

5-5-2017

# Investigating the Role of Surface Hydrophobicity in Protein Aggregation

Elizabeth Zecca

University of Connecticut - Storrs, [elizabeth.zecca@uconn.edu](mailto:elizabeth.zecca@uconn.edu)

Follow this and additional works at: <https://opencommons.uconn.edu/dissertations>

---

## Recommended Citation

Zecca, Elizabeth, "Investigating the Role of Surface Hydrophobicity in Protein Aggregation" (2017). *Doctoral Dissertations*. 1488.  
<https://opencommons.uconn.edu/dissertations/1488>

# **Investigating the Role of Surface Hydrophobicity in Protein Aggregation**

**Elizabeth Zecca, PhD**

**University of Connecticut, 2017**

## **Abstract**

Hydrophobic interactions between protein molecules are considered to be a significant contributor to attractive protein-protein interactions (PPIs) in solution. Attractive PPIs play critical roles in self-association and aggregation, thus affecting the overall protein stability. Surface hydrophobicity of three model proteins was characterized by hydrophobic interaction chromatography and fluorescence spectroscopy. To compensate for known limitations of these two widely used methods, a novel approach, based upon Nuclear Magnetic Resonance Spectroscopy (NMR), was investigated as a potential alternative. The degree of decrease in the transverse relaxation time ( $T_2$ ) of small molecule probe, such as phenol, due to its interaction with the protein of interest, was monitored to reflect the surface hydrophobicity. Utilization of this multi-method approach emphasized the differences in surface hydrophobicity of the three proteins and to distinguish the effects of two types of hydrophobic amino acids, aromatic and aliphatic, on surface hydrophobicity.

Protein unfolding, interactions and aggregation mediated at the air/water interface were monitored. It was found that aggregation was not induced by mechanical stress for the studied proteins. Furthermore, the propensities to unfold or interact with the air/water interface were only influenced by the changes in pH and not by the degree of surface hydrophobicity. Building upon the knowledge gained from the three model proteins, the surface hydrophobicity of three unknown monoclonal antibodies (MAbs) was characterized and aggregation was monitored

under mechanical stress at different ionic strength conditions. Our findings suggest that even when attractive interactions are significant, as in the case for MAb Y, the surface hydrophobicity alone is not the major factor affecting protein aggregation.

Further, antibody aggregation was studied under thermal stress. Upon heating the MAbs, unfolding and the increase in their aggregation was observed. Additionally, the aggregation propensity of MAb Y was subjected to a combination of mechanical and thermal stresses, and it was found that the aggregation increased when more energy was applied to stress the protein.

These results demonstrate that the hydrophobicity of a protein molecule is highly dependent on solution conditions and conformational changes of the protein. Therefore, protein surface hydrophobicity alone cannot be directly related to the protein propensity to aggregate and a combination of both the average and surface hydrophobicity should be taken into account.

**Investigating the Role of Surface Hydrophobicity in Protein Aggregation**

**Elizabeth Zecca**

B.S. (Chemistry), University of North Carolina Wilmington, 2011

A Dissertation

Submitted in Partial Fulfillment of the

Requirements for the Degree of

Doctor of Philosophy

at the

University of Connecticut

2017

Copyright by  
Elizabeth Zecca

2017

APPROVAL PAGE

Doctor of Philosophy Dissertation

Investigating the Role of Surface Hydrophobicity in Protein Aggregation

Presented by

Elizabeth Zecca, B.S.

Major Advisor \_\_\_\_\_

Devendra S. Kalonia

Associate Advisor \_\_\_\_\_

Michael J. Pikal

Associate Advisor \_\_\_\_\_

Robin H. Bogner

Associate Advisor \_\_\_\_\_

Olga Vinogradova

University of Connecticut  
2017

*Dedication*

*For My Mom, Dad and Sister*

## **Acknowledgments**

I would like to gratefully acknowledge a number of people without whom; this dissertation would not have been possible.

I would like to first thank my major advisor, Dr. Devendra S. Kalonia for the opportunity to learn and study in his lab at UConn. His continued enthusiasm for science and challenging questions has allowed me to learn basic concepts and grow as a scientist. His mentoring style has pushed me to become an independent researcher, which I know will serve me well in my career ahead. Thank you for your patience, pushing me out of my comfort zone and helping me grow into a more confident person.

I would like to thank my associate advisors: Dr. Michael J. Pikal and Dr. Robin H. Bogner, for always having words of encouragement, suggestions and offering support. Thank you for having faith in my abilities and bringing out the best in me. Thank you for your excitement in regards to teaching; it was truly a pleasure to learn from you. I am also very thankful to Dr. Olga Vinogradova for her scientific input, kindness and time she dedicated to our collaboration and research.

I am thankful to the pharmaceutical sciences faculty for the comprehensive coursework and seminars during my graduate research. Thank you all for your help and guidance throughout my teaching assistantships.

I would also like to thank:

- The Pharmaceutical staff in the School of Pharmacy Leslie LeBel, Mark Armati, Kathy Koji, Sharon Giovenale, Jackie Maliga, Elizabeth Anderson, Skip Copeland and others.
- The Graduate School at the University of Connecticut, Singiser Fellowships and the PhRMA



Foundation for providing financial support.

- The graduate students in Dr. Anson Ma, Dr. Xuiling Lu and Dr. Mu-Ping Neih lab, especially Sahil and Don for training me and allowing me to use the facilities in their labs.
- Dr. Michael Siedler and Dr. Vishwesh Patel at Abbvie Bioresearch Center for providing me the opportunity and a great learning experience to work as a summer intern.

I am grateful for my collaborator and friend, Khiem for the countless hours discussing NMR and proteins over the last five years. Thank you for training and sharing your knowledge with me.

I am thankful for my past and present lab mates: Shermeen, Shubhadra, Nitin, Rajni, Ash, Masha, Lauren and Japneet for their friendship and support. A special thanks to Masha whose mentorship and advice was invaluable throughout this process and Lauren who was always there to provide feedback and thoughtful suggestions.

Thank you to my friends at UConn: Mike, Pooja, Rui, Arushi, Namita, Rajan, Janki, Shreya and Pavel for all of the advice and wonderful times that we have shared. Thank you Sanne for your warm hugs and contagious joy and to Catherine who has been a constant source of encouragement, and a wonderful roommate and friend. You may not have been the first person I shared a house with, but you are the first person who made here feel like home.

My heartfelt thanks to Chelsea, Madison, Cole, Marissa, Daniela, Rachel, Gina, Taylor, Katie and Kate; for your friendship and constant support.

Thank you to Japneet. There is no doubt in my mind that UConn would not have been the same without you. Although this journey has many ups and downs, having a friend along the way to share stories of success and to carry burdens of failure, made it feel a little more like home.

There is no one I would rather laugh down the halls with.

To my family – Uncle Frank, Aunt Marlene, Aunt Rosemarie, Uncle Ed and cousins. Yes I am graduating, no I am not a pharmacist and no I do not work with cells. Thank you for the amount of love, laughter and words of encouragement (especially the emails Uncle Ed). Aunt Regina; your ability to keep me up to date on all the latest Broadway trends is only matched by the love and support you have showed me while here at UConn. My sister, Lauren and brother-in-law Chris, your encouragement, pick-me-up board game nights and constant support were always appreciated. Having a sister (brudder) means being born with a best friend and I am lucky enough to have an older sister who always believes in me and was always a phone call away. Thank you to my favorite nephew, Jackson who always puts a smile on my face and distracted me from getting my work done faster. Lastly, I would like to thank my parents Grace and Marty, for their endless amount of love, encouragement and for believing in me every step along the way. Thank you both for shaping me into who I am today, and for always being there. I love you all!

## Table of Contents

	Page
<b>Approval Page</b>	<b>iii</b>
<b>Dedication</b>	<b>iv</b>
<b>Acknowledgments</b>	<b>v</b>
<b>Table of Contents</b>	<b>viii</b>
<b>Chapter 1:</b>	<b>1</b>
Introduction, Aims and Organization of the Thesis	
<b>Chapter 2:</b>	<b>8</b>
Protein Hydrophobicity: A review of techniques and implications from a pharmaceutical perspective	
<b>Chapter 3:</b>	<b>36</b>
NMR as a Semi-Quantitative Tool for Evaluating Protein Surface Hydrophobicity	
<b>Chapter 4:</b>	<b>69</b>
Evaluating the Role of Protein-Surface Interactions in Aggregation of Proteins in Solution	
<b>Chapter 5:</b>	<b>103</b>
Physical Stability of Monoclonal Antibodies: Investigating the Link Between Protein Surface Hydrophobicity and Aggregation	

<b>Chapter 6:</b>	<b>138</b>
Summary	
<b>Appendix</b>	<b>142</b>

## **Chapter 1**

### **Introduction, Aims and Organization of the thesis**

## 1. Introduction

Protein therapeutic drugs, especially monoclonal antibodies continue to be a growing area of research and development in the pharmaceutical industry. Development of MAbs and protein-based therapeutics aid in the treatment of diseases including immunological disorders, cancers, cardiovascular diseases and infections and has seen significant growth over the last thirty years with more than 300 molecules currently in development.<sup>1-4</sup> MAbs are highly target specific, and have a large therapeutic effect however a relatively high dose is required for efficacy.<sup>5</sup> Delivery of these drugs is often via a low volume subcutaneous injection; this makes the preparation of a high concentration protein formulation essential. However, in these highly concentrated solutions many problems arise from a formulation standpoint. Both physical and chemical stability of monoclonal antibodies can compromise the safety, efficacy and shelf life of the drug.<sup>6,7</sup>

Physical degradation comprises of protein self-association, aggregation, opalescence, and phase separation and is often influenced by several stages of development such as filtration, purification, storage, formulation and delivery.<sup>5,8</sup> In addition, solution conditions as well as protein-protein interactions also affect the conformational and structural stability of protein molecules, which can often lead to physical degradation. Hydrophobic and electrostatic (dipole-dipole, dipole-induced dipole, induced dipole-induced dipole, specific ion) protein interactions make significant contributions to the net short-range attractions.<sup>9-13</sup> Although, hydrophobic interactions are known to be present and contribute to attractive protein-protein interactions, they cannot be directly measured.

Hydrophobic amino acids are present on both the surface of the protein molecule as well as in the interior.<sup>14,15</sup> Methods that measure surface hydrophobicity are often influenced by solution

conditions and therefore do not accurately predict hydrophobic interactions in protein solutions. Moreover, slight structural perturbations of the protein structure can change the degree of protein hydrophobicity therefore surface hydrophobicity measurements become inaccurate. Although, hydrophobicity is often thought to play an integral part in physical stability issues such as self-association,<sup>14,16,17</sup> aggregation<sup>18</sup> and adsorption to interfaces,<sup>19</sup> experimental correlations are lacking.<sup>13,20</sup> Thereby, it is important to understand the relative contribution of hydrophobicity compared to other molecular interactions regarding physical stability issues during the early formulation and development stages of protein molecules.

## **2. Objective**

The present dissertation focuses on investigating the surface hydrophobicity of protein molecules and studying the relationship between hydrophobic interactions with protein aggregation.

The Specific Aims of the project were:

1. Developing a multi-method approach to characterize the surface hydrophobicity of protein solutions
2. To understand the role of surface hydrophobicity in aggregation mediated by protein-surface interactions.
3. Investigating the link between protein surface hydrophobicity and aggregation of monoclonal antibodies formulations

## **3. Chapter Organization and Outline**

**Chapter 2** reviews methods to measure protein hydrophobicity and the relevant consequences of hydrophobicity in protein solutions. It begins with a brief thermodynamic

introduction of the hydrophobic effect and classical hydrophobic interactions. Techniques and methods to measure both average and surface hydrophobicity are highlighted, specifically discussing the advantages and disadvantages as well as the usefulness to distinguish between aromatic and aliphatic nonpolar amino acids. An overview of the interactions involved in pi-pi interactions is discussed. Extrinsic factors such as mechanical and thermal stresses and solution conditions affecting protein unfolding are reviewed. Finally, specific cases from literature where hydrophobicity is known to be the cause of self-association and aggregation are discussed.

**Chapter 3** discusses the current methods in literature and introduces a novel method to measure surface hydrophobicity using Nuclear Magnetic Resonance (NMR). Several different small molecular probes were tested to determine the hydrophobicity of BSA,  $\alpha$ -Chymotrypsinogen A and  $\beta$ -Lactoglobulin A. To determine the validity of the hydrophobicity measurements of the proteins from NMR, characterizing the surface hydrophobicity using hydrophobic interaction chromatography (HIC) and extrinsic fluorescence spectroscopy were also conducted.

The work in **chapter 4** focuses on the relationship between surface hydrophobicity and surface induced aggregation of protein molecules. An understanding of the effect of mechanical stress (shaking) on the adsorption and unfolding at the air/water interface and subsequent aggregation of the proteins at pH 7.0 has been investigated. Protein-protein interactions and viscoelastic parameters at different solution conditions has been studied for each protein molecule. The work presented in **chapter 5** investigates the surface hydrophobicity of three monoclonal antibodies and the impact this may have on protein aggregation via mechanical stress. HIC, fluorescence and NMR are used to measure the surface hydrophobicity at pH 7.0 and the physical stability was assessed. The purpose of this work was to determine if the surface



hydrophobicity of the antibodies influences aggregation *via* mechanical stress, thermal stress or a combination of the two. Additionally, studies were done to investigate the effect of aromatic excipients on attractive protein-protein interactions.

**Chapter 6** presents a summary of the entire work.

## References

1. Ecker, D. M., Jones, S. D. & Levine, H. L. The therapeutic monoclonal antibody market. *mAbs* **7**, 9–14 (2014).
2. Geng, X. *et al.* Research and development of therapeutic mAbs: An analysis based on pipeline projects. *Human Vaccines & Immunotherapeutics* **11**, 2769–2776 (2015).
3. Daugherty, A. L. & Mersny, R. J. Formulation and delivery issues for monoclonal antibody therapeutics. *Advanced Drug Delivery Reviews* **58**, 686–706 (2006).
4. Elvin, J. G., Couston, R. G. & van der Walle, C. F. Therapeutic antibodies: Market considerations, disease targets and bioprocessing. *International Journal of Pharmaceutics* **440**, 83–98 (2013).
5. Goswami, S., Wang, W., Arakawa, T. & Ohtake, S. Developments and Challenges for mAb-Based Therapeutics. *Antibodies* **2**, 452–500 (2013).
6. Manning, M. C., Chou, D. K., Murphy, B. M., Payne, R. W. & Katayama, D. S. Stability of Protein Pharmaceuticals: An Update. *Pharm Res* **27**, 544–575 (2010).
7. Wang, W. Instability, stabilization, and formulation of liquid protein pharmaceuticals. *International Journal of Pharmaceutics* **185**, 129–188 (1999).
8. Shire, S. J., Shahrokh, Z. & Liu, J. Challenges in the development of high protein concentration formulations. *journal of pharmaceutical sciences* **93**, 1390–1402 (2004).
9. Israelachvili, J. N. *Intermolecular and surface forces*. (2011).
10. Chari, R., Jerath, K., Badkar, A. V. & Kalonia, D. S. Long- and Short-Range Electrostatic Interactions Affect the Rheology of Highly Concentrated Antibody Solutions. *Pharm Res* **26**, 2607–2618 (2009).
11. Saluja, A. & Kalonia, D. S. Nature and consequences of protein–protein interactions in high protein concentration solutions. *International Journal of Pharmaceutics* **358**, 1–15 (2008).
12. Weiss, W. F., IV, Young, T. M. & Roberts, C. J. Principles, approaches, and challenges for predicting protein aggregation rates and shelf life. *journal of pharmaceutical sciences* **98**, 1246–1277 (2009).
13. Roberts, C. J., Das, T. K. & Sahin, E. Predicting solution aggregation rates for therapeutic proteins: Approaches and challenges. *International Journal of Pharmaceutics* **418**, 318–333 (2011).
14. Jones, S. & Thornton, J. M. Protein-protein interactions: a review of protein dimer structures. *Progress in biophysics and molecular biology* **63**, 31–65 (1995).
15. Kauzmann, W. Some factors in the interpretation of protein denaturation. *Advances in protein chemistry* **14**, 1–63 (1959).
16. Gokarn, Y. R. *et al.* Ion-specific modulation of protein interactions: Anion-induced, reversible oligomerization of a fusion protein. *Protein Science* NA–NA (2008). doi:10.1002/pro.20
17. Esfandiary, R. *et al.* A systematic multitechnique approach for detection and characterization of reversible self-association during formulation development of therapeutic antibodies. *journal of pharmaceutical sciences* **102**, 3089–3099 (2013).
18. Chennamsetty, N., Helk, B., Voynov, V., Kayser, V. & Trout, B. L. Aggregation-Prone Motifs in Human Immunoglobulin G. *Journal of Molecular Biology* **391**, 404–413 (2009).
19. Horbett, T. A. & Brash, J. L. Proteins at interfaces: current issues and future prospects. (1987). doi:10.1021/bk-1987-0343.ch001;page:string:Article/Chapter

20. Shieh, I. C. & Patel, A. R. Predicting the Agitation-Induced Aggregation of Monoclonal Antibodies Using Surface Tensiometry. *Mol. Pharmaceutics* **12**, 3184–3193 (2015).

## **Chapter 2**

### **Protein Hydrophobicity: A review of techniques and implications from a pharmaceutical perspective**

## **Contents**

### **Chapter 2**

1. Introduction
2. Thermodynamics of the Hydrophobic Effect
3. Measuring Average Hydrophobicity
  - 3.1. Transfer Free Energy
  - 3.2. Aromatic Amino Acids
4. Surface Hydrophobicity
  - 4.1. Methods to Measure Surface Hydrophobicity
    - 4.1.1. Fluorescence Spectroscopy
    - 4.1.2. Chromatography
    - 4.1.3. Aqueous Two-Phase Systems
    - 4.1.4. Surface Tension
5. Protein Unfolding
  - 5.1. Factors Affecting Unfolding
    - 5.1.1. pH
    - 5.1.2. Excipients
    - 5.1.3. Temperature
    - 5.1.4. Mechanical Stress
6. Consequences of hydrophobicity
7. Future
8. References
9. Figures

## 1. Introduction

Hydrophobic interactions play a critical role in protein folding, often being recognized as the major driving force for the tertiary structure of a protein molecule.<sup>1,2</sup> The native structure of a protein is imperative for most proteins to remain active and have a stable shelf life.<sup>3</sup> Consequently, hydrophobic interactions can also compromise the stability of a protein formulation through adsorption to the air/water or solid/water interface, self-association and aggregation.

The primary amino acid sequence of a protein is made up of amino acids that vary in polarity. There have been many attempts to characterize the hydrophobicity of these amino acids, however a general consensus between hydrophobicity scales is difficult to obtain.<sup>4,5</sup> Using the hydrophobicity values of individual amino acids, the average hydrophobicity of protein molecules has been calculated. Although the average hydrophobicity represents all of the nonpolar amino acids in the primary sequence, some of these nonpolar residues will not be buried in the core of the protein. These nonpolar amino acids can be among very hydrophilic, charged residues such as glutamic acid and lysine. Removal of these charged residues from water (unfavorable) would have to occur in order to bury the nearby nonpolar amino acids. Therefore, a considerable amount of a protein's surface is nonpolar and exposed to the aqueous solvent.<sup>6,7</sup>

The nonpolar amino acids patches represent the surface hydrophobicity of a protein. Similar to most protein-protein interactions, hydrophobic interactions are influenced by solution conditions and external factors. Both experimental and theoretical methods have been used to determine the surface hydrophobicity of various proteins, however due to these influences as well as the conformational stability of the protein, achieving a hydrophobic value for a protein continues to be difficult. Moreover, the connection between the surface hydrophobicity

measurements to protein aggregation does not always hold true. This is because the measured surface hydrophobicity does not account for the exposure of previously buried hydrophobic amino acids when the protein undergoes unfolding, which may contribute to these instabilities. Thus, relating any hydrophobic value, surface or average to a stability issue is challenging.

The following review will discuss how both, the average and surface hydrophobicity of proteins are measured by various techniques. The advantages and disadvantages will be mentioned, however the difference in measuring between aliphatic and aromatic nonpolar amino acids will be highlighted. The influence of hydrophobic interactions on protein stability will also be discussed and the recent advances in the connection between protein hydrophobicity and its impact on aggregation.

## **2. Thermodynamics of the hydrophobic effect**

Hydrophobicity was first described by studying the surface activity of hydrocarbon molecules and further explored by studying the transfer of a hydrocarbon from an aqueous solvent to a nonpolar solvent.<sup>2,7-10</sup> These principles first established with alcohols and hydrocarbons were used to describe the hydrophobic effect.<sup>2</sup> The thermodynamic contribution for the hydrophobic effect at room temperature comes from an increase in entropy and can be described by the Gibbs free energy equation below.

$$\Delta G = \Delta H - T\Delta S \quad (1)$$

Where  $\Delta G$  is the change in Gibbs free energy,  $\Delta H$  is the change in enthalpy term and  $\Delta S$  is the change in entropy. Water molecules surrounding hydrophobic amino acids become ordered

due to the lack of interaction with water. This absent interaction between nonpolar amino acids and water, results in negative or small positive values of enthalpy ( $\Delta H$ ) and an unfavorable change in entropy ( $\Delta S < 0$ ). In turn, most of the nonpolar amino acids bury within the core of the protein leading to an increase in entropy of the solution ( $-T\Delta S > 0$ ) and an overall favorable free energy ( $\Delta G < 0$ ).<sup>1,7,11-13</sup> The initial decrease in entropy is the driving force for the hydrophobic effect. The negative entropy is attributed to the ordering of the surrounding water molecules. In addition, there is a small positive heat capacity change ( $\Delta C_p$ ) signature to the hydrophobic effect.<sup>14-16</sup> The heat capacity of a folded protein compared to an unfolded protein is shown in figure 1. Although the total heat capacity change is more positive for an unfolded protein due to the hydration of nonpolar amino acid residues, the heat capacity is still slightly positive for a folded protein.<sup>17</sup>

### 3. Measuring Average hydrophobicity

#### 3.1. Transfer free energy

A number of authors have proposed hydrophobicity scales using several organic solvents to mimic the protein core. Tanford determined the change in free energy of measuring the solubility of amino acids in water and then in ethanol at 25 °C. Using the equation below,

$$\Delta F_t = RT \ln(N_{EtOH}/N_{H2O})$$

Where  $N_{H2O}$  is the solubility in water and  $N_{EtOH}$  is the solubility in ethanol.<sup>9</sup> The transfer free energies of each amino acid were measured and in order to determine the free energy contribution of only the side chain, the free energy of the amino acid was subtracted from the



free energy of glycine. Other studies have chosen different solvents that better represents the protein core, such as using N-Methylacetamide,<sup>18</sup> Hexane,<sup>19</sup> Dioxane,<sup>20</sup> Octanol,<sup>21,22</sup> and N-cyclohexyl-2-pyrrolidone.<sup>23</sup> The hydrophobicity of amino acids has also been determined by relating physical properties such as surface tension to the polarity of individual amino acids.<sup>24,25</sup> Due to the importance of hydrophobic amino acids involved in protein folding, numerous hydrophobicity scales have been developed. However, a consensus of the order of amino acids is lacking. A collection of most of the hydrophobicity scales for amino acids are compiled and the occurrence of each amino acid is ranked and presented in a review article.<sup>4</sup> It can be seen from the subtle differences in how the hydrophobicity is measured, the rank order of hydrophobicity for amino acids is very different thus making it difficult to generate a universal scale. Using the transfer free energies of individual amino acids, the hydrophobicity of a protein can also be calculated. Bigelow et al. uses the average hydrophobicity value of the amino acids and divides by the number of residues in the given protein resulting in the total calculated hydrophobicity value of that protein.<sup>26</sup> Other hydrophobicity methods including chromatography and accessible surface area (ASA) of the protein have also been compared to one another described by Biswas et al.<sup>5</sup>

All hydrophobicity scales contain both aliphatic nonpolar amino acids as well as aromatic nonpolar amino acids. This is a true representation as both contribute to hydrophobic interactions, but the changes in free energy associated with aromatic moieties is much larger than the transfer free energy with aliphatic amino acids. Aliphatic amino acids are said to interact solely due to their inability to form hydrogen bonds with water molecules (entropic effect), however for aromatic amino acids this is not the case. Aromatic amino acids have other contributing interactions such as Van der Waals and electrostatic interactions that accompany

hydrophobic interactions (aversion for water) and thus contribute to the overall thermodynamics of the interaction.<sup>27-29</sup>

### 3.2. *Aromatic Amino Acids*

Aromatic amino acids in protein molecules consist of tyrosine, tryptophan and phenylalanine. These aromatic amino acids contain portions of nonpolar moieties in their structure, such as the benzene ring in both phenylalanine and tyrosine and these structures contribute to classical hydrophobic interactions between both aromatic and aliphatic amino acids.<sup>28</sup> Moreover, the interaction between two aromatic amino acids is stronger than aliphatic-aliphatic side chains because it involves additional interactions between the molecules.<sup>14,30</sup> Since classical hydrophobic interactions do not govern  $\pi$ - $\pi$  interactions solely in solution, thermodynamically the entropy driven hydrophobic effect (small enthalpy) is not the sole responsible driving force for these interactions.<sup>31</sup>

The interactions that contribute to  $\pi$ - $\pi$  interactions are Van der Waals, hydrophobic and electrostatic interactions.<sup>32,33</sup> Although hydrophobic interactions are not a dominant role in aromatic interactions,<sup>34-36</sup> they are suggested to still be involved.<sup>28</sup> The contribution from electrostatic interactions is most significant because electrostatic interactions govern the most favorable geometries between the two aromatic side chains.<sup>27,28,30,37</sup>

Theoretical models and energy simulations have comprehensively studied the most favorable geometries between aromatic molecules. While the term “ $\pi$ - Stacking” is often used, two aromatic moieties are electrostatically repulsed when stacked on top of one another. The two most favorable geometries illustrated by figure 2 is the edge-face “T-shaped” and off-stacked geometries.<sup>37-39</sup> For proteins specifically, it was seen that phenylalanine interacts most favorable with itself, while trp and tyr prefer to pair dissimilar to itself.<sup>40</sup> Since there is a disparity between

different energies and geometries of aromatic and aliphatic interactions, an increased understanding of the different types of hydrophobic interactions would be beneficial in further understanding of a protein folded structure as well as the formation of associated species.

#### **4. Surface Hydrophobicity**

The average protein hydrophobicity does not distinguish between those amino acids that are buried in the protein core, compared to the ones that are solvent exposed. Therefore, experimental techniques have been used to qualitatively and quantitatively measure the relative surface hydrophobicity of proteins. In the following section, advantages and disadvantages will be presented for methods that measure surface hydrophobicity as well the implications of surface hydrophobicity contributing to protein instabilities in solutions will also be discussed.

##### *4.1. Methods to measure surface hydrophobicity*

###### **4.1.1. Fluorescence spectroscopy**

Fluorescence spectroscopy is a useful technique to determine structural changes of protein molecules in solution. Intrinsic fluorescence is due to the fluorophores in a protein, phenylalanine, tyrosine and tryptophan. These residues of a protein are sensitive to environmental changes within the protein.<sup>41</sup> Extrinsic fluorescence uses an extrinsic dye, which interacts non-covalently with a protein molecule. Extrinsic dyes come in a myriad of different structures, charged or uncharged in solution and have solubility issues in different solvent systems. The advantage of these dyes is that they are scarcely fluorescence in an aqueous environment, but exhibit an increase and shift in wavelength in a nonpolar environment.

The most common extrinsic dyes are cis-parinarate (CPA),<sup>42</sup> Nile Red<sup>43</sup>, 1-(anilino)-naphthalene-8-sulfonate (ANS), 4,4'-bis[1-(phenylamino)-8-naphthalenesulfonate] (bis-ANS),

6-propionyl-2 - (N, N-dimethylamino) naphthalene (Prodan),<sup>44</sup> 6-(ptoluidinyl) naphthalene-2-sulfonate (TNS<sup>-</sup>),<sup>45</sup> and Bromophenol blue.<sup>46</sup> These dyes are different in size, charge and structure. CPA only contains long hydrocarbon chains, whereas ANS contains a naphthalene ring and Bis-ANS is much larger (twice the size of ANS). The extrinsic dyes that are charged in solution have an advantage of an increased solubility, whereas those that are not charged (i.e. Nile Red) have to be dissolved in an organic solvent due to the limited solubility in water. However the major disadvantage of using charged probes is that the type of interaction between the protein and dye is not solely through hydrophobic interactions because there are electrostatic interactions that also contribute. These electrostatic contributions can over/under estimate the hydrophobicity value and give incorrect results. Haskard and Chan performed experiments with ANS and Prodan as a function of ionic strength to illustrate that as the charges are screened for both the protein and the dye, the surface hydrophobicity value varies as seen in figure 3.<sup>47</sup> Pashar and Chan also studied this overestimation of hydrophobic interactions by comparing ANS- and CPA-, which are both anionic, and Prodan, which has no charge, while also changing the pH of the protein solution.<sup>48</sup> Their results indicated that there were differences between the charged and uncharged probes, as well as differences seen between structurally different dyes CPA and ANS.<sup>41,49</sup> The difference between interactions for an aliphatic dye, CPA and aromatic dye, ANS illustrates that structurally different dyes will interact with the protein by both  $\pi$ - $\pi$  as well as hydrophobic interactions. A recent study compared traditional dyes, ANS and PRODAN to five new 4-bora-3a,4a-diaza-s-indacene (BOPIDY) hydrophobic sensors (HP) to determine the surface hydrophobicity of proteins.<sup>50</sup> They concluded that the HPsensor 2 was the most effective dye out of five for measuring surface hydrophobicity and can be incorporated with other methods to characterize protein hydrophobicity. Using fluorescence spectroscopy enables the detection of

surface hydrophobicity on specific patches of a protein, however the interaction will be affected by the size, charge and structure of both the nonpolar patch as well as the extrinsic dye.

#### 4.1.2. Chromatography

Traditionally used for purification, hydrophobic interaction chromatography (HIC) is a useful tool for separating proteins by their hydrophobicity in a less harsh environment (as in RPC).<sup>51</sup> The proteins are injected into a nonpolar column that is equilibrated with a high concentration of salt buffer.<sup>52</sup> The type of salt used is based off of the Hofmeister series, certain salts promoting hydrophobic interaction to the column more than others.<sup>53</sup> As the salt concentration in the mobile phase decreases, the proteins will elute off the column, and the order will indicate the relative surface hydrophobicity. Comparing the relative hydrophobicity of many proteins has been successfully achieved by this method.<sup>42</sup>

Choosing appropriate parameters such as a suitable salt (mobile phase), flow rate, injection volume, pH, concentration of salt, and column will all impact the retention times of the proteins.<sup>53-57</sup> Using different stationary columns can evaluate the type of hydrophobic interactions between the protein and the column. Aliphatic substituents like butyl and ethyl have been used for HIC experiments, as well as the aromatic phenyl moiety. The degree of binding has been said to be stronger for phenyl than the alkyl ligand support column.<sup>52</sup> Goheen et al. made this inference by using HIC to determine the hydrophobicity of BSA on both a butyl and phenyl column. A difference in the number of peaks, one peak eluted off the butyl column while two peaks eluted off the phenyl column, illustrated a difference in binding between BSA and the structurally different supports. They attributed this to the difference in selectivity between aromatic and aliphatic columns.<sup>58</sup> However, other conclusions can be drawn from these observations such as structural changes of BSA induced by ammonium sulfate, or the difference

in the density of the support. Although these hypotheses do occur in systems, there needs to be more research performed in order to further clarify. Further studies to elucidate the difference in amino acid retention on an HIC column was performed by monitoring the retention times of various aliphatic and aromatic amino acids on an HIC support column. From the results it was shown that aromatic amino acids were retained significantly longer than aliphatic amino acid residues.<sup>59</sup>

The surface hydrophobicity distribution of a protein will also affect the way the protein interacts with the column. This is evident in the difference in retention times for two ribonucleases, despite having similar hydrophobicity.<sup>60</sup> This can give a false prediction of the surface hydrophobicity of the whole molecule. Lienqueo et al. uses the three-dimensional structure of the protein, along with amino acid hydrophobicity scales to determine the surface hydrophobicity of the proteins and predict the retention times on the column.<sup>61</sup>

#### 4.1.3. Aqueous Two-Phase Systems

Aqueous two-phase systems consist of a PEG/salt or PEG/dextran system and the partition coefficient ( $\log K$ ), is related to the free energy. The partition coefficient is measured for each protein and gives a rank order of hydrophobicity for protein molecules.<sup>62</sup> This method to measure protein surface hydrophobicity has been used to correlate with techniques such as hydrophobic interaction chromatography, reverse phase-HPLC and precipitation by ammonium sulfate (inverse solubility). The authors found no correlation between the measured partition coefficient and both of the chromatographic methods (HIC and RPC). However, the partition coefficient that was observed, correlated well with the measured hydrophobicity by precipitation (ammonium sulfate).<sup>63-65</sup> However, this suggests that both of these methods (ATPS and precipitation) depend on a proteins solubility, rather than hydrophobicity. Although the

hydrophobicity of a protein will have an affect on a proteins solubility measurement; other factors will contribute to protein solubility. It has also been suggested that measuring the surface hydrophobicity by ATPS, may not be accurate because the measured partition coefficient ( $\log K$ ) could be a result of changes in the protein conformation or association between protein molecules.<sup>66</sup>

#### 4.1.4. Surface Tension

Surface tension has been used to determine the hydrophobic characteristics of individual amino acids as well as globular proteins.<sup>24</sup> The interfacial tension of proteins (protein solution/corn oil) was compared to both HIC and  $\Delta\log K$  hydrophobic methods. The results indicate a negative correlation with both techniques, the more hydrophobic a protein was, the more the interfacial tension decreased. A positive correlation between the interfacial tension and the hydrophobicity measured by fluorescence spectroscopy,  $S_0$  using CPA as the dye was also observed.<sup>42</sup> Recently, Amrhein et al. developed a non-invasive technique to measure surface tension and relate the surface tension measurements of different proteins to their surface hydrophobicity measured by an established spectrophotometric method.<sup>67</sup> Thus, relating surface tension to protein hydrophobicity can give an indication of the surface hydrophobicity of a protein.

To get a true representation of the surface hydrophobicity measured by the methods above, the protein must remain in its tertiary structure. However, the proteins conformational stability is influenced by a number of factors and solution conditions. If the protein begins to partially unfold at specific pH values or after being exposed to a mechanical stress, the measured surface hydrophobicity by these techniques will change. Therefore, understanding the specific factors

that affect unfolding is important to determine the extent to which surface hydrophobicity measurements hold true.

## **5. Protein Unfolding**

Proteins undergo conformational changes and denaturation due to a number of different factors. For most proteins, maintaining a native structure is essential for the protein to remain active and stable.<sup>3</sup> A main stability issue that can occur due to protein unfolding is irreversible protein aggregation and eventual precipitation out of solution, which can be detrimental to the stability of the protein formulation.<sup>68,69</sup>

When a protein unfolds, the hydrophobic amino acids are exposed to the solvent, increasing the free energy of the system. This increase in free energy is a result of an increase in enthalpy and a decrease in entropy (small but remains positive). The entropy decreases but remains positive because although more nonpolar amino acids are exposed and structure water molecules, there is an increase in configurationally entropy due to the unfolded protein. As a protein unfolds there is also a large increase in heat capacity, which is attributed to the solvation of nonpolar amino acids.<sup>1</sup>

External factors such as temperature, pH, ionic strength and mechanical stress are some factors that can accelerate or facilitate protein denaturation. Protein unfolding can also be influenced by different interfaces, solid/liquid, liquid/liquid and liquid/air. For protein pharmaceuticals, solid/liquid (interaction between the glass vial and the solution) and air/water interfaces are of importance because it can lead to protein aggregation in the bulk solution. Hydrophobic amino acids have been known to contribute to adsorption of proteins onto hydrophobic surfaces and at the air/water interface, leading to unfolding and potential



aggregates.<sup>70,71</sup> Understanding the specific factors that promote unfolding is important to determine how the formulation will behave during purification, filtration, manufacturing, and transportation of the product. The factors that promote unfolding and the subsequent consequences are essential to understanding the role of protein hydrophobicity in aggregation.

### *5.1. External Factors Affecting Unfolding of Proteins*

#### *5.1.1. pH*

Maintaining the pH of the solution is important to assure a stable protein formulation. While some proteins are stable at pH values close to their isoelectric point (pI), others aggregate due to protein–protein interactions or surface hydrophobicity that is higher at the protein pI. Protein unfolding can become an issue as the pH of the solution is formulated far from the proteins isoelectric point. As the pH is increased or decreased away from the pI, the protein becomes very charged, leading to charge repulsions and can result in partial unfolding of the protein structure.<sup>1,68</sup> Extreme pH values towards acidic or basic conditions can also alter the protein conformations leading to a more flexible conformation, causing aggregation.<sup>72</sup> Examples of structural changes as a function of pH are HSA,<sup>73</sup> Lysozyme,<sup>74</sup> and BSA.<sup>75</sup>

#### *5.1.2. Excipients*

The effect of salt also can influence the conformational stability of a protein depending on the type of salt and concentration used. The Hofmeister series ranks salts based on their kosmotropic or chaotropic nature, similar to their effect on the solubility of proteins. Kosmotropic salts such as  $\text{CO}_3^{2-}$  and  $\text{SO}_4^{2-}$  promote precipitation of proteins and prevent protein unfolding, whereas chaotropic salts like  $\text{ClO}_4^-$  and  $\text{SCN}^-$  promote denaturation and increase solubility.<sup>76-78</sup> Some salts, which are used in formulations such as NaCl, are in the middle of the series and have a neutral effect.<sup>79</sup>

Preferential interaction of co-solutes is a major stabilization effect of excipients. Preferential interactions imply the proteins will interact with either the water or the co-solute. When an excipient stabilizes a protein, the proteins prefers to interact with water therefore excluding the presence of the excipient from the protein surface (preferential exclusion) which subsequently stabilizes the protein structure.<sup>80</sup> Sucrose is a widely known and used stabilizer.<sup>81</sup> Types of stabilizers vary from different sugars, polyols, amino acids, polymers, PEGS and surfactants.<sup>79,82,83</sup> Other excipients may promote unfolding by preferential binding, especially at high concentrations including denaturants (guanidinium chloride, urea) and preservatives (phenol, benzyl alcohol).<sup>76,79,84</sup>

#### 5.1.3. Temperature

Protein stability is often measured by thermal unfolding usually by differential scanning calorimetry (DSC). The higher the melting temperature ( $T_m$ ), the more stable the protein. Using the onset of unfolding and the melting temperature, protein stability has been inferred from this information. High and low temperatures can denature a protein, which will result in aggregation and precipitation.<sup>85-88</sup>

#### 5.1.4. Mechanical stress

Mechanical stress (shaking, stirring and shear) can facilitate protein unfolding by generating new air/water interfaces. Kiese et al. performed a comprehensive study comparing the two stresses, shaking and stirring, imposed on an IgG monoclonal antibody<sup>89</sup>. Fill volume, concentration of surfactant and protein concentrations were varied to determine the conditions vulnerable for aggregates. Total Aggregation, monitored by SEC, turbidity and DLS was different for the two stresses. Other studies have looked into shaking speed and type of container

to determine the impact of shaking on the proteins.<sup>90</sup> Shear stress can also influence unfolding and aggregation especially in the presence of the air/water interface.<sup>91</sup>

An example of predicating antibody stability by observing surface properties such as surface pressure, surface excess and hydrophobicity to determine the aggregation propensity of monoclonal antibodies by shaking stress.<sup>92</sup> Subjecting protein formulations to mechanical stress is a predictive tool to determine how the protein will behave under difference stresses throughout the product development process such as stirring, pumping, purification, filtration and delivery.

## **6. Consequences of hydrophobicity**

Generally, hydrophobicity is known to be a dominant force in the formation of associated species or aggregates in protein solutions. However, determining the relationship between either the average and/or surface hydrophobicity measurement of a protein and these stability issues is still unresolved.

Self-association of protein molecules is the reversible formation of native monomer units. Formation of dimers, trimers and higher molecular weight species can impact solution viscosity and injectability to the patient.<sup>93</sup> Attractive interactions between two protein molecules can promote self-association through both hydrophobic and electrostatic interactions.<sup>94-96</sup> In order to mitigate this issue, excipients are added to the formulation, and from the results one can determine the source of the attractive interactions. One study shows that there was a significant decrease in association of protein molecules after adding hydrophobic amino acids, with a substantial decrease seen after adding phenylalanine and tryptophan.<sup>97</sup> Gokarn et al monitored self-association by observing the sedimentation coefficient using AUC. It was observed that as hydrophobic aromatic amino acids were added to the antibody solution, self-association

decreased.<sup>98</sup> This emphasizes that hydrophobic excipients replaced unwanted hydrophobic interactions between protein molecules, thus decreasing the stability issue. The interior, interface (between two dimers) and exterior amino acid composition was investigated for 32 proteins and it was observed that hydrophobic amino acids had a greater probability to be at the interface between two protein-associated molecules.<sup>99</sup> Aromatic amino acids were also observed to be present at the interface at an elevated rate.<sup>99,100</sup>

In concentrated protein solutions, while both attractions and repulsions are present, attractions between protein molecules become significant. In one study, concentrated proteins showed an increase in viscosity. As mentioned earlier, associations of protein molecules affect viscosity, which is heightened at higher concentrations. Salts such as NaCl and KI can decrease the viscosity effectively. However, Du et al shows that cations or anions attached to hydrophobic moieties termed “hydrophobic salts” noticeably decreased the viscosity to a greater extent than the inorganic salts.<sup>101</sup> The work highlighted here shows the importance of surface hydrophobicity of protein molecules by decreasing the stability issue (self-association and viscosity) after it has occurred. Determining the hydrophobicity of a protein prior to self-association or an increase in viscosity and then establishing a link to these instabilities would be beneficial.

Hydrophobicity also impacts the formation of irreversible aggregates between partially or fully unfolded protein molecules. As the protein denatures, hydrophobic interactions will contribute to the attractive interactions in solution and the eventual formation of aggregates. This was seen in the case of Lysozyme.<sup>102</sup> Aggregation has also been predicted for monoclonal antibodies using a spatial aggregation propensity (SAP) modeling system.<sup>103-105</sup> Areas of hydrophobic patches were mutated to make more hydrophilic antibodies and accelerated stability studies were performed by thermal stress. Enhanced stability was observed in the DSC scans and

turbidity assay in both the mutant antibodies A and B compared to the wild type. This method predicts the hydrophobic sites on monoclonal antibodies that may contribute to stability issues, however stability studies are tested at high temperature conditions. Therefore, if temperature were used to unfold the protein, neither the surface hydrophobicity nor the average hydrophobicity would be a good predictor of stability.

## **7. Future**

It is evident that hydrophobic interactions play a significant role in protein structure and stability. A number of methods have been established to determine the hydrophobicity of a protein, however the degree of hydrophobicity does not always correlate to stability issues in protein molecules. The established methods that measure hydrophobicity are divided into two differing categories. Measuring the average hydrophobicity of the amino acid sequence of a protein accounts for all nonpolar amino acids, however all of these residues will not participate in hydrophobic protein interactions. Surface hydrophobicity methods measure the hydrophobicity of a native protein structure, but this requires the protein to remain in its folded state. Aggregation particularly occurs when a proteins structure has been compromised by different solution conditions or external factors.<sup>69</sup> Therefore, the hydrophobicity that needs to be measured is one that accounts for the structural perturbations of a protein as it behaves in solution. This also requires that the observed hydrophobicity measurement be taken under solution conditions where other interactions are present, thus mimicking protein conditions in therapeutic formulations. The differences in aromatic and aliphatic hydrophobic amino acids contributing to stability issues will be important to determine the excipients that can be used to minimize stability issues, as well as the types of amino acids that have an increased probability

of participating in association or aggregation. Determining the degree of hydrophobicity of a protein molecule is an ongoing area of research and is important in order to effectively understand physical instabilities of protein molecules.

## 8. References

1. Dill, K. A. Perspectives in Biochemistry. *Biochemistry* (1990).
2. Kauzmann, W. Some factors in the interpretation of protein denaturation. *Advances in protein chemistry* **14**, 1–63 (1959).
3. Goswami, S., Wang, W., Arakawa, T. & Ohtake, S. Developments and Challenges for mAb-Based Therapeutics. *Antibodies* **2**, 452–500 (2013).
4. Trinquier, G. & Sanejouand, Y. H. Which effective property of amino acids is best preserved by the genetic code? *Protein engineering* (1998).
5. Biswas, K. M., DeVido, D. R. & Dorsey, J. G. Evaluation of methods for measuring amino acid hydrophobicities and interactions. *Journal of Chromatography A* **1000**, 637–655 (2003).
6. Englard, S. & Seifter, S. [22] Precipitation techniques. *Methods in Enzymology* **182**, 285–300 (1990).
7. Tanford, C. *The hydrophobic effect: formation of micelles and biological membranes*. (John Wiley & Sons, 1973).
8. Némethy, G. & Scheraga, H. A. Structure of Water and Hydrophobic Bonding in Proteins. II. Model for the Thermodynamic Properties of Aqueous Solutions of Hydrocarbons. *J. Chem. Phys.* **36**, 3401–3417 (1962).
9. Tanford, C. Contribution of Hydrophobic Interactions to the Stability of the Globular Conformation of Proteins. **84**, 4240–4247 (1962).
10. Frank, H. S. & Evans, M. W. Free Volume and Entropy in Condensed Systems III. Entropy in Binary Liquid Mixtures; Partial Molal Entropy in Dilute Solutions; Structure and Thermodynamics in Aqueous Electrolytes. *J. Chem. Phys.* **13**, 507 (1945).
11. Ben-Naim, A. Hydrophobic Interaction and Structural Changes in the Solvent. **14**, 1337–1355 (1965).
12. Livingstone, J. R., Spolar, R. S. & Record, M. T., Jr. Contribution to the thermodynamics of protein folding from the reduction in water-accessible nonpolar surface area. *Biochemistry* **30**, 4237–4244 (1991).
13. Privalov, P. L. & Gill, S. J. The hydrophobic effect: a reappraisal. *Pure and Applied Chemistry* 1097–1104 (1989).
14. Makhatadze, G. I. & Privalov, P. L. Energetics of interactions of aromatic hydrocarbons with water. *Biophysical Chemistry* **50**, 285–291 (1994).
15. Prabhu, N. V. & Sharp, K. A. HEAT CAPACITY IN PROTEINS. *Annu. Rev. Phys. Chem.* **56**, 521–548 (2005).
16. Spolar, R. S., Ha, J.-H. & Record, M. T., Jr. Hydrophobic effect in protein folding and other noncovalent processes involving proteins. *PNAS* 8382–8385 (1989).
17. Privalov, P. L. & Makhatadze, G. I. Contribution of hydration and non-covalent interactions to the heat capacity effect on protein unfolding. *Journal of Molecular Biology* **224**, 715–723 (1992).
18. Damodaran, S. & Song, K. B. The role of solvent polarity in the free energy of transfer of amino acid side chains from water to organic solvents. *J. Biol. Chem.* **261**, 7220–7222 (1986).
19. Fendler, J. H., Nome, F. & Nagyvary, J. Compartmentalization of amino acids in surfactant aggregates. *J Mol Evol* **6**, 215–232 (1975).

20. Nazaki, Y. & Tanford, C. The solubility of amino acids and two glycine peptides in aqueous ethanol and dioxane solutions. *J Biol Chem* (1971).
21. Yunger, L. M. & Cramer, R. D. Measurement and Correlation of Partition Coefficients of Polar Amino Acids. *Mol Pharmacol* **20**, 602–608 (1981).
22. Fauchere, J. L. & Pliska, V. Hydrophobic parameters  $\pi$  of amino-acid side chains from the partitioning of N-acetyl-amino-acid amides. *Eur J Med Chem* (1983).
23. Lawson, E. Q. *et al.* A simple experimental model for hydrophobic interactions in proteins. *J. Biol. Chem.* **259**, 2910–2912 (1984).
24. Bull, H. B. & Breese, K. Surface tension of amino acid solutions: A hydrophobicity scale of the amino acid residues. *Archives Of Biochemistry and Biophysics* **161**, 665–670 (1974).
25. Kyte, J. & Doolittle, R. F. A simple method for displaying the hydropathic character of a protein. *Journal of Molecular Biology* (1982).
26. Bigelow, C. C. On the average hydrophobicity of proteins and the relation between it and protein structure. *Journal of Theoretical Biology* **16**, 187–211 (1967).
27. Hunter, C. A., Lawson, K. R., Perkins, J. & Urch, C. J. Aromatic interactions. *J. Chem. Soc., Perkin Trans. 2* 651–669 (2001). doi:10.1039/b008495f
28. Waters, M. L. Aromatic interactions in model systems. *Current Opinion in Chemical Biology* **6**, 736–741 (2002).
29. Makhatasze, G. I. & Privalov, P. L. Energetics of interactions of aromatic hydrocarbons with water. *Biophysical Chemistry* **50**, 285–291 (1994).
30. Burley, S. K. & Petsko, G. A. Amino-aromatic interactions in proteins. *Federation of European Biochemical Sciences* **203**, 139–143 (1986).
31. Pereira de Araujo, A. F., Pochapsky, T. C. & Joughin, B. Thermodynamics of Interactions between Amino Acid Side Chains: Experimental Differentiation of Aromatic-Aromatic, Aromatic-Aliphatic, and Aliphatic-Aliphatic Side-Chain Interactions in Water. *Biophysical Journal* **76**, 2319–2328 (1999).
32. Gervasio, F. L., Chelli, R., Procacci, P. & Schettino, V. The nature of intermolecular interactions between aromatic amino acid residues. *Proteins* **48**, 117–125 (2002).
33. Hunter, C. A. Meldola lecture. The role of aromatic interactions in molecular recognition. *Chemical Society Reviews* (1994).
34. Newcomb, L. F. & Gellman, S. H. Aromatic Stacking Interactions in Aqueous Solution: Evidence That Neither Classical Hydrophobic Effects nor Dispersion Forces Are Important. *J. Am. Chem. Soc.* 4993–4994 (1994).
35. Ma, J. C. & Dougherty, D. A. The Cation– $\pi$  Interaction. *Chem. Rev.* **97**, 1303–1324 (1997).
36. Shepodd, T. J. & Petti, M. A. *Molecular recognition in aqueous media: donor-acceptor and ion-dipole interactions produce tight binding for highly soluble guests.* (Journal of the American ..., 1988).
37. Hunter, C. A. & Sanders, J. K. M. The Nature of  $\pi$ - $\pi$  Interactions. *J. Am. Chem. Soc.* **112**, 5525–5534 (1990).
38. Hunter, C. A., Singh, J. & Thornton, J. M.  $\pi$ - $\pi$ : Interactions: the Geometry and Energetics of Phenylalanine-Phenylalanine Interactions in Proteins. *J. Mol. Biol* **218**, 837–846 (1991).
39. McGaughey, G. B., Gagné, M. & Rappé, A. K.  $\pi$ -Stacking interactions alive and well in proteins. *J. Biol. Chem.* 15458 (1998). doi:10.1074/jbc.273.25.15458



40. Martinez, C. R. & Iverson, B. L. Rethinking the term ‘pi-stacking’. *Chemical Science* **3**, 2191–2201 (2012).
41. Moro, A., Gatti, C. & Delorenzi, N. Hydrophobicity of Whey Protein Concentrates Measured by Fluorescence Quenching and Its Relation with Surface Functional Properties. *J. Agric. Food Chem.* **49**, 4784–4789 (2001).
42. Kato, A. & Nakai, S. Hydrophobicity determined by a fluorescence probe method and its correlation with surface properties of proteins. *Biochimica et Biophysica Acta (BBA) - Protein Structure* **624**, (1980).
43. Sackett, D. L. & Wolff, J. Nile red as a polarity-sensitive fluorescent probe of hydrophobic protein surfaces. *Analytical Biochemistry* **167**, 228–234 (1987).
44. Hawe, A., Sutter, M. & Jiskoot, W. Extrinsic Fluorescent Dyes as Tools for Protein Characterization. *Pharm Res* **25**, 1487–1499 (2008).
45. Greene, F. C. Interactions of anionic and cationic fluorescent probes with proteins: The effect of charge. **3**, 167–180 (1984).
46. Bertsch, M., Mayburd, A. L. & Kassner, R. J. The identification of hydrophobic sites on the surface of proteins using absorption difference spectroscopy of bromophenol blue. *Analytical Biochemistry* **313**, 187–195 (2003).
47. Haskard, C. A. & Li-Chan, E. C. Y. Hydrophobicity of Bovine Serum Albumin and Ovalbumin Determined Using Uncharged (PRODAN) and Anionic (ANS-) Fluorescent Probes. *J. Agric. Food Chem.* **46**, 2671–2677 (1998).
48. Alizadeh-Pasdar, N. & Li-Chan, E. C. Y. Comparison of Protein Surface Hydrophobicity Measured at Various pH Values Using Three Different Fluorescent Probes. *J. Agric. Food Chem.* **48**, 328–334 (2000).
49. Alizadeh-Pasdar, N., Li-Chan, E. C. Y. & Nakai, S. FT-Raman Spectroscopy, Fluorescent Probe, and Solvent Accessibility Study of Egg and Milk Proteins. *J. Agric. Food Chem.* **52**, 5277–5283 (2004).
50. Dorh, N. *et al.* BODIPY-Based Fluorescent Probes for Sensing Protein Surface-Hydrophobicity. *Nature Publishing Group* 1–10 (2015). doi:10.1038/srep18337
51. Fausnaugh, J. L., Kennedy, L. A. & Regnier, F. E. Comparison of hydrophobic-interaction and reversed-phase chromatography of proteins. *Journal of Chromatography A* **317**, 141–155 (1984).
52. Lienqueo, M. E., Mahn, A., Salgado, J. C. & Asenjo, J. A. Current insights on protein behaviour in hydrophobic interaction chromatography. *Journal of Chromatography B* **849**, 53–68 (2007).
53. Queiroz, J. A., Tomaz, C. T. & Cabral, J. M. S. Hydrophobic interaction chromatography of proteins. *Journal of Biotechnology* 143–159 (2001).
54. Szepeszy, L. & Rippel, G. Comparison and evaluation of HIC columns of different hydrophobicity. *Chromatographia* **34**, 391–397 (1992).
55. Fausnaugh, J. L., Pfannkoch, E., Gupta, S. & Regnier, F. E. High-performance hydrophobic interaction chromatography of proteins. *Analytical Biochemistry* **137**, 464–472 (1984).
56. Oscarsson, S. Factors affecting protein interaction at sorbent interfaces. *Journal of Chromatography B* 117–131 (1997).
57. Hjertén, S. Some General Aspects of Hydrophobic Interaction Chromatography. *Journal of Chromatography* **87**, 325–331 (1973).
58. Goheen, S. C. & Gibbins, B. M. Protein losses in ion-exchange and hydrophobic

- interaction high-performance liquid chromatography. *Journal of Chromatography A* **890**, 73–80 (2000).
59. Pochapsky, T. C. & Gopen, Q. A chromatographic approach to the determination of relative free energies of interaction between hydrophobic and amphiphilic amino acid side chains. *Protein Science* 786–795 (1992).
  60. Mahn, A., Lienqueo, M. E. & Asenjo, J. A. Effect of surface hydrophobicity distribution on retention of ribonucleases in hydrophobic interaction chromatography. *Journal of Chromatography A* **1043**, 47–55 (2004).
  61. Lienqueo, M. E., Mahn, A. & Asenjo, J. A. Mathematical correlations for predicting protein retention times in hydrophobic interaction chromatography. *Journal of Chromatography A* **978**, 71–79 (2002).
  62. Shanbhag, V. P. & Axelsson, C.-G. Hydrophobic Interaction Determined by Partition in Aqueous Two-Phase Systems. *Eur. J. Biochem* **60**, 17–22 (1975).
  63. Hachem, F., Andrews, B. A. & Asenjo, J. A. Hydrophobic partitioning of proteins in aqueous two-phase systems. *Enzyme and Microbial Technology* **19**, 507–517 (1996).
  64. Andrews, B. A., Schmidt, A. S. & Asenjo, J. A. Correlation for the partition behavior of proteins in aqueous two-phase systems: Effect of surface hydrophobicity and charge. *Biotechnology and Bioengineering* **90**, 380–390 (2005).
  65. Andrews, B. A. & Asenjo, J. A. Theoretical and Experimental Evaluation of Hydrophobicity of Proteins to Predict their Partitioning Behavior in Aqueous Two Phase Systems: A Review. *Separation Science and Technology* **45**, 2165–2170 (2010).
  66. SHANBHAG, V. P. *Estimation of surface hydrophobicity of proteins by partitioning. Aqueous Two-Phase Systems* **228**, 254–264 (Methods in enzymology, 1993).
  67. Amrhein, S., Bauer, K. C., Galm, L. & Hubbuch, J. Non-invasive high throughput approach for protein hydrophobicity determination based on surface tension. *Biotechnology and Bioengineering* **112**, 2485–2494 (2015).
  68. Chi, E. Y., Krishnan, S., Randolph, T. W. & Carpenter, J. F. Physical Stability of Proteins in Aqueous Solution: Mechanism and Driving Forces in Nonnative Protein Aggregation. *Pharm Res* **20**, 1325–1336 (2003).
  69. Roberts, C. J., Das, T. K. & Sahin, E. Predicting solution aggregation rates for therapeutic proteins: Approaches and challenges. *International Journal of Pharmaceutics* **418**, 318–333 (2011).
  70. The Hydrophobic Effect. 67–84 (1992).
  71. Horbett, T. A. & Brash, J. L. Proteins at interfaces: current issues and future prospects. (1987). doi:10.1021/bk-1987-0343.ch001;page:string:Article/Chapter
  72. Fink, A. L., Calciano, L. J., Goto, Y. & Kurotsu, T. Classification of acid denaturation of proteins: intermediates and unfolded states. *Biochemistry* (1994).
  73. Dockal, M. Conformational Transitions of the Three Recombinant Domains of Human Serum Albumin Depending on pH. *J. Biol. Chem.* **275**, 3042–3050 (2000).
  74. Lu, J. R., Su, T. J. & Howlin, B. J. The Effect of Solution pH on the Structural Conformation of Lysozyme Layers Adsorbed on the Surface of Water. *J. Phys. Chem. B* **103**, 5903–5909 (1999).
  75. Noskov, B. A., Mikhailovskaya, A. A., Lin, S. Y., Loglio, G. & Miller, R. Bovine Serum Albumin Unfolding at the Air/Water Interface as Studied by Dilational

- Surface Rheology. *Langmuir* **26**, 17225–17231 (2010).
76. Zhang, Y. & Cremer, P. S. Chemistry of Hofmeister anions and osmolytes. *Annu. Rev. Phys. Chem.* (2010). doi:10.1146/annurev.physchem.59.032607.093635
  77. Majumdar, R., Manikwar, P., Hickey, J. M. & Samra, H. S. Effects of salts from the Hofmeister series on the conformational stability, aggregation propensity, and local flexibility of an IgG1 monoclonal antibody. *Biochemistry* (2013). doi:10.1021/bi400232p
  78. Collins, K. D. & Washabaugh, M. W. The Hofmeister effect and the behaviour of water at interfaces. *Quarterly Reviews of Biophysics* **18**, 323–422 (1985).
  79. Kamerzell, T. J., Esfandiary, R., Joshi, S. B., Middaugh, C. R. & Volkin, D. B. Protein–excipient interactions: Mechanisms and biophysical characterization applied to protein formulation development. *Advanced Drug Delivery Reviews* **63**, 1118–1159 (2011).
  80. Arakawa, T. & Timasheff, S. N. Preferential interactions of proteins with salts in concentrated solutions. *Biochemistry* (1982).
  81. Arakawa, T. & Timasheff, S. N. Stabilization of protein structure by sugars. *Biochemistry* **21**, 6536–6544 (1982).
  82. Wang, W. Instability, stabilization, and formulation of liquid protein pharmaceuticals. *International Journal of Pharmaceutics* **185**, 129–188 (1999).
  83. Bam, N. B. *et al.* Tween protects recombinant human growth hormone against agitation-induced damage via hydrophobic interactions. *Journal of pharmaceutical sciences* **87**, 1554–1559 (1998).
  84. Fransson, J., Hallen, D. & Florin-Robertsson, E. Solvent Effects on the Solubility and Physical Stability of Human Insulin-Like Growth Factor I. *Pharm Res* **14**, 606–612 (1997).
  85. Sahin, E. *et al.* Aggregation and pH–Temperature Phase Behavior for Aggregates of an IgG2 Antibody. *Journal of pharmaceutical sciences* **101**, 1678–1687 (2012).
  86. Privalov, P. L., Tiktopulo, E. I. & Venyaminov, S. Y. Heat capacity and conformation of proteins in the denatured state. *Journal of molecular ...* **205**, 737–750 (1989).
  87. Golub, N. *et al.* Evidence for the formation of start aggregates as an initial stage of protein aggregation. *FEBS Letters* **581**, 4223–4227 (2007).
  88. Jaenicke, R. *et al.* Protein Structure and Function at Low Temperatures [and Discussion]. *Philosophical Transactions of the Royal Society of London B: Biological Sciences* **326**, (1990).
  89. Kiese, S., Pappenger, A., Friess, W. & Mahler, H.-C. Shaken, Not Stirred: Mechanical Stress Testing of an IgG1 Antibody. *Journal of pharmaceutical sciences* **97**, 4347–4366 (2008).
  90. Eppler, A., Weigandt, M., Hanefeld, A. & Bunjes, H. Relevant shaking stress conditions for antibody preformulation development. *European Journal of Pharmaceutics and Biopharmaceutics* **74**, 139–147 (2010).
  91. Maa, Y. F. & Hsu, C. C. Effect of high shear on proteins. *Biotechnology and Bioengineering* (1996).
  92. Shieh, I. C. & Patel, A. R. Predicting the Agitation-Induced Aggregation of Monoclonal Antibodies Using Surface Tensiometry. *Mol. Pharmaceutics* **12**, 3184–3193 (2015).

93. Shire, S. J., Shahrokh, Z. & Liu, J. Challenges in the development of high protein concentration formulations. *journal of pharmaceutical sciences* **93**, 1390–1402 (2004).
94. Jones, S. & Thornton, J. M. Principles of protein-protein interactions. *PNAS* **93**, 13–20 (1996).
95. Chari, R., Jerath, K., Badkar, A. V. & Kalonia, D. S. Long- and Short-Range Electrostatic Interactions Affect the Rheology of Highly Concentrated Antibody Solutions. *Pharm Res* **26**, 2607–2618 (2009).
96. Kumar, V., Dixit, N., Zhou, L. L. & Fraunhofer, W. Impact of short range hydrophobic interactions and long range electrostatic forces on the aggregation kinetics of a monoclonal antibody and a dual-variable domain immunoglobulin at low and high concentrations. *International Journal of Pharmaceutics* **421**, 82–93 (2011).
97. Esfandiary, R. *et al.* A systematic multitechnique approach for detection and characterization of reversible self-association during formulation development of therapeutic antibodies. *journal of pharmaceutical sciences* **102**, 3089–3099 (2013).
98. Gokarn, Y. R. *et al.* Ion-specific modulation of protein interactions: Anion-induced, reversible oligomerization of a fusion protein. *Protein Science* NA–NA (2008). doi:10.1002/pro.20
99. Jones, S. & Thornton, J. M. Protein-protein interactions: a review of protein dimer structures. *Progress in biophysics and molecular biology* **63**, 31–65 (1995).
100. Thornton, J. M. & Jones, S. Review Principles of protein-protein interactions. *PNAS* **93**, 13–20 (1996).
101. Du, W. & Klibanov, A. M. Hydrophobic salts markedly diminish viscosity of concentrated protein solutions. *Biotechnology and Bioengineering* **108**, 632–636 (2010).
102. Le Brun, V., Friess, W., Bassarab, S. & Garidel, P. Correlation of protein-protein interactions as assessed by affinity chromatography with colloidal protein stability: A case study with lysozyme. *Pharmaceutical Development and Technology* **00**, 090925060905063–10 (2009).
103. Chennamsetty, N., Voynov, V., Kayser, V., Helk, B. & Trout, B. L. Design of therapeutic proteins with enhanced stability. *PNAS* **106**, 11937–11942 (2009).
104. Chennamsetty, N., Helk, B., Voynov, V., Kayser, V. & Trout, B. L. Aggregation-Prone Motifs in Human Immunoglobulin G. *Journal of Molecular Biology* **391**, 404–413 (2009).
105. Chennamsetty, N., Voynov, V., Kayser, V., Helk, B. & Trout, B. L. Prediction of Aggregation Prone Regions of Therapeutic Proteins. *J. Phys. Chem. B* **114**, 6614–6624 (2010).

## 9. Figures

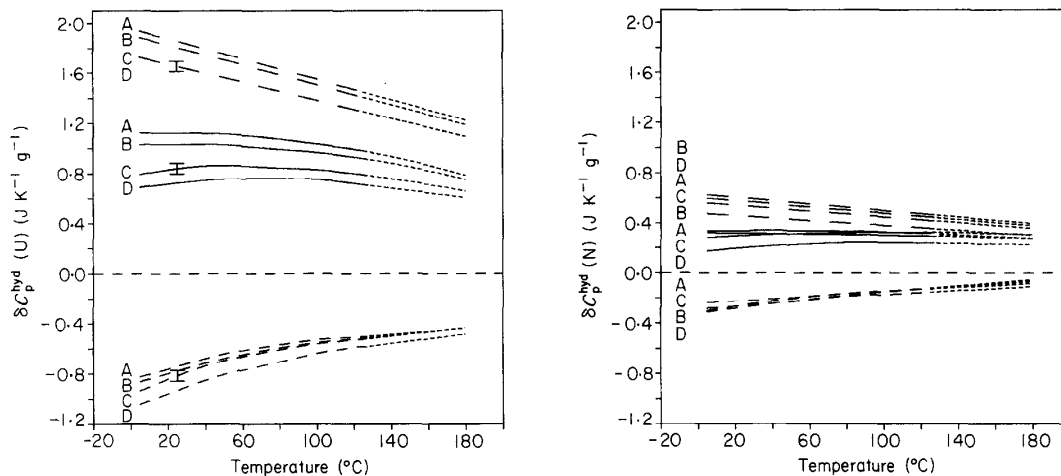


**Figure 1:** Specific heat capacity effects of hydration of the unfolded polypeptide chains (left) and native proteins (right). The continuous line; total hydration effect, long broken line; the hydration effect of nonpolar groups, broken line; the hydration effect of polar groups, short broken line; the extrapolation. A: unfolded/native apo myoglobin; B: unfolded/native apo cytochrome c; C: unfolded/native lysozyme; D: unfolded/native ribonuclease A taken from Privalov and Makhatze.<sup>17</sup>

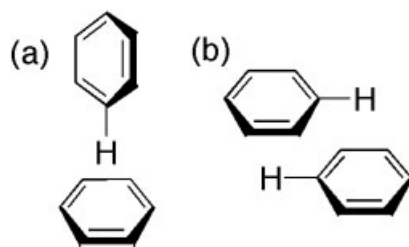


**Figure 2:** Geometries of aromatic interactions taken from Waters et al. where (a) edge-face; (b) offset stacked. <sup>105</sup>

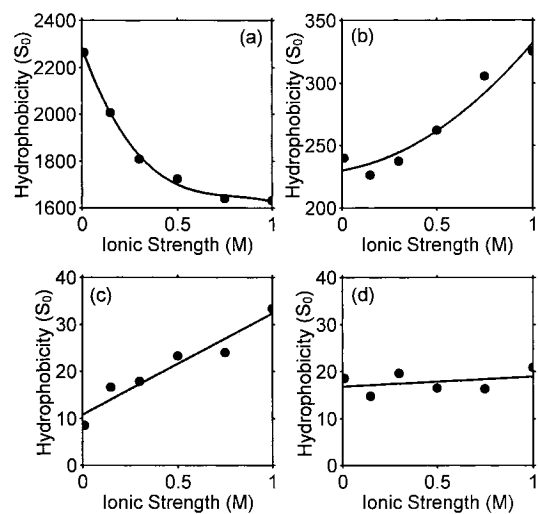


**Figure 3:** Protein surface hydrophobicity ( $S_0$ ) variation with ionic strength (0.01 - 1.0 M) taken from Haskard and Chan.<sup>47</sup> (a) BSA hydrophobicity measured with ANS; (b) BSA hydrophobicity measure with PRODAN (c) OVA hydrophobicity measured with ANS; (d) OVA hydrophobicity measured with PRODAN

## **Chapter 3**

### **NMR as a Semi-Quantitative Tool for Evaluating Protein Surface Hydrophobicity**



## **Contents**

### **Chapter 3**

1. Abstract and Keywords
2. Introduction
3. Materials and Methods
  - 3.1. Materials
  - 3.2. Methods
    - 3.2.1. Extrinsic Fluorescence Spectroscopy
    - 3.2.2. Hydrophobic Interaction Chromatography
    - 3.2.3. Sample Preparation for NMR
    - 3.2.4. Measuring Transverse Relaxation Time
4. Results and Discussion
  - 4.1. Investigation of Hydrophobicity by Fluorescence and Hydrophobic Interaction Chromatography
  - 4.2. Optimization and Applicability of NMR for Evaluating Surface Hydrophobicity
    - 4.2.1. Aliphatic vs. Aromatic Capped Probes
    - 4.2.2. Aliphatic vs. Aromatic Capped Amino Acids
  - 4.3. Comparison of Fluorescence, HIC, and NMR
5. Conclusion
6. References
7. Figures and Tables

## 1. Abstract

Nuclear Magnetic Resonance spectroscopy was used to evaluate the surface hydrophobicity of three proteins, Bovine Serum Albumin,  $\alpha$ -chymotrypsinogen A and  $\beta$ -lactoglobulin A. The surface hydrophobicity was investigated by studying the binding of small molecular probes, which were selected based on their aliphatic or aromatic moieties, to the protein of interest. The binding of the probe was quantified through its transverse relaxation time,  $T_2$ , where a significant decrease in the transverse relaxation time indicated a more pronounced hydrophobic interaction between probe and protein. For all proteins, phenol, an aromatic alcohol, acted as the most promising probe and showed that BSA is the most hydrophobic of proteins studied. The comparison between A-ChytA and B-LgA was inconclusive due the uncovered instability of A-ChytA in solution. Both HIC and fluorescence spectroscopy were in agreement with the NMR results. For HIC experiments, two columns were used to further assess the difference in aromatic and aliphatic interactions. From these results we concluded that the binding to an aromatic phenyl column was more pronounced for all proteins.

**Key Words:** Hydrophobicity; NMR Spectroscopy; Proteins; BSA.

## 2. Introduction <sup>1</sup>

Hydrophobic interactions define key protein properties, including stability, structure, and functionality.<sup>1,2</sup> Therefore, characterizing the hydrophobicity of a protein would be essential for understanding its behavior. There are two common ways to characterize hydrophobicity in a protein molecule. The **net hydrophobicity** accounts for all nonpolar side chains present, whereas the **surface hydrophobicity** deals only with solvent exposed nonpolar side chains.<sup>3,4</sup> The surface hydrophobicity is responsible for the overall stabilization of the protein's native structure and is a major contributor to physical instabilities, such as protein self-association, aggregation and adsorption to interfaces.<sup>5-7</sup>

Different experimental techniques have been used for measuring surface hydrophobicity. Hydrophobic Interaction Chromatography (HIC) is a purification method which provides high resolution and relatively mild solution conditions when compared to other chromatographic methods including Reverse Phase Chromatography.<sup>8-10</sup> Therefore, HIC has been successfully used to compare the surface hydrophobicity of different proteins. In HIC, proteins bind to a stationary phase (column) composed of a nonpolar hydrocarbon chain or phenyl residue. The mobile phase consists of a high concentration salt, such as ammonium sulfate, in order to promote binding between the protein and the weakly nonpolar stationary phase. As the salt concentration decreases, the proteins will elute off the stationary phase in order of their hydrophobicity, where the least hydrophobic protein will elute first. While HIC illustrates that one protein is more hydrophobic than another protein based on different retention times, there are limitations that have to be considered.

---

<sup>1</sup> **Abbreviations:** A-ChytA,  $\alpha$ -chymotrypsinogen; ANS, 8-Anilinonaphthalene-1-sulfonic acid; Bis-ANS, 4,4'-Bis(1-anilinonaphthalene 8-sulfonate); B-LgA,  $\beta$ -lactoglobulin A; BSA, bovine serum albumin; CPMG, Carr-Purcell-Meiboom-Gill; HIC, hydrophobic interaction chromatography; NMR, nuclear magnetic resonance spectroscopy; Prodan, N,N-Dimethyl-6-propionyl-2-naphthylamine.

First, various experimental conditions, such as the type of column, temperature, salt, and ionic strength of the mobile phase, can considerably increase or decrease retention times of proteins, contributing to the difficulty in interpretation and problems with reproducibility of results.<sup>11-16</sup> As a result, comparing protein hydrophobicity necessitates matching experimental conditions. In addition, these proteins are subjected to a very high ionic strength salt buffer, which may screen any potential electrostatic interactions and heighten hydrophobic interactions. As both electrostatic and hydrophobic interactions impact the protein stability, the outcome of the comparison could be misleading if these charges are masked, hydrophobic interactions may become dominant even if in other circumstances they are not. Furthermore, the size of the protein and the hydrophobic heterogeneity will impact the interactions between the column and the protein.<sup>14,17,18</sup> This leads to an untrue representation of the hydrophobic characteristics of the molecule as a whole. These caveats are important to keep in mind considering that solution conditions where these proteins will be formulated and stored are not equivalent to HIC conditions.

The use of extrinsic fluorescence probes, such as ANS, Bis ANS, and Prodan, is another method to assess the hydrophobicity of proteins. These probes have a low quantum yield in an aqueous environment, but once the probe enters a hydrophobic environment the quantum yield increases and there is a shift in the wavelength of maximum fluorescence.<sup>19</sup> Although this technique is fast, simple, and nondestructive, it is not a truly reliable measure of surface hydrophobicity. This is because extrinsic dyes can contain aromatic and/or aliphatic chains. Therefore, the mode of binding of the extrinsic dye to the protein can be different between dyes, which can ultimately affect the hydrophobicity value obtained.<sup>20</sup> Purely aromatic probes may interact through  $\pi$ - $\pi$  interactions with tryptophan or tyrosine residues, whereas those that are

purely aliphatic or those comprising of both aliphatic and aromatic components may bind differently to the protein surface. Along with being structurally distinct, certain probes may also acquire charge in an aqueous solution (i.e. ANS), This can lead to a potential over/under estimation of hydrophobicity due to electrostatic interactions, as charge-charge interactions can both enhance as well as reduce the interactions between dye and protein depending on the pH and ionic strength of the solution.<sup>9,21</sup> The size of these probes can also limit the ability to detect the surface hydrophobicity. If hydrophobic amino acids are only partially exposed or lay within a narrow pocket, only a smaller nonpolar probe, one that isn't affected by solution conditions and is small enough to access these residues would be efficient in exploring this hydrophobic patch.

To conclude both traditional techniques, fluorescence spectroscopy and hydrophobic interaction chromatography, have a number of experimental problems limiting their ability to provide an accurate value of hydrophobicity. Although reproducibility is an important factor, the main problem that needs to be addressed is that the values obtained are only relative numbers, having no real significance to the hydrophobic character of a protein, unless compared to the values measured for another protein. This stresses the importance of establishing a multi-method quantitative measurement protocol to define surface hydrophobicity, which provides sufficient sensitivity to differentiate hydrophobic interactions from aromatic contributions, independent of experimental conditions.

This paper focuses on using Nuclear Magnetic Resonance (NMR) to understand the surface hydrophobicity of proteins. NMR is a sensitive and robust technique that can be used to study the binding between a small molecule (probe) and a larger macromolecule (protein) by observing the transverse relaxation time ( $T_2$ ).<sup>22</sup> Monitoring the relaxation time of the small molecule in the absence and presence of a protein will reflect the degree of interaction, providing useful

information about the hydrophobic surface of the protein. Aromatic or aliphatic small molecules can be used to analyze hydrophobic interactions with the potential to separate the  $\pi$ - $\pi$  effect, the ability that was previously not achieved.

In this study, the sensitivity of NMR to measure surface hydrophobicity was explored by comparing the binding between various probes and three well-known proteins. More traditional HIC and fluorescence data for these three proteins was also obtained and compared with the NMR results. Positive correlation in the relative hydrophobicity measured by different methods was confirmed and substantiated by additional information.

### **3. Materials and Methods**

#### *3.1. Materials*

Bovine Serum Albumin (BSA),  $\alpha$ -Chymotrypsinogen A from Bovine Pancreas (A-ChytA), and  $\beta$ -Lactoglobulin A (B-LgA) from Bovine Milk, N-Acetyl-L-Leucine Methyl Ester and N-Acetyl-L-Phenylalanine Ethyl Ester were purchased from Sigma (St. Louis, Mo). Acetyl-Valine-Methyl Ester was purchased from Bachem Americas Inc., N-Acetyl-L-tryptophan Ethyl Ester was purchased from TCI Chemicals and N-Acetyl-L-Tyrosine Ethyl Ester was purchased from MP Biomedicals, LLC. ANS (8-anilino-1-naphthalenesulfonic acid) was purchased from Molecular Probes. The Hiscreen Butyl HP column and Hiscreen Phenyl HP column was purchased from GE Healthcare. All buffers and protein stock solutions were filtered through 0.22  $\mu$ m filters.

#### *3.2. Methods*

##### *3.2.1. Extrinsic Fluorescence Spectroscopy*

Fluorescence measurements were conducted using Photon Technology International (PTI) TimeMaster<sup>TM</sup> TM-200 LED lifetime strobe spectrofluorometer (Birmingham, New Jersey).

Studies were performed at 25 °C with a slit width of 2 nm and each spectrum was collected 4 times at a scan rate of 2 nm/sec. A 1 mM ANS stock solution was prepared. The stock's concentration was verified prior to the preparation of the final ANS concentration (50  $\mu$ M) for each fluorescence experiment. Concentrations of ANS stock solutions were determined using Solo VPE, using molar absorption coefficient  $\epsilon_{350} = 4.95 \times 10^3 \text{ M}^{-1}\text{cm}^{-1}$ .<sup>23</sup> Stock solutions of BSA, A-ChytA, and B-LgA were prepared with the same buffer and filtered through a 0.22  $\mu$ M filter. The final concentrations of protein were 0.0125 mg/ml, 0.025 mg/ml, 0.05 mg/ml, 0.1 mg/ml, 0.2 mg/ml, 0.3 mg/ml and 0.4 mg/ml (except for BSA, which saturated the signal at this concentration). Samples of protein and ANS were made prior to measurement and stored in a dark place for 15 minutes covered with aluminum foil. Relative fluorescence intensities (RFI) of each solution (including buffer blank and buffer + probe blank) were measured. The RFI of protein blank samples (without ANS) were also prepared for the same concentrations. The net relative fluorescence intensities were obtained by subtracting the protein blanks (without ANS) from the protein samples that contained ANS. Measurements were done in duplicate. A fluorescence emission spectrum was recorded from 400 nm to 650 nm for all proteins and an excitation wavelength of 375 nm was selected. Similarly to what has been put forward by Kato and Nakai, the surface hydrophobicity was determined from the protein concentration vs. fluorescence intensity at 470 nm plot and the initial slope,  $S_0$ , is related to surface hydrophobicity.<sup>3</sup>

### 3.2.2. Hydrophobic Interaction Chromatography

HIC was used with an in-line UV detector at 280 nm. 1.0 mg/ml protein solutions were filtered and prepared in 20 mM ionic strength sodium phosphate buffer (pH  $7.0 \pm 0.05$ ) and were injected into a high salt mobile phase of 20 mM sodium phosphate buffer with 1 M ammonium

sulfate ( $\text{pH } 7.0 \pm 0.05$ ). The pH of both buffers was adjusted with NaOH to maintain a pH of 7.0. The column was equilibrated with 100% 1.0 M ammonium sulfate in sodium phosphate buffer prior to injection until a stable baseline was reached. Three proteins, BSA, B-LgA and A-ChytA, were injected separately into the column with an injection volume of 100  $\mu\text{L}$ . Elution was accomplished by a 30-minute linear gradient from 100% 1.0 M to 0.0 M ammonium sulfate buffer at a flow rate of 0.5 ml/min. At the end of the 30 minutes, the column continued to run in 20 mM sodium phosphate buffer until the protein eluted off the column entirely and the baseline returned. Each sample was filtered with a 0.22  $\mu\text{M}$  filter and injected in triplicates on both the butyl HP and Phenyl HP column.

### 3.2.3. Sample preparation for NMR

Stock Samples were buffer exchanged in a pH 7.0 (Mono and Dibasic sodium phosphate) 15 mM buffer ionic strength (8.5 mM buffer strength). A similar sodium phosphate pH 7.0 buffer was prepared at the same buffer and ionic strength using nitrogen flushed  $\text{D}_2\text{O}$  as the solvent for NMR samples. For probe:protein ratio studies, the small molecular probes were held a constant concentration of 3 mM and the ratios used were 1:20, 1:50, 1:200, 1:400 and 1:1000. These ratios correspond to 150  $\mu\text{M}$ , 60  $\mu\text{M}$ , 30  $\mu\text{M}$ , 20  $\mu\text{M}$ , 15  $\mu\text{M}$ , 7.5  $\mu\text{M}$ , and 3  $\mu\text{M}$  of protein (BSA, A-ChytA, or B-LgA), respectively. A 1:50 ratio was used for a comparative study between probes, which correspond to 1.5 mM probe and 30  $\mu\text{M}$  protein. Concentrations of 1.5 mM, 3 mM or 6 mM for each of the probes alone were also investigated. The use of internal and external references were initially explored, however it was observed that internal references may bind to the protein leading to invalid measurements, while external references complicated the acquisition process due to problems associated with shimming of two different compartments simultaneously. Therefore, the samples did not contain any reference compounds.



Probes were selected based on their structural characteristics. Aliphatic alcohol probes selected were *tert*-butyl alcohol, 1-propanol, and 1-butanol and for aromatic interactions, phenol was chosen. Capped amino acids were also selected as probes to mimic protein-protein interactions. Likewise, the capped amino acids were also chosen based on their aliphatic and aromatic side chains, with the aliphatics being N-acetyl-L-leucine methyl ester, and N-acetyl-L-valine methyl ester, and the aromatics were N-acetyl-L-phenylalanine ethyl ester, N-acetyl-L-tryptophan ethyl ester, and N-acetyl-L-tyrosine ethyl ester.

#### 3.2.4. Measuring Transverse Relaxation Time

$T_2$  measurements were performed on a Varian 600 MHz NMR spectrometer equipped with a triple resonance cryogenic probe. All samples were prepared in a 2.0 mL eppendorf tube, nitrogen flushed and transferred to 535-PP-7 NMR tubes (Wilmad Labglass, Vineland NJ). The water signal was suppressed by presaturation at power level 6 dB for 3 seconds. The experimental temperature was held at 25 °C. Binding between the probes and the proteins was determined by measuring the transverse relaxation time ( $T_2$ ) of the probe. Experiments were performed using the Carr-Purcell-Meiboom-Gill (CPMG)  $T_2$  pulse sequence without temperature compensation.<sup>24</sup> The pulse sequence is shown in figure 1, the acquisition delay (d1-satdly) was set to 22 seconds. This is the time between acquisitions for the nuclear spins to return back to equilibrium. The 90° pulse width (pw) is the amount of time the pulse of energy applied to a sample is applied to flip all spins to the X-Y plane. The 180 ° pulse width is indicated at (p1). This pulse sequence continues to repeat between initial pulse and data acquisition as is suggested by the selected Big Tau parameter. For these experiments, there was a bias towards smaller times values to improve the exponential fit. The bigtau values were different between samples due to variability of the relaxation of the probes and are given in the appendix (A1). Under these

conditions, no sample heating was observed as judged by the lack of temperature-dependent perturbations in chemical shifts. No alterations in peak shifts due to J-coupling<sup>25</sup> was noticed either.

The integral for the probe peak of interest was taken in each spectrum of the array. Errors originating from overlapping peaks were minimized by base-line correction, which involves subtracting a spectrum of the protein alone from the spectrum of the probe with additional correction factors to account for concentration differences. The intensities for the peak of interest were also taken and used to compare exponential fitting parameters (see supporting information). The fit was carried out using the VnmrJ v3.2 T<sub>2</sub> analysis module. The equation used for the fit was:

$$y = m_0 * e^{\left(\frac{-x}{T_2}\right)} + m_1 \quad (1)$$

$m_0$  is a constant that corrects for the scaling factor of the integral and  $m_1$  is a constant that corrects for baseline issues. The T<sub>2</sub> measurements were done in triplicates and the average T<sub>2</sub> was calculated for further analysis.

## 4. Results and Discussion

### 4.1. Investigation of Hydrophobicity by Fluorescence and Hydrophobic Interaction

#### *Chromatography*

We have first established relative hydrophobicity's for the three proteins of choice by employing traditional methods, fluorescence spectroscopy and hydrophobic interaction chromatography. Using the extrinsic fluorescence probe ANS, the surface hydrophobicity ( $S_0$ ) was measured for the three proteins and results are shown in figure 2. The  $S_0$  for BSA was 90-fold higher than the  $S_0$  for B-LgA and ~500-fold higher than the  $S_0$  for A-ChytA. A limitation of

using ANS is that it is negatively charged in solution, signifying that the interaction between the dye and protein is not only due to hydrophobic interactions. The  $S_0$  value measured for BSA at pH 7.0 at a low ionic strength of 15 mM, will give a different value if measured at high ionic strength conditions. As the ionic strength is increased, the charge on ANS will be screened and therefore interact differently with the protein. The charges on the surface of BSA will also be screened as the ionic strength is increased and therefore may produce a different hydrophobic  $S_0$  value. This has been seen in literature when comparing the charged probe ANS to an uncharged probe PRODAN under different ionic strength conditions.<sup>21</sup> The pH of the solution can also affect the local environment of the protein surface and affect interaction with a charge probe. Since the two types of interactions, electrostatic and hydrophobic cannot be separated; the fluorescence data cannot give a reliable quantitative measure of hydrophobicity. Moreover, due to the fact that both the surface and the probe are influenced by solution conditions (i.e. pH, ionic strength etc.), the initial slope method, which produces an estimation of surface hydrophobicity, only tells the hydrophobic character of a protein at particular conditions. Therefore, these values should be used with caution when comparing proteins at different solution conditions and with different extrinsic dyes.

Hydrophobic Interaction Chromatography was also used to determine the surface hydrophobicity of the proteins. A butyl column was used for hydrophobic aliphatic interactions, and separately an aromatic phenyl column was used for  $\pi$ - $\pi$  interactions between the phenyl ring and aromatic residues. A more hydrophobic protein will elute from the column at longer times. Figure 3 shows the results for the three proteins injected separately and as a mixture in two different columns. The order of hydrophobicity is similar for both columns. A-ChytA elutes off the column first, followed by B-LgA and BSA. This indicates that of the three proteins, BSA is

most hydrophobic. Similar behavior was seen with the retention times of BSA and B-LgA using an HIC linear gradient method.<sup>26</sup> All three proteins have multiple peaks, which indicates heterogeneity in the sample based on molecular weight (fragments or aggregates) or different conformational species present in the sample. Multiple peaks can also relate to changes induced by different ammonium sulfate concentrations or the strength of the hydrophobic stationary column.<sup>27</sup> Ueberbacher and coworkers used ATR FTIR to show that at high isocratic concentrations of ammonium sulfate, BSA does change conformation after being bound to the butyl HP column<sup>28</sup>. At a high ammonium sulfate concentration, the change in conformation could promote BSA aggregates, which may have different binding strengths leading to the difference in retention. Ueberbacher also states that partially unfolded proteins have a difficult time eluting off of the column, which may be why we see BSA having very broad peaks on both the phenyl and butyl columns. Though our elution patterns for BSA is not very different between the two columns, BSA may undergo structural changes and/or aggregate, making it difficult to assess the aromatic and aliphatic interactions.

The elution profile for B-LgA is significantly different between the two columns, where the peak is relatively sharper for the phenyl column as well as having a small secondary peak eluting at a later time. This could be due to B-LgA having stronger  $\pi$ - $\pi$  interactions. The least hydrophobic protein, A-ChytA has distinct peaks on both columns, having three peaks on the butyl column, and four peaks on the phenyl column.<sup>29</sup> Multiple peaks present for A-ChytA may indicate numerous conformations at the pH and ionic strength studied as well as aromatic binding between these conformations to the phenyl column. These HIC results pose difficulties when trying to compare relative hydrophobicity's of these three proteins. Comparing the results from the phenyl HIC column, to the fluorescence spectroscopy data, A-ChytA showed the least

amount of binding to ANS even though both ANS and the phenyl column contain aromatic residues. This lack of increase in fluorescence intensity could be due to the lack of hydrophobic accessible binding sites on the protein surface.<sup>30</sup>

These results demonstrate that surface hydrophobicity is an interplay between both aliphatic and aromatic amino acids. It is also clear that because of the difference in solution conditions, which alter the amount of hydrophobic binding between techniques, finding additional information beyond the relative surface hydrophobicity is still a challenging task when using established methods.

#### *4.2. Optimization and Applicability of NMR for Evaluating Surface Hydrophobicity*

Interactions between small molecular weight probes and large proteins can be observed by monitoring changes in the chemical shift and line broadening of the NMR spectrum.<sup>31</sup> However, in practice the line-width is affected by artifacts,  $\vartheta_{actual} = \vartheta_{1/2} + \vartheta_{non-hom}$ . These artifacts are associated with magnetic field non-homogeneity caused by the lack of identical shims for each sample, subsequently causing large errors. To resolve this issue, one can track changes in the probe's relaxation time to minimize magnetic field inhomogeneity.<sup>32-35</sup> The line width is inversely proportional to the transverse relaxation time,  $T_2$  and both parameters are related by the equation,  $\vartheta_{1/2} = \frac{1}{\pi T_2}$ . Large molecules such as macromolecules are characterized by longer correlation times and relax faster in solution than small molecules. Thus, when a small molecular weight probe binds to the protein, the probe relaxation rate increases and the probe will relax faster in solution.<sup>36</sup> The  $T_2$  relaxation is determined by fitting the data points (peak integrals) in time array to equation 1 as demonstrated in Figure 4.

Since peak intensities are more sensitive to a number of factors not particularly related to binding, such as variations in line shapes and possible shifts in resonance frequencies due to

temperature instability,<sup>37</sup> the exponential decay is monitored by peak integration. One drawback with using peak integration is the chance of overlapping peaks, broad protein peaks located underneath the sharp probe peak, thus producing problems with fitting the data. Integration over this region would combine the areas of both, the signal of interest and unwanted peaks, which may cause difficulties with fitting the data to a single exponential function and result in inaccurate  $T_2$  measurements. Therefore, when there is no option to choose other probe peaks where overlapping peaks are not present, protein peak subtraction before fitting is necessary.

Aliphatic and aromatic small molecular probes were chosen to determine the contributions of different nonpolar structures to protein hydrophobicity. Phenol and t-butyl alcohol were the first two small molecules tested for interactions with BSA, A-ChytA and B-IgA and were tested at various ratios (probe to protein). Hydrophobic interactions are weak non-covalent interactions; therefore non-specific interactions between the probe and protein (with  $K_d$ s, dissociation constants, in high mM range) were expected. In order to ensure the measurements were sensitive enough to reflect ligand/receptor kinetics, it was assumed that the equilibrium between the free probe and the probe bound to the protein is in fast exchange.<sup>33</sup> Thus, the peaks observed correspond to a population average of the two states in fast exchange, the free probe in solution ([S]) and the one bound to a target protein ([SP]). The averaged peak would then have a relaxation rate that is weighted summation of the free and bound states as shown in the equation 2 below.

$$\frac{1}{T_{2obs}} = f_b \frac{1}{T_{2b}} + (1 - f_b) \frac{1}{T_{2free}} \quad \text{where} \quad f_b = \frac{[SP]}{[S]_{total}} \quad (2)$$

The  $T_{2obs}$  is the measured relaxation time of the probe with protein in solutions,  $T_{2f}$  is the relaxation time of the probe alone,  $T_{2b}$  is the relaxation time of the probe in its bound state (a constant value equal to the relaxation time of only the protein), and  $f_b$  is the fraction of probe

bound. The  $^1\text{H}$  transverse relaxation times of the proteins were measured and the values used are 0.030 s, 0.020 s, and 0.003 s for B-LgA, A-ChytA and BSA, respectively. Solving equation 2 for  $f_b$  results:

$$f_b = \frac{T_{2b}(T_{2f} - T_{2obs})}{T_{2obs}(T_{2f} - T_{2b})} \quad (3)$$

Multiple binding sites for nonspecific interactions between a small molecule probe and a protein are probable. Therefore, one can assume that there are  $n$  binding sites and that each binding site is equivalent:

$$\frac{[SP]}{[P_o]} = n \left( \frac{[S]}{[S + K_d]} \right) \quad (4)$$

Rearranging equation 4, the model equation can be obtained below.

$$f_b = \alpha - \sqrt{(\alpha^2 - \beta)} \quad (5)$$

where

$$\alpha = \frac{[S]_o + n[P]_o + K_d}{2[S]_o} \quad (6)$$

and

$$\beta = \frac{n[P]_o}{[S]_o} \quad (7)$$

It is possible to fit the equation to obtain  $K_d$  and  $n$  because the concentration of the probe and protein are known. However, this is highly dependent on how it's fit<sup>38</sup> and could lead to unreliable results. Instead, the fraction bound of probe with respect to the concentration of target protein was plotted (Figure 5), where the steepness of the linear fit can be considered as a semi-quantitative measurement of protein hydrophobicity. The greater amount of probe that is bound correlates to a steeper slope. Therefore, it can be concluded that BSA is the most hydrophobic whereas B-LgA is the least hydrophobic based on phenol. *Tert*-butyl alcohol has appreciably less

affinity for BSA than phenol and exhibited no significant interaction with either A-ChytA or B-LgA.

Figure 5 also elucidates the inconsistency of  $T_2$  measurements for A-ChytA, where it could be more or less hydrophobic depending on the sample history preparation. It was found that these inconsistencies are due to the tendency of A-ChytA to degrade/oligomerize over time (see appendix figure for time dependency, A3), which could be potentially related to the autocatalysis from trace impurities of chymotrypsin.<sup>39</sup> It is observed in literature that chymotrypsin is less hydrophobic than its zymogen, A-ChytA.<sup>18</sup> Therefore, further studies are needed to explore differences in  $T_2$  values and time-dependent changes in hydrophobicity of A-ChytA. Although unexpected, variations in the  $T_2$  values determined by NMR can be used as an indicator for changes in sample integrity.

Furthermore, to explore the use of different hydrophobic probes, the interaction between a protein with various probes can be studied at one ratio, rather than performing a more extensive concentration-dependent titration (as presented in Figure 5). When comparing  $T_2$  values at one particular ratio, a sufficient amount of probe bound is necessary in order to have more confidence in the measured differences in the  $T_2$  (and correlated fraction bound values). For this, a ratio of 1:50 (from the titration curves for the phenol and *tert*-butyl) was chosen and the data for various probes are highlighted in Table 1. Instead of showing the absolute  $T_2$  values of the probes, the percent reductions upon binding are presented. Evaluating the interaction between protein and probe this way makes analysis more intuitive: as each probe has its own unique  $T_2$  value, it is difficult to compare the changes between probes looking just at the raw numbers. The greater percent reduction/change indicates a greater degree of interaction between probe and



protein. The different probes tested and the subsequent interactions with each protein are discussed below.

#### 4.2.1. Aliphatic vs. Aromatic Small Probes

Each small molecule was chosen to emphasize the difference in aliphatic and aromatic contribution to hydrophobic interactions. According to Table 1, the interaction between the proteins and the aromatic probes is different compared to the interaction between aliphatic probes and the proteins. When comparing the free probe to BSA-bound, there is a notable drop in the  $T_2$  values for all aliphatic (tert-butyl, butanol, propanol) and aromatic (phenol) probes. However, the decrease (97%) is much more significant for BSA interacting with phenol, rather than BSA interacting with t-butyl alcohol (21% decrease). Although BSA does interact with all aliphatic probes (73% decrease in 1-butanol and 60% 1-propanol), it is the only protein of the three to exhibit any interaction at all with the aliphatic probes. Both A-ChytA and B-IgA observed changes in  $T_2$  measurements within experimental error. However, Phenol is only probe that demonstrates interaction with all three proteins.

#### 4.2.2. Aliphatic vs. Aromatic Capped Amino Acids

One advantage of using certain probes in NMR (as opposed to probes in fluorescence spectroscopy) is for the interaction between protein and probe to be based solely on hydrophobic interactions without an added contribution from electrostatic interactions. Therefore to use amino acids as probes, which are typically charged under physiological conditions, the N and C-terminus were capped to eliminate electrostatic interactions. The results were similar to what was previously seen with small alcohol probes. The aliphatic amino acids, leucine and valine displayed no binding to A-ChytA and B-IgA, while showing a slight interaction in the presence of BSA. Leucine relaxes very fast (0.67 s); therefore the 9% decrease seen after interacting with A-

ChytA (0.61 s) can be attributed to its very fast relaxation behavior and not due to interaction between probe and protein. Although interactions between aliphatic probes and proteins were negligible, a decrease in  $T_2$  for the aromatic amino acid tryptophan was seen with all proteins. Surprisingly tyrosine and phenylalanine did not demonstrate binding to all proteins even though their structure is analogous to phenol.

Since Capped Phe and Tyr did not interact with the proteins as expected, it is hypothesized that the capped C- and N-terminus may likely be responsible. These amino acids are capped on the C-terminus with ethyl esters and N-terminus with an acetyl group; thus they have an increased bulkiness, which may result in steric hindrance. It was also seen that different conformations of capped amino acids are found in solution. Generally, the different conformations of capped amino acids are readily interconverted in solution, so the corresponding peaks in  $^1\text{H}$  NMR spectrum represent an average of the conformations. We have found that capped amino acids have different conformations in slow exchange, leading to two (or, in some cases, even more) distinct conformations of non-equal populations.

The different conformations of Trp alone and bound to the three proteins are shown in figure 6. Trp has only five unique aromatic hydrogens, however the pattern of peaks in the aromatic region is more complex than expected (figure 6A). This is evidence that there are different conformations of capped-Trp in solution. Additionally, the disappearance of particular conformations in protein/probe solutions makes the use of this probe challenging. This is apparent by looking at the left most hydrogen (two doublets) in figure 6A. The left most doublet at 7.54 ppm disappears in the presence of BSA (Figure 6B) and moderately disappears when interacting with B-IgA (6D), but is present with A-ChytA (6C). Similarly, the right doublet at 7.48 ppm disappears with A-ChytA, but remains with BSA and B-IgA.

This characteristic of a probe is very problematic because different conformations complicate the exponential fit as they may have a different binding capability to the protein and therefore can no longer be fit to a single exponential. For example, taking the integral over the range from 7.56 ppm to 7.45 ppm to examine the  $T_2$  of one hydrogen would not be appropriate for analysis as the observed peaks correspond to two or three unique hydrogen's, some of which can entirely disappear either due to the shift in equilibrium between conformations or due to line-broadening beyond detection upon tight binding. Thus,  $T_2$  values defined from these experiments become questionable.

Tryptophan was not the only amino acid that was observed to have different conformations upon binding. Leucine and tyrosine also displayed conformational changes whereas phenylalanine and valine did not. Nevertheless, using these capped amino acids as probes still pose potential problems regarding their size and potential steric clashes. However, further experiments using the different conformations of these amino acids could make interesting observations on the geometry and conformation of how tryptophan interacts with proteins in solution. However for the purpose of these studies, capped amino acids bring unnecessary complications and do not seem suitable molecules for our studies.

#### *4.3. Comparison of Fluorescence, HIC, and NMR*

The present techniques have all been used in an orthogonal approach to characterize the hydrophobicity of three different proteins. While HIC has the potential to distinguish between aliphatic and aromatic interactions, this technique along with fluorescence spectroscopy are both highly influenced by experimental conditions and contributions from additional types of interactions. NMR is the most sensitive to protein stability as highlighted in the case of A-ChytA,

while under the pH and ionic strength conditions are prone to aggregation and could autocatalyze its degradation from chymotrypsin impurities, which led to remarkably different  $T_2$  values.

In pharmaceutical protein formulations, aggregation, precipitation and opalescence are critical issues. However, the role of hydrophobicity in these phenomena is not clear. It is recognized that protein molecules will have a combination of various interactions, some of which can be modulated by pH and ionic strength of the solution. This method serves as an attempt to provide tools to better quantify the hydrophobic effect. The focus of this investigation is to quantitate the hydrophobicity (entropic/dispersion forces etc.) of the protein without any influence of electrostatic or steric influences.

## **5. Conclusions**

Solution NMR is a fast and robust technique that is able to investigate the interaction between small molecular probes and proteins. In our search to define the hydrophobicity of proteins, it was found that there is a difference between the non-specific binding capabilities of aliphatic and aromatic probes. There was a significant drop in  $T_2$  values for phenol in every protein solution tested, whereas there were no signs of binding for any aliphatics tested to A-ChytA or B-LgA. The same observations of the preferable aromatic interactions were found to be the case for capped amino acids, where the aliphatics Leu and Val did not bind to A-ChytA or B-LgA, but Trp, an aromatic, did. Intriguingly though, Phe and Tyr interacted only with BSA, hypothesizing that it was most probably due to the steric clashes with bulky capped ends. Therefore, use of capped amino acids as hydrophobicity probes is not suggested for future studies despite the potential advantage of mimicking protein-protein interactions.

The reliability of the NMR for measuring the surface hydrophobicity was determined by comparing it to two well-known techniques, which were HIC and extrinsic fluorescence spectroscopy. All techniques showed that BSA was the most hydrophobic. Fluorescence data indicated that A-ChytA is the least hydrophobic, whereas NMR and HIC were not conclusive. Though the findings here are promising, there still remain questions that need to be answered. For instance, further studies are needed to better characterize phenol as an optimal binding probe (or possibly find another small aromatic probe), to determine a suitable method for quantification of surface hydrophobicity by NMR, to understand how and when aliphatic probes bind, and how sample integrity relates to the observed differences  $T_2$ . Nonetheless, NMR is a versatile technique with vast potential. It is a sensitive technique for measuring the surface hydrophobicity of proteins, specifically focused on differences between aromatic and aliphatic binding modes. This approach can be further used for protein targets with specific pharmaceutical significance.

## 6. References

1. Kauzmann, W. Some Factors in the Interpretation of Protein Denaturation. **14**, 1–63 (1979).
2. Tanford, C. Contribution of Hydrophobic Interactions to the Stability of the Globular Conformation of Proteins. **84**, 4240–4247 (1962).
3. Kato, A. & Nakai, S. Hydrophobicity determined by a fluorescent probe method and its correlation with surface properties of proteins. *Biochim Biophys Acta, Protein Struct* **624**, 13–20 (1980).
4. Bigelow, C. C. On the average hydrophobicity of proteins and the relation between it and protein structure. *Journal of Theoretical Biology* **16**, 187–211 (1967).
5. Amin, S., Barnett, G. V., Pathak, J. A., Roberts, C. J. & Sarangapani, P. S. Protein aggregation, particle formation, characterization & rheology. *Current Opinion in Colloid & Interface Science* **19**, 438–449 (2014).
6. Wang, W. Instability, stabilization, and formulation of liquid protein pharmaceuticals. *International Journal of Pharmaceutics* **185**, 129–188 (1999).
7. Haynes, C. A. & Norde, W. Globular proteins at solid/liquid interfaces. *Colloids and Surfaces. B, Biointerfaces* **2**, 517–566 (1994).
8. Roettger, B. F. & Ladisch, M. R. Hydrophobic interaction chromatography. *Biotechnology Advances* **7**, 15–29 (1989).
9. Cardamone, M. & Puri, N. K. Spectrofluorimetric assessment of the surface hydrophobicity of proteins. *Biochem. J.* **282**, 589–593 (1992).
10. Rassi, El, Z. Recent progress in reversed-phase and hydrophobic interaction chromatography of carbohydrate species. *Journal of Chromatography A* **720**, 93–118 (1996).
11. Melander, W. & Horváth, C. Salt Effects on Hydrophobic Interactions in Precipitation and Chromatography of Proteins: An Interpretation of the Lyotropic Series'. *Archives Of Biochemistry and Biophysics* 200–215 (1977).
12. Mahn, A., Lienqueo, M. E. & Asenjo, J. A. Optimal operation conditions for protein separation in hydrophobic interaction chromatography. *Journal of Chromatography B* **849**, 236–242 (2007).
13. Queiroz, J. A., Tomaz, C. T. & Cabral, J. M. S. Hydrophobic interaction chromatography of proteins. *Journal of Biotechnology* **87**, 143–159 (2001).
14. Fausnaugh, J. L. & Regnier, F. E. Solute and Mobile Phase Contributions to Retention in Hydrophobic Interaction Chromatography of Proteins. *Journal of Chromatography A* 131–146 (1986).
15. Goheen, S. C. & Gibbins, B. M. Protein losses in ion-exchange and hydrophobic interaction high-performance liquid chromatography. *Journal of Chromatography A* **890**, 73–80 (2000).
16. Rassi, Z. E. & Horváth, C. Hydrophobic Interaction Chromatography of t-RNA's and Proteins. *Journal of Liquid Chromatography* **9**, 3245–3268 (1986).
17. Mahn, A., Lienqueo, M. E. & Asenjo, J. A. Effect of surface hydrophobicity distribution on retention of ribonucleases in hydrophobic interaction chromatography. *Journal of Chromatography A* **1043**, 47–55 (2004).
18. Fausnaugh, J. L., Kennedy, L. A. & Regnier, F. E. Comparison of hydrophobic-

- interaction and reversed-phase chromatography of proteins. *Journal of Chromatography A* **317**, 141–155 (1984).
19. Hawe, A., Sutter, M. & Jiskoot, W. Extrinsic Fluorescent Dyes as Tools for Protein Characterization. *Pharm Res* **25**, 1487–1499 (2008).
  20. Alizadeh-Pasdar, N., Li-Chan, E. C. Y. & Nakai, S. FT-Raman Spectroscopy, Fluorescent Probe, and Solvent Accessibility Study of Egg and Milk Proteins. *J. Agric. Food Chem.* **52**, 5277–5283 (2004).
  21. Haskard, C. A. & Li-Chan, E. C. Y. Hydrophobicity of Bovine Serum Albumin and Ovalbumin Determined Using Uncharged (PRODAN) and Anionic (ANS-) Fluorescent Probes. *J. Agric. Food Chem.* **46**, 2671–2677 (1998).
  22. Pellecchia, M., Sem, D. S. & Wüthrich, K. NMR in drug discovery. *Nature Reviews Drug Discovery* (2002). doi:10.1038/nrd748
  23. Weber, G. & Young, L. B. Fragmentation of Bovine Serum Albumin by Pepsin. *The Journal of Biological Chemistry* **239**, 1415–1423 (1964).
  24. Meiboom, S. & Gill, D. Modified Spin-Echo Method for Measuring Nuclear Relaxation Times. *Rev. Sci. Instrum.* **29**, 688 (1958).
  25. Aguilar, J. A., Nilsson, M., Bodenhausen, G. & Morris, G. A. Spin echo NMR spectra without J modulation. *Chem. Commun.* **48**, 811–813 (2012).
  26. Hachem, F., Andrews, B. A. & Asenjo, J. A. Hydrophobic partitioning of proteins in aqueous two-phase systems. *Enzyme and Microbial Technology* **19**, 507–517 (1996).
  27. Wu, S.-L., Figueroa, A. & Karger, B. L. Protein Conformational Effects in Hydrophobic Interaction Chromatography. *Journal of Chromatography* **371**, 3–27 (1986).
  28. Ueberbacher, R., Haimer, E., Hahn, R. & Jungbauer, A. Hydrophobic interaction chromatography of proteins. *Journal of Chromatography A* **1198-1199**, 154–163 (2008).
  29. Fausnaugh, J. L., Kennedy, L. A. & Regnier, F. E. Comparison of Hydrophobic-Interaction and Reversed Phase Chromatography of Proteins. *Journal of Chromatography* **317**, 141–155 (1984).
  30. Greene, F. C. Interactions of anionic and cationic fluorescent probes with proteins: The effect of charge. *Journa of Protein Chemistry* **3**, 1–14 (1984).
  31. Ross, A., Schlotterbeck, G., Klaus, W. & Senn, H. Automation of NMR measurements and data evaluation for systematically screening interactions of small molecules with target proteins. *J Biomol NMR* **16**, 139–146 (2000).
  32. Hahn, E. L. Spin echoes. *Physical review* (1950).
  33. Lepre, C. A., Moore, J. M. & Peng, J. W. Theory and Applications of NMR-Based Screening in Pharmaceutical Research. *Chem. Rev.* **104**, 3641–3676 (2004).
  34. Fielding, L. NMR methods for the determination of protein–ligand dissociation constants. *Progress in Nuclear Magnetic Resonance Spectroscopy* **51**, 219–242 (2007).
  35. Dubois, B. W. & Evers, A. S. Fluorine-19 NMR spin-spin relaxation (T2) method for characterizing volatile anesthetic binding to proteins. Analysis of isoflurane binding to serum albumin. *Biochemistry* **31**, 7069–7076 (1992).
  36. Fischer, J. J. & Jardetzky, O. Nuclear Magnetic Relaxation Study of Intermolecular Complexes. The Mechanism of Penicillin Binding to Serum Albumin". *J. Am. Chem. Soc.* **87**, 3237–3244 (1965).

37. Viles, J. H. *et al.* Potential bias in NMR relaxation data introduced by peak intensity analysis and curve fitting methods. *J Biomol NMR* **21**, 1–9 (2001).
38. Fielding, L., Rutherford, S. & Fletcher, D. Determination of protein-ligand binding affinity by NMR: observations from serum albumin model systems. *Magn. Reson. Chem.* **43**, 463–470 (2005).
39. Velez, O. D., Kaler, E. W. & Lenhoff, A. M. Protein Interactions in Solution Characterized by Light and Neutron Scattering: Comparison of Lysozyme and Chymotrypsinogen. *Biophysical Journal* **75**, 2682–2697 (1998).



## 7. Figures and Tables

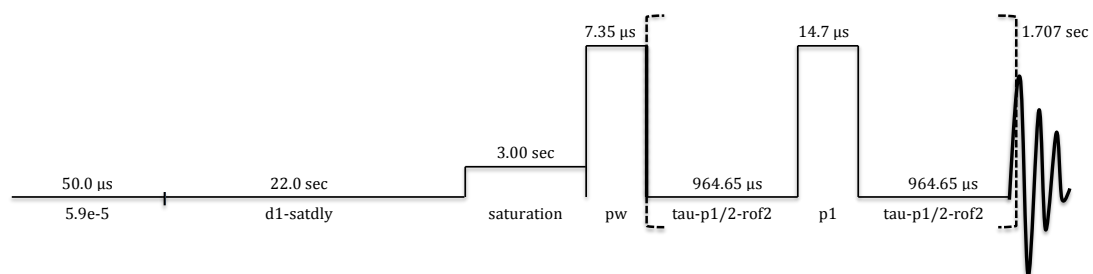
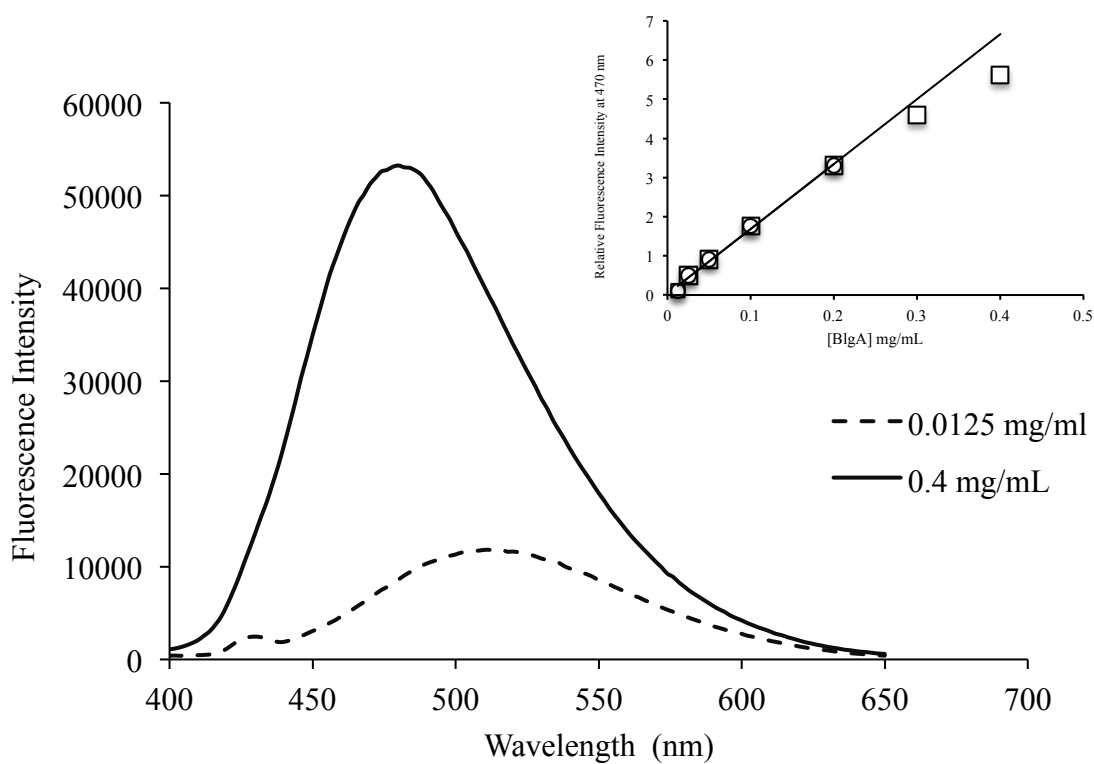


**Figure 1.** CMPG-T<sub>2</sub> pulse sequence for NMR measurements.



Protein	Surface Hydrophobicity ( $S_0$ )
BSA	1355.2
B-LgA	16.6
A-ChytA	2.8

**Figure 2.** Fluorescence Intensity of ANS as a function of B-IgA concentration. Concentrations shown here represent the minimum and maximum concentrations used. Relative fluorescence Intensity (RFI) at 470 nm as a function of B-IgA concentration is shown in the inset. The initial slope of the line is used to represent the surface hydrophobicity. The table shows the initial slopes ( $S_0$ ) of ANS bound to BSA, B-LgA and A-ChytA.

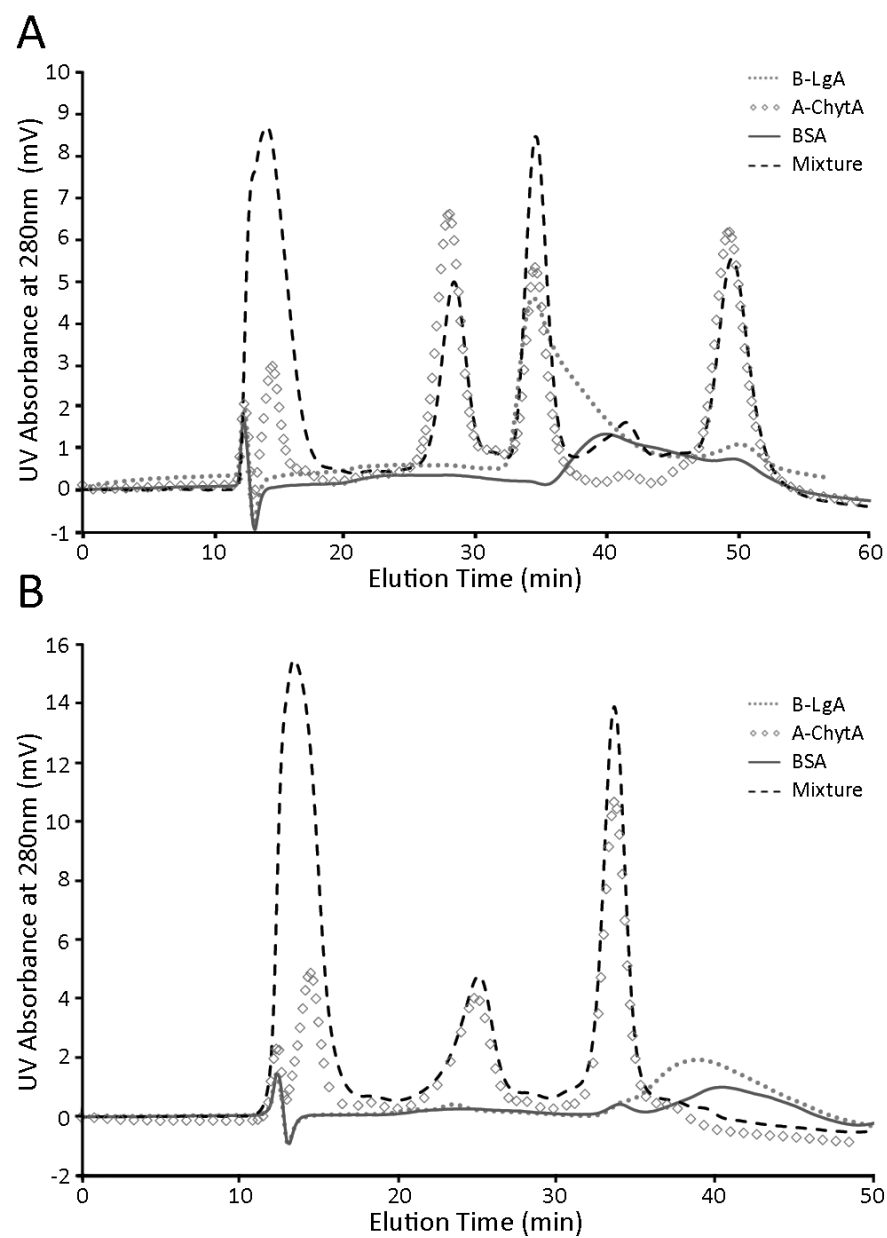


**Figure 3.** The HIC elution profile of BSA, A-ChytA, B-LgA, and Mixture on (a) Phenyl HP (b) Butyl HP column.

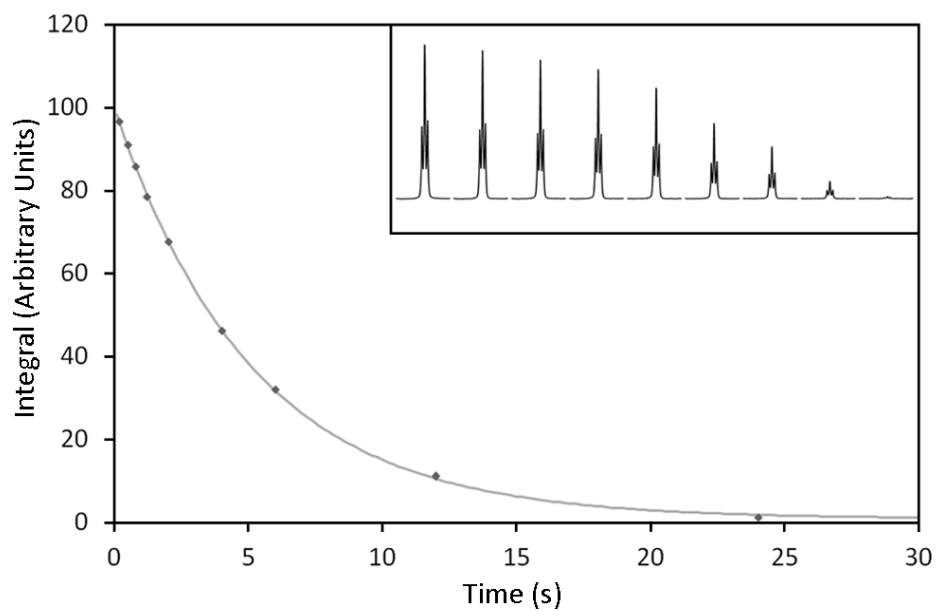


**Figure 4.** A sample exponential decay (of 3 mM phenol) obtained from the CMPG- $T_2$  experiment. The exponential is fit with equation 1. The variables of the fit were  $m_0 = 99.2$ ,  $m_1=0.88$ , and  $t_2=5.147$  s. The inset depicts the peak of interest (triplet at 7.34ppm) at consequent time points in the array.

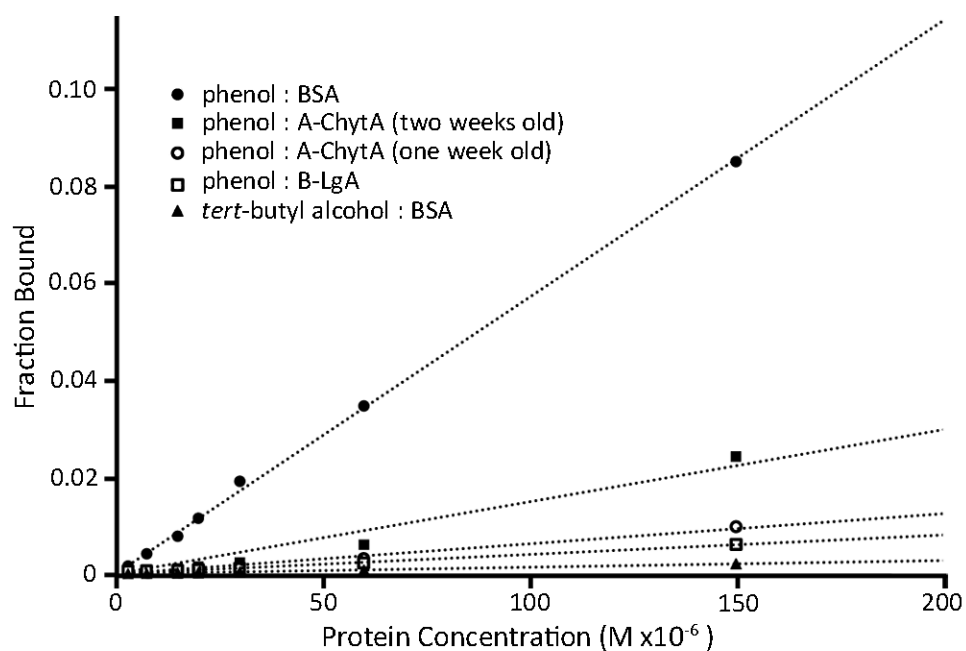


**Figure 5.** Plot showing the fraction bound of probe vs. the concentration of protein. The probe:protein mixtures are labeled and a linear fit of each data set is shown. Two sets of data are shown for phenol:A-ChytA to better represent the variability of  $T_2$ s obtained, which is due to protein degradation/activation at different time points of protein preparation.

**Table 1:** Percent Reduction in T<sub>2</sub> Relaxation Times of the Probes upon Binding to the Proteins.

Protein Probe	BSA	A-ChytA	B-LgA
<i>Tert</i> -butyl alcohol	21	NB	NB
1-butanol	73	NB	NB
1-propanol	60	NB	NB
Phenol	97	11	18
Capped Amino Acids			
Leucine	58	9	NB
Valine	17	NB	NB
Phenylalanine	84	NB	8
Tryptophan	94	21	19
Tyrosine	79	6	NB

The values shown above are the percent change in T<sub>2</sub> when compared to the T<sub>2</sub> of the free probe using the average T<sub>2</sub> value obtained, where percent change =  $100 * (T_{2f} - T_{2obs})/T_{2f}$ . Percent changes of less than 5% were within experimental error and are denoted with NB (no binding).

The ratio for protein:probe is 1:50, where the protein concentration is 0.03 mM and the probe is 1.49 mM. T<sub>2</sub> of the free probes and integration regions are: *tert*-butyl alcohol = 2.32s (1.28-1.18ppm), 1-butanol = 2.69 s (0.86-0.6 ppm), 1-propanol = 3.32 s (0.86-0.6 ppm), phenol = 5.16 s (7.4-7.26 ppm), leucine = 0.67 s (0.84-0.7 ppm), valine = 0.83 s (0.95-0.6 ppm), phenylalanine = 2.04 s (7.28-7.08 ppm), tryptophan = 2.20 s (7.56-7.45 ppm), tyrosine = 1.46 s (7.14-6.86 ppm).

Protein Probe	BSA	A-ChytA	B-LgA
<i>Tert</i> -butyl alcohol	0.21	-0.05	0.004
1-butanol	0.73	-0.02	-0.02
1-propanol	0.60	-0.03	0.02
Phenol	0.97	0.11	0.18
Capped Amino Acids			
Leucine	0.58	0.09	0.00
Valine	0.17	-0.03	-0.03
Phenylalanine	0.84	-0.01	0.08
Tryptophan	0.94	0.21	0.19
Tyrosine	0.79	0.06	-0.03

The values shown above are the fraction change in  $T_2$  when compared to the  $T_2$  of the free probe using the average  $T_2$  value obtained, where fraction change =  $(T_{2f} - T_{2obs})/T_{2f}$ . The ratio for protein:ligand is 1:50, where the protein concentration is 0.029 mM and the ligand is 1.490 mM.  $T_2$  of the free probes and integration regions are: *tert*-butyl alcohol = 2.32 s (1.28-1.18ppm), 1-butanol = 2.69 s (0.86-0.6ppm), 1-propanol = 3.32 s (0.86-0.6ppm), phenol = 5.16 s (7.4-7.26ppm), leucine = 0.67 s (0.84-0.7ppm), valine = 0.83 s (0.95-0.6ppm), phenylalanine = 2.04 s (7.28-7.08ppm), tryptophan = 2.20 s (7.56-7.45ppm), tyrosine = 1.46 s (7.14-6.86ppm).

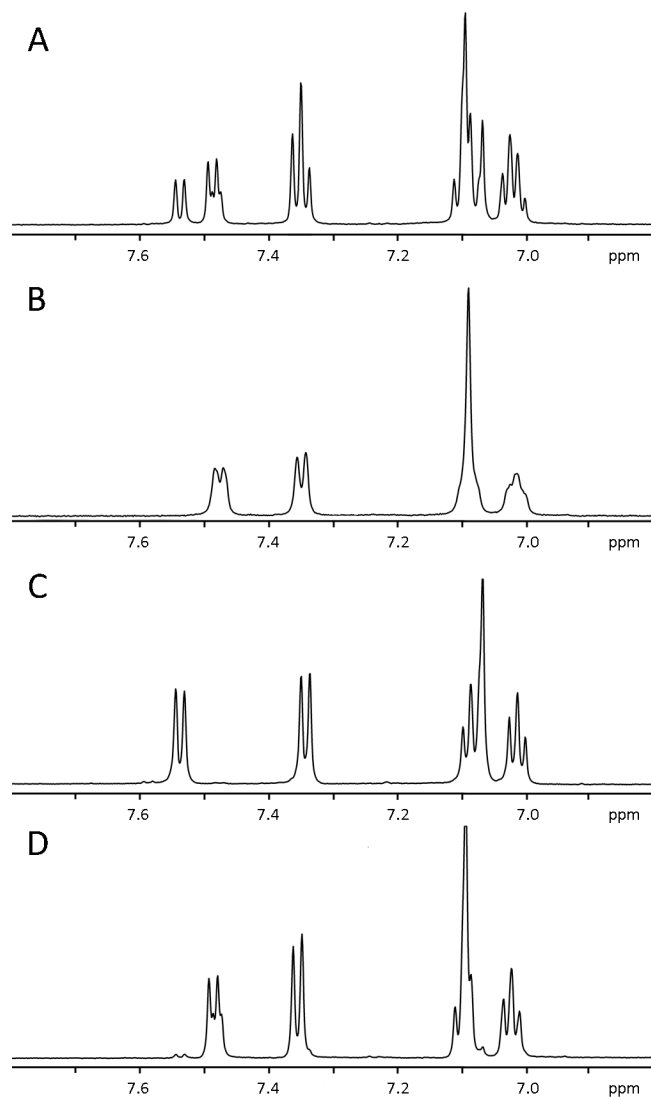


**Figure 6.** Capped-Trp spectra are shown zoomed on the aromatic region. The concentrations of Trp (shown for Trp alone in A) are 3 mM and the ratio of Trp to proteins, (shown for BSA in B, for A-ChytA in C, and for B-LgA in D), is 1:100. Integration areas are: 7.56-7.45ppm = 0.99, 7.4-7.3ppm = 1.02, 7.15-7.06ppm = 2.0, 7.05-6.98ppm = 0.99. This correlates to the five aromatic protons of Trp.



## **Chapter 4**

### **Evaluating the Role of Protein-Surface Interactions in Aggregation of Proteins in Solution**

## **Contents**

### **Chapter 4**

1. Abstract and Keywords
2. Introduction
3. Materials
4. Methods
  - 4.1. Stability Studies of BSA, A-ChytA and B-IgA Solutions at pH 7.0
    - 4.1.1. Mechanical (Shaking) Stress
    - 4.1.2. Monitoring Protein Unfolding
    - 4.1.3. Thermal Denaturation Studies
  - 4.2. Protein-Protein Interactions
  - 4.3. Differential Scanning Calorimetry
  - 4.4. Interfacial Rheology
  - 4.5. Surface Tension Measurements
5. Results
  - 5.1. Protein Unfolding and Aggregation
  - 5.2. Effect of pH on Elasticity at the Surface
  - 5.3. Protein Aggregation after Mechanical Stress
  - 5.4. Protein-Protein interactions
  - 5.5. Temperature Induced Unfolding and Aggregation
6. Discussion
  - 6.1. Unfolding and Mechanical Stress Induced Aggregation

6.2. Rheology Studies

6.3. Temperature Induced Aggregation

6.4. Relationship Between Hydrophobicity and Aggregation

7. Conclusion

8. References

9. Figures and Tables

## 1. Abstract

Three proteins were stressed *via* mechanical stress to determine the extent of aggregation in solution over time. The three proteins, Bovine Serum Albumin,  $\alpha$ -chymotrypsinogen A and  $\beta$ -lactoglobulin A have different surface hydrophobicity's measured previously. However, the hydrophobicity order had no bearing on the effect on aggregation by mechanical stress. After three days of shaking, BSA exhibited no aggregation, whereas A-ChytA and B-IgA displayed aggregates that were to the same extent as solutions that were kept as controls (no stress).

Surface elasticity was also measured for each protein as a function of pH. The elastic modulus did vary, as a function of pH for the three proteins, however did not change or depend on the hydrophobic nature of the proteins or any applied 24-hour stress. Unfolding and aggregation as a function of temperature was determined for BSA by monitoring light scattering and fluorescence spectroscopy simultaneously. Aggregation was observed as the protein began to unfold for BSA, however aggregation was unable to be detected for both A-ChytA and B-IgA.

**Key Words:** Hydrophobicity; Shaking Stress; Bovine Serum Albumin; Protein Unfolding; Fluorescence; Protein Adsorption; Interfacial Rheology

## 2. Introduction

Developing protein therapeutic drugs, especially monoclonal antibodies, to treat chronic illnesses such as cancer and autoimmune diseases continues to be an emerging field in the pharmaceutical industry.<sup>1-4</sup> However the stability of a protein can be compromised at various stages of formulation and development.<sup>5</sup> In order for protein therapeutics to remain safe, stable and efficacious for the entire shelf life of the drug, an understanding of the multiple degradation pathways is essential. One common form of physical degradation is protein aggregation.<sup>6</sup> Aggregates are formed when native, partially unfolded or fully denatured proteins interact in solution to form new species.<sup>7,8</sup> These interactions can be covalent or non-covalent in nature. Non-covalent interactions are comprised of Van der Waals forces (dipole-dipole, dipole-induced dipole, and induced dipole-induced dipole), hydrogen bonding, electrostatic and hydrophobic interactions.<sup>9-12</sup>

Hydrophobic interactions between protein molecules have been suggested as a major pathway leading to aggregation.<sup>8,13-16</sup> Hydrophobic amino acids are mainly present inside the core of the protein molecule away from water, but some are also located on the surface, exposed to the solvent.<sup>17-19</sup> Determining the surface hydrophobic patches on the protein structure that are prone to aggregation has been investigated.<sup>14,16,20,21</sup> However, aggregation is induced at elevated temperatures thus, the protein first unfolds and then aggregates in solution. The surface hydrophobicity of an unfolded protein is different than the surface hydrophobicity of the protein in its native structure. Other methods use the average hydrophobicity determined by the primary amino acid sequence to relate to protein aggregation, however not all of these amino acids are solvent exposed and not all contribute to aggregate formation. Although there are different views

on how to identify hydrophobicity of a protein molecule and relate to aggregation, the issue is still unresolved and continues to remain an area of active research.<sup>22,23</sup>

Aggregation can also be influenced by external stresses such as temperature and mechanical stresses.<sup>24,25</sup> Exposure to elevated temperatures can lead to protein unfolding and cause proteins to favorably interact in solution. Mechanical stress, such as shaking, can occur during manufacturing, shipping and handling of the protein formulation.<sup>26,27</sup> Shaking stresses are known to create air/water interfaces, and subjecting the protein to this type of stress could result in aggregates due to structural changes at the interface.<sup>28-31</sup> It is proposed that a protein will spontaneously diffuse to the interface and will undergo a structural rearrangement where the protein will rearrange to expose the hydrophobic amino acids to the air while exposing the more hydrophilic amino acids to the aqueous solvent.<sup>32-34</sup> These denatured proteins will interact at the interface, aggregate and fall back into the bulk solution, or the denatured protein will fall back into solution and aggregate in the bulk.<sup>30,35</sup> However questions still remain regarding the impact that surface hydrophobicity has on protein aggregation mediated by the air/water interface.

The objective of the present work is to determine whether protein association/aggregation is governed by the surface hydrophobicity or by the propensity of a protein to unfold. To achieve this, mechanical (shaking) stress is applied to model proteins (Bovine Serum Albumin (BSA),  $\alpha$ -Chymotrypsinogen A (A-ChytA) and  $\beta$ -lactoglobulin A (B-IgA) with known hydrophobicity values, while monitoring unfolding and aggregation at different solution conditions. Rheological properties of the proteins are also assessed to understand the behavior of the protein at the air/water interface and the resulting impact on protein aggregation.

### 3. Materials

All buffer reagents and chemicals used were of reagent grade or the highest purity.  $\beta$ -lactoglobulin A (B-IgA), Bovine Serum Albumin (BSA) and  $\alpha$ -Chymotrypsinogen A (A-ChytA) were all purchased from Sigma Aldrich (St. Louis, MO). Triple distilled water was used to prepare all solutions. Solutions of pH 4.0 (acetic acid-sodium acetate), pH 5.0 (acetic acid-sodium acetate), pH 7.0 (mono and dibasic sodium phosphate), pH 9.0 (N,N Bis(2-hydroxyethyl)glycine (Bicine) buffers were prepared to maintain the solution pH. For each buffer, concentrations were selected to maintain the ionic strength at 15 mM without any additional salt. For ionic strength studies, the buffer solution was adjusted to 150 or 300 mM with sodium chloride. Prior to analysis, protein solutions were buffer exchanged to prepare stock solutions using Amicon Centrifuge units (10 kD cutoff) to obtain desired pH. Concentrations were determined using SoloVPE with absorptivity's equal to 0.667, 2.02 and 0.96 mL/(mg\*cm) for BSA, A-ChytA and B-IgA, respectively. These stock solutions were used to prepare solutions for further analysis. For shaking studies, 20R (Schott) Fiolax clear vials (55.0 mm height and 30.0 mm OD) and Stelmi C1404 20 mm bromobutyl stoppers were used.

### 4. Methods

#### *4.1. Stability Studies of BSA, A-ChytA and B-IgA Solutions at pH 7.0*

##### *4.1.1. Mechanical (Shaking) Stress*

Samples of 1 mg/ml were filtered through a 0.22  $\mu$ M syringe and filled in a 20 mL glass vial, with a 5 mL fill. Then they were placed vertical on a New Brunswick Scientific platform shaker plate and rotated at 200 rpm for the specified amount of time. The presence of aggregates during shaking studies was determined using Dynamic Light Scattering measurements using Malvern

Zetasizer Nano series (Worcestershire, UK) at a wavelength of 632.8 nm and a scattering angle of 173°. Monomer peaks were chosen based on size by being less than 12 nm in diameter. In the DLS measurements where there were multiple peaks present, the second and third peaks were designated as aggregate peaks and the diameter was no greater than 1000 nm.

#### 4.1.2. Monitoring Protein Unfolding

The unfolding propensity of BSA and A-ChytA was measured while being stressed for 48 hours by using a Photon Technology International (PTI) TimeMaster™ TM-200 fluorescence spectrofluorometer with a xenon arc lamp. 50 µM of ANS at pH 7.0 (15 mM ionic strength) was added prior to stress of each protein sample. An aliquot from each sample was taken out of both of the stressed and unstressed vials after 6, 18 and 48 hours. Fluorescence measurements were performed at an excitation wavelength of 375 nm. The same samples were then monitored for aggregation using dynamic light scattering.

#### 4.1.3. Thermal Denaturation Studies

Fluorescence measurements were performed on a Photon Technology International (PTI) spectrofluorometer and temperature was controlled within the cuvette cell with a temperature control device from Quantum Northeast (Spokane WA). Protein stock solutions of 10 mg/ml were prepared in a pH 7.0 sodium phosphate buffer with an ionic strength of 15 mM (buffer strength of 8.5 mM) and filtered through a 0.22 µm syringe filter. For proteins A-ChytA and B-IgA, the sample was diluted to 1 mg/ml with excitation and emission slit widths set to 0.5 nm. BSA was diluted to 0.5 mg/ml and the excitation and emission slit widths were set to 0.2 nm. 50 µM ANS was added to the final protein concentration solutions. Heating was increased at 1 °C/min with an equilibration time of 120 seconds once the temperature was reached. Samples were checked periodically for micro air bubbles. For each sample, the protein and ANS were at a



constant concentration. For each scan, the excitation wavelength was set to 375 nm and the emission spectra were collected between 350 nm to 650 nm at a rate of 2 nm/sec for all samples. Four scans were collected for each sample and each protein was analyzed in triplicate.

#### *4.2. Protein-Protein Interactions*

DLS studies were performed on Malvern's Zetasizer Nano Series at a wavelength of 632.8 nm and an angle of 173°. All samples and buffers were filtered through 0.22 microns before measurements. Measurements were performed in duplicate, except for A-ChytA, which were performed in triplicate. Concentrations of proteins range from 2 mg/ml to 10 mg/ml. After each measurement, the sample was checked on Solo VPE for correct concentration. Using Malvern's software, Diffusion coefficients ( $D_m$ ) were obtained from the correlation function. The measured diffusion coefficient is plotted as a function of protein concentration ( $c$ ) in mL/g, and a linear line can provide information to obtain the  $D_s$  (self-diffusion coefficient) and the  $k_D$  (interaction parameter).<sup>36</sup>

$$D_m = D_s(1 + k_D c)$$

The interaction parameter is obtained by the slope/intercept. A positive  $k_D$  indicates repulsive protein-protein interactions, while a negative  $k_D$  represents attractive interactions are dominant in solution.  $k_D$  has both contributions from thermodynamic and hydrodynamic properties.<sup>37</sup>

#### *4.3. Differential Scanning Calorimetry*

DSC experiments were performed on a nano-DSC (TA instruments) to determine  $T_m$  and onset of unfolding for the proteins in a pH 7.0 sodium phosphate buffer at 15 mM, 150 mM and 300 mM ionic strength. 1 mg/ml of each protein sample was filtered through a 0.22  $\mu$ m syringe filter and checked for concentration prior to experiment. Each sample was run at a scan rate of 1°C/min from 25 °C to 90 °C with a pre-scan equilibration time of 600 seconds. The

corresponding buffer was also run at the same conditions for baseline subtraction. The thermal scans were analyzed; baseline subtracted and fitted using the Nano Analyze software.

#### *4.4. Interfacial Rheology*

An AR-G2 rheometer with a Du Nouy ring attachment was used to measure the viscoelastic properties at the air/liquid interface. A platinum/iridium ring was attached to a stress motor with a radius of 10 mm and a thickness of 0.36 mm. The ring was aligned with a Delrin trough, which holds the sample at a temperature of 25 °C regulated by a water bath and Peltier plate. Samples were placed in the trough at a concentration of 1 mg/ml at a constant volume of 9600 µL. The ring was lowered manually each time to make contact with the surface. For each protein, strain sweeps were performed at constant frequency and frequency sweeps were performed at constant strains to obtain information about the linear-viscoelastic region. Once parameters were chosen in the linear regime, time sweeps were performed for all solutions. All samples were measured in duplicate at pH 4.0; at pH 5.0; duplicate measurements were performed for B-IgA and BSA; while four measurements were made for A-ChytA. At pH 7.0; BSA was measured seven times, while B-IgA and A-ChytA were measured four times. At pH 9.0, duplicates measured for A-ChytA.

#### *4.5. Surface Tension Measurements*

Surface tension measurements were performed using a microbalance with a Wilhelmy plate perpendicular to the interface. The protein concentration was 1 mg/ml for each protein and was measured after measurements were taken. Samples were diluted and placed in a petri dish after the Wilhelmy plate was at the correct height for the surface tension reading. Between readings, the Wilhelmy plate was cleaned by flame for several seconds. Within a single measurement, the petri dish was swirled by hand for thirty seconds before a second reading was performed.

To determine the impact of mechanical stress on the samples, surface tension measurements were taken prior to shaking. Following the measurement, samples were placed in a 20 mL glass vial and were shaken at 200 rpm for 20-22 hours. After the stress, the surface tension was measured for a second time. For each sample, a 150- $\mu$ L aliquot was taken to determine concentration and aggregation by dynamic light scattering.

## 5. Results

### 5.1. Protein Unfolding and Aggregation

The unfolding propensity of BSA and A-ChytA while being stressed for 48 hours was monitored by adding 50  $\mu$ M of ANS at pH 7.0 (15 mM ionic strength). An aliquot from each sample was taken out of both of the stressed and unstressed vials at specific time points. Aggregates were measured by dynamic light scattering (figure 1) according to size and then the same samples were analyzed by fluorescence spectroscopy to determine if the protein unfolded during the applied stress (figure 2). It can be seen from figure 1, that after shaking BSA for 42 hours, aggregation is not detected in any of the vials (scattering intensity remained unchanged). However for A-ChytA in the presence of ANS, aggregates were present in both the stressed and unstressed vials. At 48 hours, the vials that were exposed to the stress, aggregated more than those held at room temperature. Figure 2 captures the environment of ANS when exposed to the two proteins, which is determined by the shift in maximum wavelength of fluorescence intensity. A blue shift to lower wavelengths indicates that ANS is in a more nonpolar environment and a red shift to higher wavelength illustrates a more polar environment. It is observed that there is no shift in wavelength for BSA. However, there is a shift in  $\lambda_{Max}$  over time for A-ChytA but it does not differ between stressed and not stressed vials. Further shaking studies are performed and the

results are shown in section 5.3 to determine the effect of solution conditions on protein aggregation during shaking stress.

### *5.2 Effect of pH on elasticity at the Surface*

**Figure 3** shows a time (a), strain (b) and frequency (c) sweeps for 1 mg/ml BSA at pH 5.0 to determine the linear viscoelastic region and parameters to use for further studies. These results are similar to what has been determined previously in literature.<sup>38</sup> Using 0.6% as the strain rate, and 0.1 Hz as the frequency, time sweeps were performed for one hour for each protein at different pH conditions. The time sweeps at different pH conditions for 1 mg/ml BSA solutions, A-ChytA and B-IgA can be found in the Appendix (A4). For all proteins, the linear viscoelastic regions showed a more pronounced elastic response ( $G' > G''$ ). BSA plateaus around 20 minutes, therefore to compare all proteins, the  $G'$  at 50.4 minutes was obtained and plotted in figure 4. Figure 4 illustrates that there is a difference in the  $G'$  (elastic modulus) as a function of pH for each of the proteins. Both B-IgA (pI 5.1) and BSA (pI 4.9) have the highest elasticity at pH 5.0, their isoelectric point. The  $G'$  value is reduced for both proteins as the solution pH is increased to pH 7.0 and decreased to pH 4.0. The behavior for A-ChytA does not follow this pattern: the pI of the protein is ~9.0, but  $G'$  does not change significantly between pH 4.0, 7.0 or 9.0. The only pH that affects the elastic modulus of A-ChytA is pH 5.0. The surface rheology and surface tension were also monitored before and after 24 hours of mechanical stress, however there was no impact on the elastic modulus and surface tension before and after shaking stress (data not shown).

### *5.3 Protein Aggregation after Mechanical Stress*

Dynamic light scattering measurements were performed at different solution conditions to monitor aggregation as a function of time for A-ChytA, BSA and B-IgA. BSA (figure 5) shows no aggregation present in the stressed or unstressed vials for all ionic strengths studied at pH 7.0. It can be seen from figure 6, that A-ChytA aggregated at low ionic strength (15 mM) due to the decrease in monomer scattering intensity, but aggregation is absent at higher ionic strength conditions. For ionic strength conditions 150 mM and 300 mM, there is no aggregation present therefore lines representing 100% monomer scattering intensity overlap. Aggregation is present for A-ChytA at 15 mM after 24 hours and continues to increase as time increases. However, as time increases to 72 hours, there is no difference in the rate of aggregation for either the control non-shaking vial, or the shaking vial at 72 hours. This aggregation behavior is in agreement with what has been observed in literature as a property of this protein.<sup>39</sup> B-IgA aggregation is shown in figure 7. The vials at 15 mM ionic strength show aggregation to a greater extent than the higher ionic strength condition (300 mM) seen by the decrease in monomer scattering intensity. Both BSA and A-ChytA also underwent mechanical stress at pH 5.0 15 mM and 300 mM (data not shown) and it was concluded that both proteins were not influenced by the mechanical stress since aggregation was minimal for both.

### *5.4 Protein-Protein Interactions*

The nature of interactions in dilute solutions was measured by dynamic light scattering, (DLS). DLS measures the diffusion coefficients of a solute, and using this information, the interaction parameter,  $k_D$  can be found. A negative  $k_D$  implies attractive interactions, whereas a positive  $k_D$  indicates repulsive interactions in solution.<sup>37</sup> Figure 8 shows the  $k_D$  values as a function of ionic strength for the three proteins at pH 7.0. At low ionic strength, 15 mM, BSA is

highly repulsive whereas A-ChytA is significantly attractive. As ionic strength is increased to 150 mM and 300 mM, these repulsions and attractions are diminished, and the interactions appear to be net neutral for both proteins. B-IgA is net neutral at pH 7.0 at high and low ionic strength.

### *5.5 Temperature Induced Unfolding and Aggregation*

DSC scans are shown in figure 9 for both BSA and A-ChytA at pH 7.0 as a function of ionic strength. As the ionic strength is increased for both proteins, the unfolding temperatures increase towards higher temperatures indicating the conformational stability of the proteins increase as ionic strength is increased. Therefore it would require more energy to unfold the proteins at higher ionic strengths. Using these temperatures as guides to monitor unfolding and aggregation of the proteins by heat denaturation, figure 10 illustrates aggregation and fluorescence spectroscopy for BSA. The excitation wavelength, 375 nm was used to monitor aggregation due to light scattering occurring at the wavelength of incident light. As the temperature exceeds the melting temperature for BSA, the protein begins to aggregate as seen by the increase in light scattering (closed squares) at 376 nm. The fluorescence intensity of ANS will increase in a non-polar environment and will shift towards lower wavelengths. Therefore, choosing a wavelength in the range of emission wavelengths for ANS, one can monitor the fluorescence intensity. Interaction between ANS and BSA initially shows a shift in the wavelength from  $\lambda_{Max}$  of 500 nm in water to a  $\lambda_{Max}$  of 468 nm in the presence of BSA. However as temperature increases, the intensity at 470 nm decreases (no shift) which is likely due to ANS being quenched by water.

## 6. Discussion

### 6.1 Unfolding and Mechanical Stress Induced Aggregation

After 42 hours of shaking, changes in the  $\lambda_{max}$  were observed for A-ChytA, but not for BSA as seen in figure 2. The unfolding seen by the change in  $\lambda_{max}$  of A-ChytA occurs in both stressed and unstressed vials, however aggregation was more significant in the vials that were stressed. This difference in behavior could suggest that the vials that were shaken with ANS increased the chances for collisions between proteins molecules. Therefore, aggregation would be more significant for vials that were stressed, compared to vials that weren't.

However further shaking studies with only A-ChytA in solution (figure 6) revealed that the protein aggregates to a lesser extent compared to when ANS was in the solution (figure 1). A-ChytA is prone to aggregation even without any stress to the sample. It has been reported in the literature that A-ChytA (at pH 7.0) has a large dipole moment and electrostatic attractions that are diminished at high ionic strength conditions.<sup>39</sup> Therefore, during the shaking studies with ANS (low ionic strength), electrostatic interactions between the charged probe and the protein may have promoted aggregation to a much higher degree than the protein would have aggregated alone. The evidence of electrostatic interactions can also be confirmed by the  $k_D$  values measured at different ionic strengths. The  $k_D$  is negative at low ionic strengths (15 mM) illustrating significant attractive protein-protein interactions. As the ionic strength of the solution is increased to 150 mM and 300 mM, A-ChytA attractions significantly decrease indicating that the attractions are electrostatic in nature. Furthermore, A-ChytA at pH 7.0 possesses a positive charge, whereas ANS is negatively charged in solution. This would suggest, that ANS which is charged in solution, facilitates an increased aggregation propensity for those stressed vials.

Mechanical stress studies were performed for BSA and B-IgA as well to determine aggregation induced by shaking. Stressing all three proteins (including A-ChytA) for 72 hours did not significantly impact aggregation of any of the proteins at any ionic strength. It is worth mentioning that aggregates seen in DLS are biased towards the larger species and do not reflect quantitatively the amount of aggregates present in solution. These results only suggest that aggregates are present, the concentration or percent of aggregate is unknown. The results of the shaking studies suggest that for the proteins studied, a larger energy than that provided by shaking used here is required to observe unfolding and promote aggregation. Protein unfolding may occur at the interface for protein molecules, however in these studies unfolding at the interface did not lead to protein aggregation. For surface hydrophobicity to impact aggregation, the  $k_D$  values for the proteins would have to be attractive in nature, whereas for these proteins the protein-protein interactions are either repulsive or attractive due to electrostatic interactions.

## *6.2. Rheology Studies*

When the solution pH is equal to the isoelectric point (pI) of a protein molecule, the protein exhibits a low net charge.<sup>40</sup> This allows closer contacts between molecules, which would result in a more rigid interface (higher  $G'$ ).<sup>41</sup> Hydrophobic interactions are significant when the charge on the protein is low. However as the pH moves units away from the pI, the net charge on the protein increases. Depending on the nature of the charge and thus the subsequent protein-protein interactions that can occur, the protein elastic modulus can be impacted.<sup>42</sup> Therefore evaluating the surface rheology of these three proteins at different solution conditions can give insight into whether any interactions of proteins are occurring at the interface.

The elastic/storage modulus ( $G'$ ) which measures the rigidity of the molecule at the interface, is at its highest for B-IgA and BSA at pH 5.0, while the isoelectric points for the proteins are 5.1



and 4.9 respectively.<sup>43</sup> Therefore, both proteins have a net neutral charge and thus the hydrophobic interactions are significant and the elasticity at the interface is greatest at this pH. However at conditions where electrostatic interactions are more substantial such as pH 7.0, the  $G'$  for both proteins decrease compared to pH 5.0. These two proteins' elastic modulus is affected by solution pH, and at pH 7.0 when the charge interactions significantly govern protein-protein interactions; hydrophobicity plays a less significant role. However, BSA, which has been shown to have the highest surface hydrophobicity out of molecules studied here, has the smallest  $G'$  value at pH 7.0 of the three proteins. At this pH, BSA is highly repulsive shown by the positive  $k_D$  (+21.28). Due to these repulsions at this pH, the decrease in  $G'$  from pH 5.0 to 7.0 is expected. The elastic properties of BSA are highest at pH 5.0 and decrease further at pH 4.0 and 7.0. A similar decrease is seen when authors Noskov et al study BSA using dilatation shear stress as a function of pH.<sup>44</sup>

The elastic modulus for B-IgA at pH 5.0 ( $pH=pI$ ) is greatest out of the conditions studied, with a value of about 0.13 Pa. It has been observed that B-IgA transitions through various molecular weight species as a function of pH. Between pH 3.7 and 5.1, B-IgA exists as an octamer and dissociates to form dimers below pH 3.7 and above pH 5.1.<sup>45,46</sup> Further decreasing/increasing the pH eventually results in monomer formation. Therefore, for this protein, the octamer formation (gelation propensity) at pH 5.0 contributes to the high  $G'$  exhibited at the interface.<sup>47</sup> The elasticity for A-ChytA does not depend on pH, except for pH 5.0. At this pH, the attractions and repulsions present for A-ChytA are balanced which is supported by previous studies of  $B_{22}$  values as a function of pH.<sup>39</sup> At low ionic strength conditions and at pHs less than 5.25, interactions of  $\alpha$ -Chymotrypsinogen A are highly repulsive and at pHs greater than 5.25 interactions are highly attractive. A-ChytA also has an asymmetric

charge distribution therefore at pH conditions away from pH 5.0, the uneven charge distribution may cause lateral interactions leading to an increase in elasticity.<sup>48</sup>

### 6.3. *Temperature induced aggregation*

Temperatures of the protein samples were increased as light scattering measured aggregation and simultaneously fluorescence spectroscopy monitored protein unfolding. An increase in the extrinsic dye, ANS as well as an accompanied shift in the maximum wavelength towards lower wavelengths would indicate that the dye is in a more nonpolar environment. The dye and protein were excited at 375 nm; therefore monitoring the emission at 375 nm, which represents Raleigh light scattering, would be an indicator of aggregation. The larger the molecule, the more light is scattered. Additionally, fluorescence of ANS was studied. Any observed shift in wavelength and increase/decrease in intensity of ANS would indicate a structural event. However, for these three globular proteins, as temperature is increased, the fluorescence intensity of ANS decreases. Thus, to monitor the unfolding of the protein pre-aggregation or during aggregate formation is challenging. Furthermore as the protein is heated in solution, the scattering intensity for BSA increases well after the melting temperature is reached as seen by DSC. For both A-ChytA and B-IgA, the scattering intensity does not increase as the melting point for the two proteins is reached. This could be due to not enough equilibration time for the proteins to nucleate and aggregate.

### 6.4. *Relationship Between Hydrophobicity and Aggregation*

Protein molecules are amphipathic molecules, having both hydrophilic and hydrophobic amino acids on the surface exposed to the solvent. The spontaneous adsorption of protein molecules to the air/water interface is described by the following equation,<sup>49,50</sup>

$$\Delta G_{ads} = \Delta H_{ads} - T\Delta S_{ads} < 0$$

Where,  $\Delta S_{ads}$ ,  $\Delta H_{ads}$  and  $\Delta G_{ads}$  are the changes in entropy, enthalpy and the free energy upon adsorption, and T is the temperature. The driving force for adsorption to the interface is an increase in entropy resulting from structured water molecules surrounding nonpolar amino acids located on the protein surface. However, depending on the conformational stability of a protein in solution and at the interface, the partially unfolded protein adsorbed to the interface will also result in a gain of entropy for the surrounding water molecules, decreasing the free energy of the system. Renewal of the molecules at the interface through shaking or stirring, can allow these unfolded proteins to diffuse into the bulk creating an unfavorable system. However, in such cases, in order to minimize free energy the unfolded protein will form aggregates in solution.<sup>50</sup>

Surface hydrophobicity measurements were discussed for the three proteins in the previous chapter (chapter 3). In this chapter, studies were carried out to determine if the hydrophobicity results have any bearing on aggregation. If the nonpolar amino acids on the surface were accessible to interact and self-associate in solution, surface hydrophobicity measurements would be reliable. However the conformational stability of the proteins studied here were not altered enough to promote denaturation and aggregation in solution. Solutions conditions can often impact and alter the conformational stability<sup>50</sup> of a protein and therefore the surface hydrophobicity measurements become invalid. In addition, solution conditions are often manipulated for the specific technique and therefore cannot always be a reliable measurement at the intended formulation condition.

## 7. Conclusion

While surface hydrophobicity might be a contributing force to adsorption at the interface, experiments carried out in this chapter could not establish whether surface hydrophobicity facilitates aggregation to a great extent. Of the three proteins, BSA was the most hydrophobic protein based on HIC, Fluorescence and NMR methods (chapter 3). However, BSA showed no sign of aggregation induced by mechanical stress. This is plausible due to the fact, that BSA is very soluble in solution, had repulsive protein-protein interactions at the condition where mechanical stress was applied, and the lowest surface rigidity at the pH measured. For the two proteins that showed signs of aggregation,  $\alpha$ -chymotrypsinogen A and  $\beta$ -lactoglobulin A, the aggregation was present in the sample regardless of the stress. Furthermore, aggregation of A-ChytA and B-IgA was most likely due to other types of interactions (electrostatic interactions in the case of A-ChytA). Surface hydrophobicity is not an absolute measure, and thus cannot be directly related to aggregation. This is partially due to the way hydrophobicity is measured, and the dependence of the measurement validity on solution conditions.

## 8. References

1. Harris, M. Monoclonal antibodies as therapeutic agents for cancer. *The Lancet Oncology* **5**, 292–302 (2004).
2. Stern, M. & Herrmann, R. Overview of monoclonal antibodies in cancer therapy: present and promise. *Critical Reviews in Oncology/Hematology* **54**, 11–29 (2005).
3. Geng, X. *et al.* Research and development of therapeutic mAbs: An analysis based on pipeline projects. *Human Vaccines & Immunotherapeutics* **11**, 2769–2776 (2015).
4. Niwa, R. & Satoh, M. The Current Status and Prospects of Antibody Engineering for Therapeutic Use: Focus on Glycoengineering Technology. *journal of pharmaceutical sciences* **104**, 930–941 (2015).
5. Cromwell, M. E. M., Hilario, E. & Jacobson, F. Protein aggregation and bioprocessing. *The AAPS Journal* **8**, E572–E579 (2006).
6. Shire, S. J., Shahrokh, Z. & Liu, J. Challenges in the development of high protein concentration formulations. *journal of pharmaceutical sciences* **93**, 1390–1402 (2004).
7. Roberts, C. J., Das, T. K. & Sahin, E. Predicting solution aggregation rates for therapeutic proteins: Approaches and challenges. *International Journal of Pharmaceutics* **418**, 318–333 (2011).
8. Chi, E. Y., Krishnan, S., Randolph, T. W. & Carpenter, J. F. Physical Stability of Proteins in Aqueous Solution: Mechanism and Driving Forces in Nonnative Protein Aggregation. *Pharm Res* **20**, 1325–1336 (2003).
9. Chari, R., Jerath, K., Badkar, A. V. & Kalonia, D. S. Long- and Short-Range Electrostatic Interactions Affect the Rheology of Highly Concentrated Antibody Solutions. *Pharm Res* **26**, 2607–2618 (2009).
10. Curtis, R. A., Prausnitz, J. M. & Blanch, H. W. Protein-Protein and Protein-Salt Interactions in Aqueous Protein Solutions Containing Concentrated Electrolytes. **57**, 11–21 (1998).
11. Saluja, A. & Kalonia, D. S. Nature and consequences of protein–protein interactions in high protein concentration solutions. *International Journal of Pharmaceutics* **358**, 1–15 (2008).
12. Manning, M. C., Chou, D. K., Murphy, B. M., Payne, R. W. & Katayama, D. S. Stability of Protein Pharmaceuticals: An Update. *Pharm Res* **27**, 544–575 (2010).
13. Thornton, J. M. & Jones, S. Review Principles of protein-protein interactions. *PNAS* **93**, 13–20 (1996).
14. Chennamsetty, N., Voynov, V., Kayser, V., Helk, B. & Trout, B. L. Prediction of Aggregation Prone Regions of Therapeutic Proteins. *J. Phys. Chem. B* **114**, 6614–6624 (2010).
15. Bothra, A., Bhattacharyya, A., Mukhopadhyay, C., Bhattacharyya, K. & Roy, S. A Fluorescence Spectroscopic and Molecular Dynamics Study of bis-ANS/Protein Interaction. *Journal of Biomolecular Structure and Dynamics* **15**, 959–966 (1998).
16. Chennamsetty, N., Voynov, V., Kayser, V., Helk, B. & Trout, B. L. Design of therapeutic proteins with enhanced stability. *PNAS* **106**, 11937–11942 (2009).
17. Klotz, I. M. Comparison of molecular structures of proteins: helix content; distribution of apolar residues. *Archives Of Biochemistry and Biophysics* **138**, 704–706 (1970).
18. Horsley, D., Herron, J., Hlady, V. & Andrade, J. D. Human and hen lysozyme adsorption:

- a comparative study using total internal reflection fluorescence spectroscopy and molecular graphics. (1987). doi:10.1021/bk-1987-0343;article:article:10.1021/bk-1987-0343.ch019
19. Norde, W. & Haynes, C. A. *Thermodynamics of protein adsorption*. (1996).
  20. Chennamsetty, N., Helk, B., Voynov, V., Kayser, V. & Trout, B. L. Aggregation-Prone Motifs in Human Immunoglobulin G. *Journal of Molecular Biology* **391**, 404–413 (2009).
  21. Agrawal, N. J. *et al.* Aggregation in Protein-Based Biotherapeutics: Computational Studies and Tools to Identify Aggregation-Prone Regions. *journal of pharmaceutical sciences* **100**, 5081–5095 (2011).
  22. Esfandiary, R., Parupudi, A., Casas-Finet, J., Gadre, D. & Sathish, H. Mechanism of Reversible Self-Association of a Monoclonal Antibody: Role of Electrostatic and Hydrophobic Interactions. *journal of pharmaceutical sciences* n/a–n/a (2014). doi:10.1002/jps.24237
  23. Shieh, I. C. & Patel, A. R. Predicting the Agitation-Induced Aggregation of Monoclonal Antibodies Using Surface Tensiometry. *Mol. Pharmaceutics* **12**, 3184–3193 (2015).
  24. Kiese, S., Pappenberg, A., Friess, W. & Mahler, H.-C. Shaken, Not Stirred: Mechanical Stress Testing of an IgG1 Antibody. *journal of pharmaceutical sciences* **97**, 4347–4366 (2008).
  25. Wang, W., Li, N. & Speaker, S. *External Factors Affecting Protein Aggregation. Aggregation of Therapeutic Proteins* **289**, 119–204 (John Wiley & Sons, Inc., 2010).
  26. Shire, S. J. Formulation and manufacturability of biologics. *Current Opinion in Biotechnology* **20**, 708–714 (2009).
  27. Carpenter, J. F., Kendrick, B. S. & Chang, B. S. [16] Inhibition of stress-induced aggregation of protein therapeutics. *Methods in ...* **309**, 236–255 (1999).
  28. Dickinson, E. Adsorbed protein layers at fluid interfaces: interactions, structure and surface rheology. *Colloids and Surfaces. B, Biointerfaces* **15**, 161–176 (1999).
  29. A Bos, M. & van Vliet, T. Interfacial rheological properties of adsorbed protein layers and surfactants: a review. *Advances in Colloid and Interface Science* **91**, 437–471 (2001).
  30. Hensen, A. F., Mitchell, J. R. & Mussellwhite, P. R. The Surface Coagulation of Proteins During Shaking. *Journal of Colloid and Interface Science* **32**, 162 (1970).
  31. Mahler, H.-C., Müller, R., Frieß, W., Delille, A. & Matheus, S. Induction and analysis of aggregates in a liquid IgG1-antibody formulation. *European Journal of Pharmaceutics and Biopharmaceutics* **59**, 407–417 (2005).
  32. Kato, A. & Nakai, S. Hydrophobicity determined by a fluorescent probe method and its correlation with surface properties of proteins. *Biochim Biophys Acta, Protein Struct* **624**, 13–20 (1980).
  33. Brash, J. L. & Horbett, T. A. in *Proteins at Interfaces II* **602**, 1–23 (American Chemical Society, 2009).
  34. Andrade, J. D., Hlady, V., Feng, L. & Tingey, K. Proteins at interfaces: principles, problems, and potential. *Bioprocess Technol* (1996).
  35. Cumper, C. W. N. & Alexander, A. E. The surface chemistry of proteins. *Trans. Faraday Soc.* **46**, 235–19 (1950).
  36. Brown, W. *Dynamic Light Scattering: The method and some applications*. **49**, (Oxford University Press, 1993).
  37. Yadav, S., Shire, S. J. & Kalonia, D. S. Factors Affecting the Viscosity in High Concentration Solutions of Different Monoclonal Antibodies. *journal of pharmaceutical*

- sciences* **99**, 4812–4829 (2010).
38. Mondy, L., Brooks, C., Grillet, A. & Moffat, H. Surface Rheology and Interface Stability. *Biochemistry* (2010).
  39. Velev, O. D., Kaler, E. W. & Lenhoff, A. M. Protein Interactions in Solution Characterized by Light and Neutron Scattering: Comparison of Lysozyme and Chymotrypsinogen. *Biophysical Journal* **75**, 2682–2697 (1998).
  40. Horbett, T. A. & Brash, J. L. Proteins at interfaces: current issues and future prospects. (1987). doi:10.1021/bk-1987-0343.ch001;page:string:Article/Chapter
  41. Benjamins, J. *Static and dynamic properties of proteins adsorbed at liquid interfaces*. (2000).
  42. Pezennec, S. The protein net electric charge determines the surface rheological properties of ovalbumin adsorbed at the air–water interface. *Food Hydrocolloids* **14**, 463–472 (2000).
  43. Graham, D. E. & Phillips, M. C. Proteins at liquid interfaces. *Journal of Colloid and Interface Science* **76**, 240–250 (1979).
  44. Noskov, B. A., Mikhailovskaya, A. A., Lin, S. Y., Loglio, G. & Miller, R. Bovine Serum Albumin Unfolding at the Air/Water Interface as Studied by Dilational Surface Rheology. *Langmuir* **26**, 17225–17231 (2010).
  45. Schwenke, K. D. *Proteins at Liquid Interfaces*.
  46. Wishnia, A. & Pinder, T. W., Jr. *Hydrophobic interactions in proteins. The alkane binding site of  $\beta$ -lactoglobulins A and B*. (Biochemistry, 1966).
  47. la Fuente, de, M. A., Singh, H. & Hemar, Y. Recent advances in the characterisation of heat-induced aggregates and intermediates of whey proteins. *Trends in Food Science Technology* **13**, 262–274 (2002).
  48. Malmsten, M. *Biopolymers at interfaces*. (2003).
  49. Haynes, C. A. & Norde, W. Globular proteins at solid/liquid interfaces. *Colloids and Surfaces. B, Biointerfaces* **2**, 517–566 (1994).
  50. Norde, W. & Hayes, D. B. *Interfacial Phenomena and Bioproducts*. 123–143 (1996).

## 9. Figures and Tables

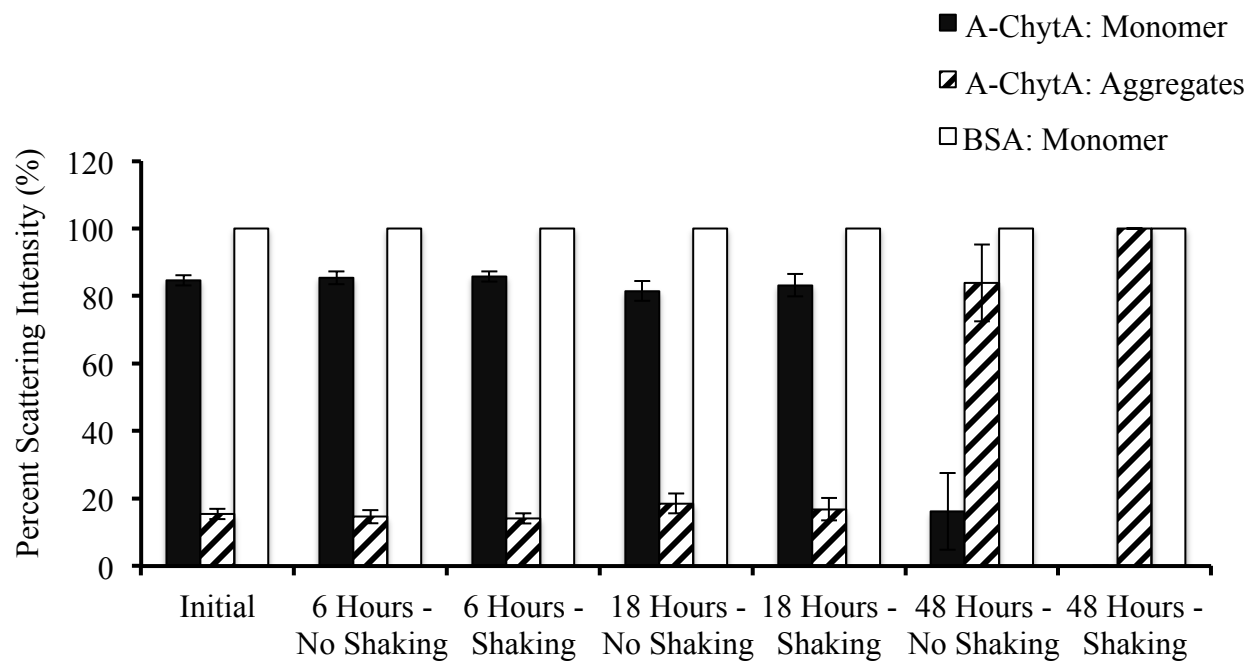


**Figure 1:** Percent Scattering intensity monitoring physical stability of BSA and A-ChytA at pH 7.0 (15 mM) during 48 hours of mechanical stress. Each sample has 50  $\mu$ M of ANS in solution.



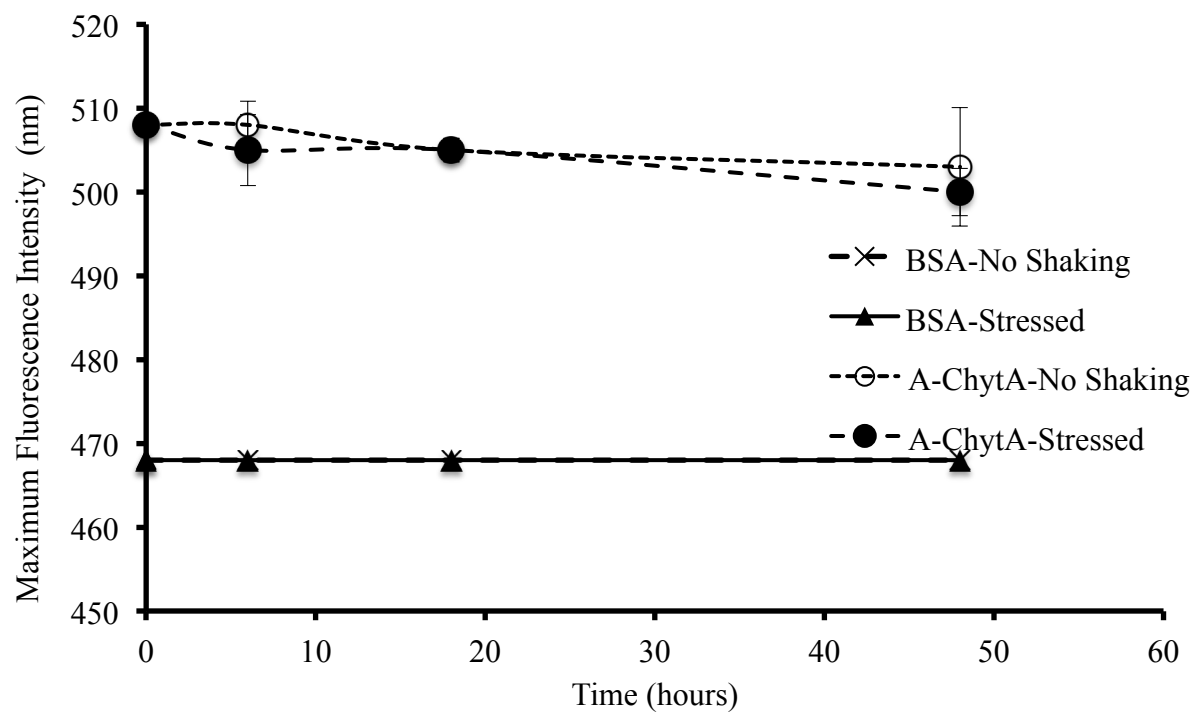
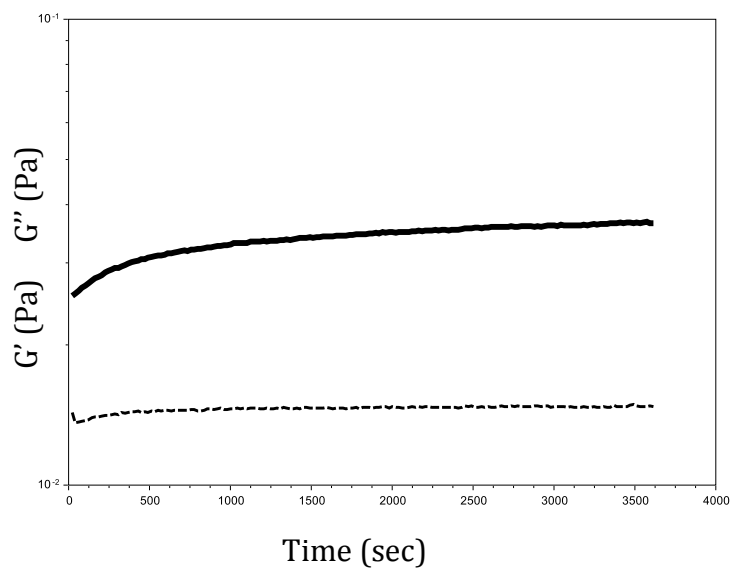
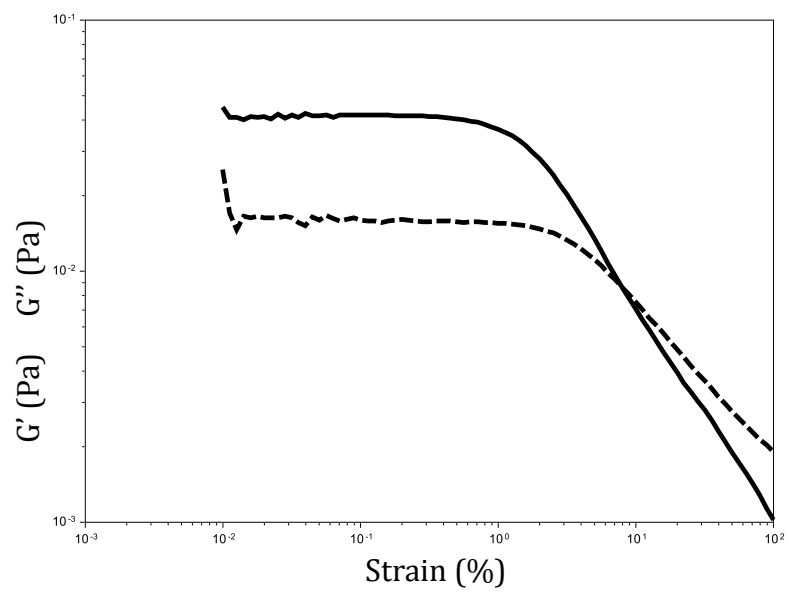


**Figure 2:** Shift in  $\lambda_{max}$  for BSA and A-ChytA at pH 7.0 (15 mM). Aliquots taken for measurement at specific time points from vials undergoing mechanical stress



(a)



(b)

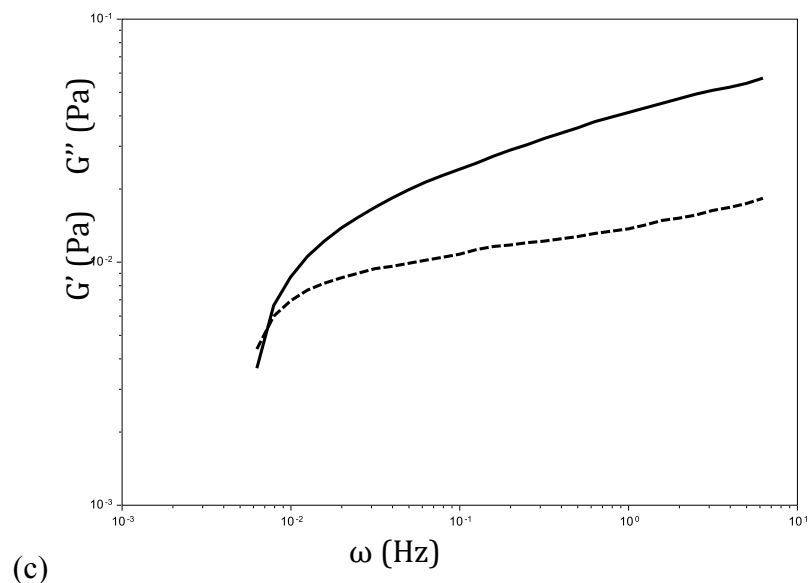


**Figure 3:** Time (a), strain (b) and frequency (c) sweeps of 1 mg/ml BSA at pH 5.0 (15 mM ionic strength) were monitored on a Du Nouy Ring ARG2 rheometer. The parameters  $G'$  (solid line) and  $G''$  (dashed line) are on the y-axis. Time sweeps were performed for 0 to 60 minutes, strain sweeps from 0.01 to 100 % and frequency sweeps from 0.001 to 1 Hz.

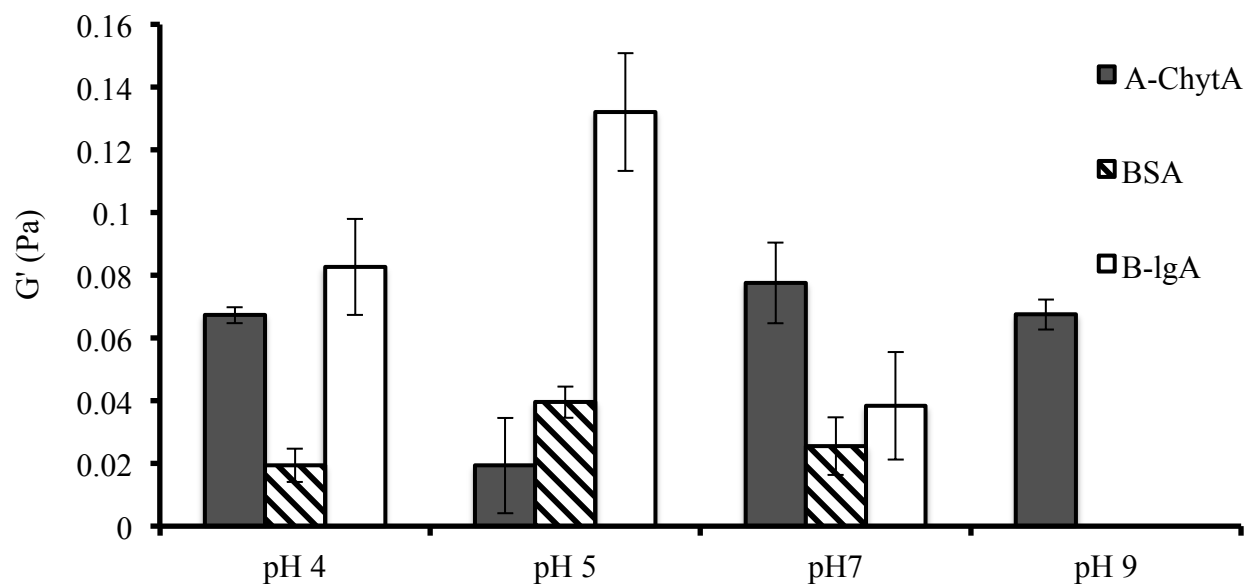


**Figure 4:** Storage modulus of BSA, BlgA and A-ChytA as a function of pH 4.0, 5.0, 7.0 and 9.0.

G' values were taken from the 1 hour time sweep at 50.4 minutes for each protein.

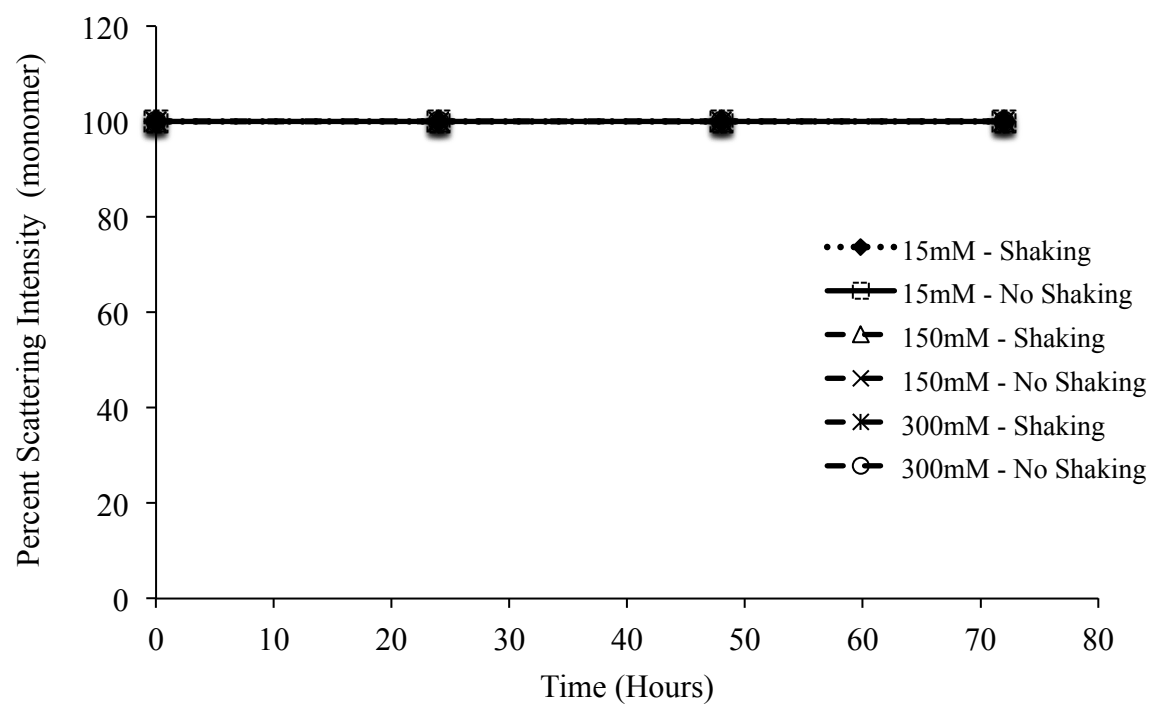


**Figure 5:** Percent scattering intensity monitoring physical stability over 72 hours of mechanical stress for 1 mg/ml BSA. Solutions conditions for both stressed and unstressed vials were pH 7.0 at 15 mM, 150 mM and 300 mM.

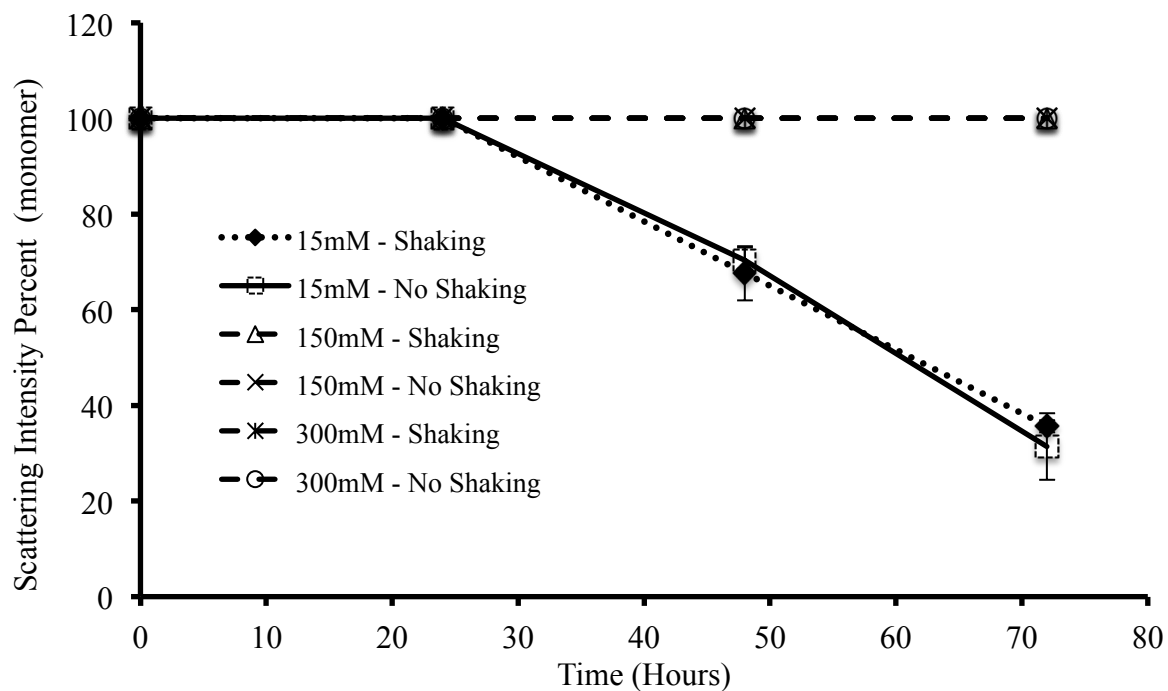


**Figure 6:** Percent scattering intensity monitoring physical stability over 72 hours of mechanical stress for 1 mg/ml A-ChytA. Solutions conditions for both stressed and unstressed vials were pH 7.0 at 15 mM, 150 mM and 300 mM.

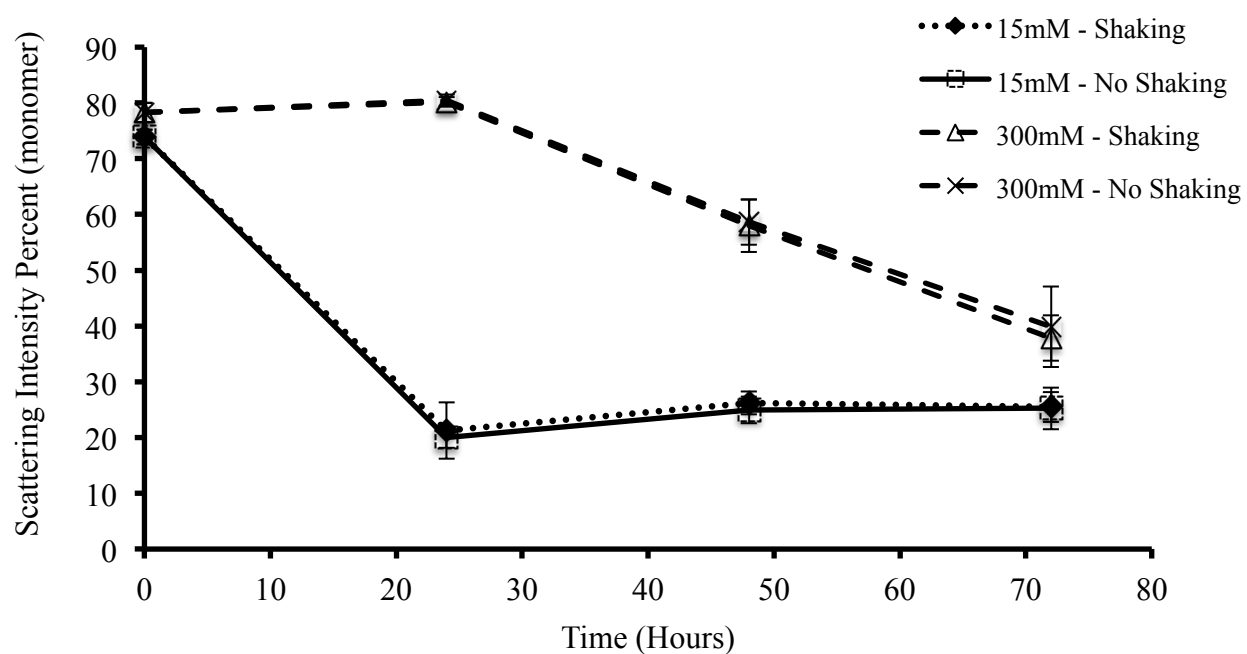


**Figure 7:** Percent scattering intensity monitoring physical stability over 72 hours of mechanical stress for 1 mg/ml B-IgA. Solutions conditions for both stressed and unstressed vials were pH 7.0 at 15 mM and 300 mM.

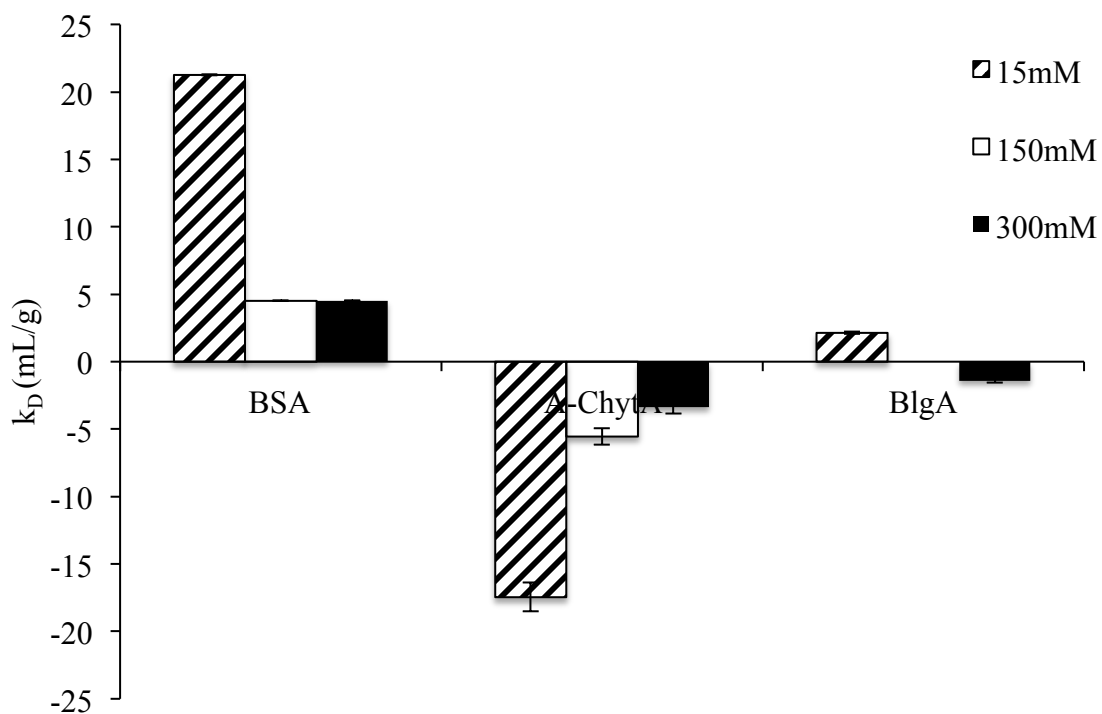
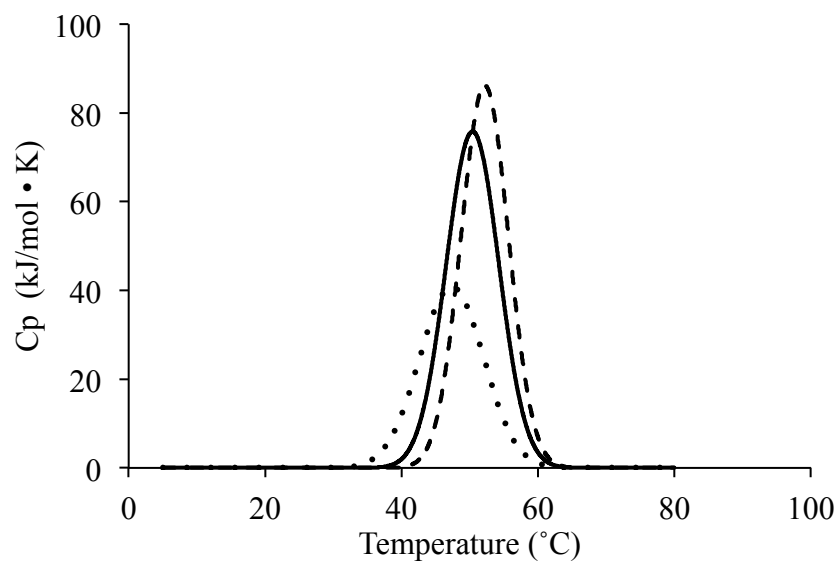


**Figure 8:** Protein-protein interactions illustrated by  $k_D$  of three proteins at pH 7.0 at 15 mM, 150 mM and 300 mM ionic strengths. The error bars for BSA and B-IgA indicate standard error, and for A-ChytA represent standard deviation.



A.



B.

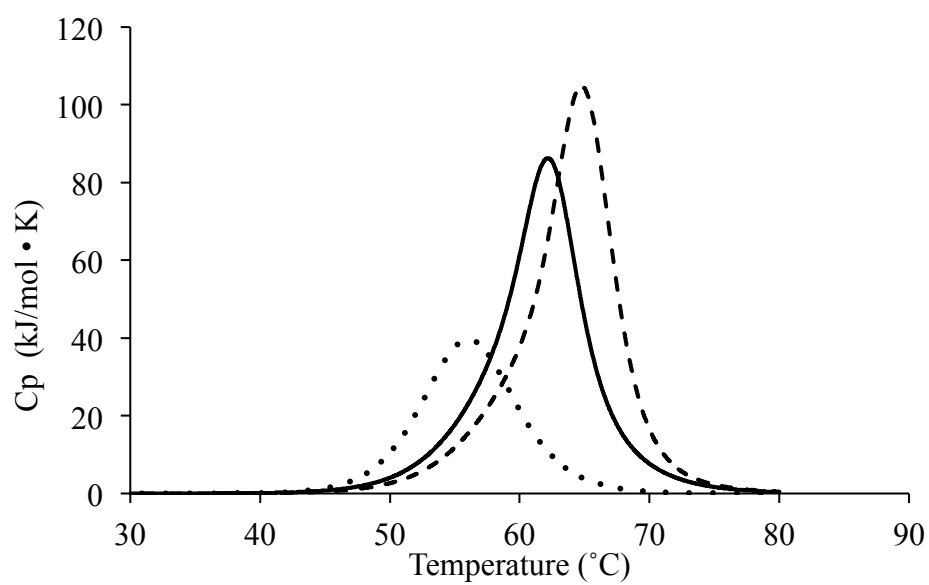


**Figure 9:** DSC scans of 1 mg/ml Alpha (A) and BSA (B) as a function of ionic strength at pH 7.0. Ionic strengths used were 15 mM; dotted line (···), 150 mM; solid line (—) and 300 mM; dashed line (- - -). Runs were made in duplicates.

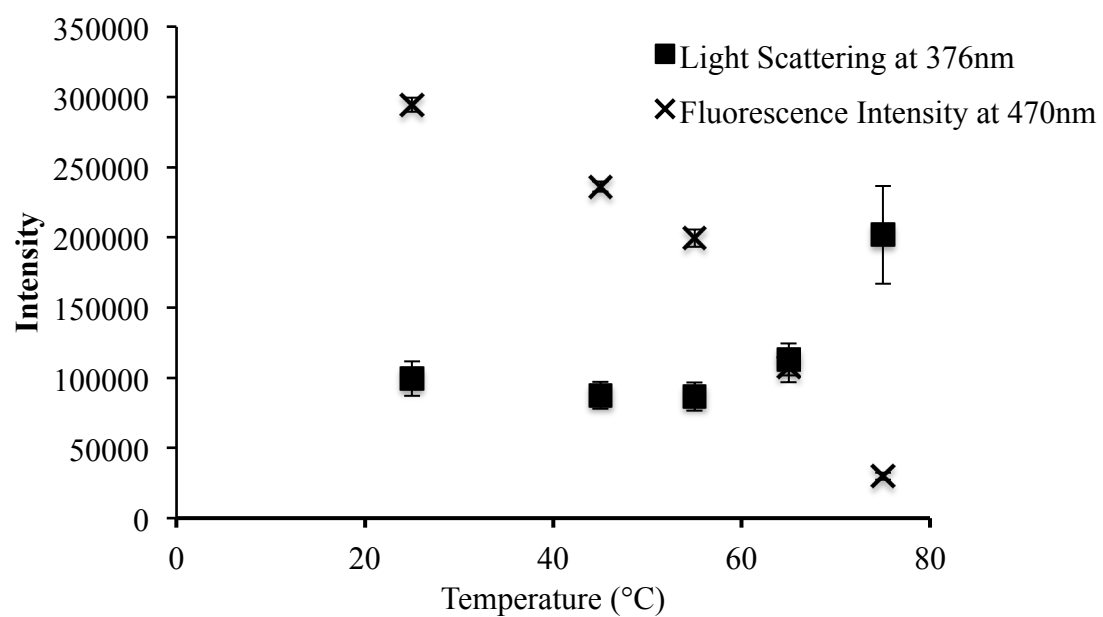


**Figure 10:** Aggregation (376 nm) and unfolding (470 nm) of BSA measured on a fluorescence spectrofluorometer at pH 7.0 (15 mM ionic strength).

## **Chapter 5**

### **Physical Stability of Monoclonal Antibodies: Investigating the Link Between Protein Surface Hydrophobicity and Aggregation**

## **Contents**

### **Chapter 5**

1. Abstract and Keywords
2. Introduction
3. Materials and Methods
  - 3.1. Materials
  - 3.2. Methods
    - 3.2.1. Fluorescence Spectroscopy
    - 3.2.2. Hydrophobic Interaction Chromatography
    - 3.2.3. Nuclear Magnetic Resonance: Transverse Relaxation Time Measurements
    - 3.2.4. Dynamic Light Scattering
    - 3.2.5. Mechanical Stress (Shaking) of Antibodies at  $25\text{ }^{\circ}\text{C} \pm 2.0^{\circ}\text{C}$
    - 3.2.6. Size Exclusion High-Performance Liquid Chromatography
    - 3.2.7. Differential Scanning Calorimetry
4. Results and Discussion
  - 4.1. Hydrophobicity Characterization
  - 4.2. Physical Stability of MAb X, Y and Z.
    - 4.2.1. Effect of Ionic Strength on the Interaction Parameter ( $k_D$ )
    - 4.2.2. Aggregation of MAb X, Y and Z under Mechanical Stress
    - 4.2.3. Aggregation of MAb X, Y and Z under Thermal Stress.
  - 4.3. Effect of Aromatic Excipients on Protein-Protein Interactions of MAb X.
    - 4.3.1. Protein-Protein Interactions after the Addition of Aromatic Excipients

5. Conclusion

6. References

7. Figures and Tables

## 1. Abstract

In this study the surface hydrophobicity of three antibodies was measured by Nuclear Magnetic Resonance, Hydrophobic Interaction Chromatography and fluorescence spectroscopy. Antibody solutions at pH 7.0 (15 mM and 300 mM) were stressed via mechanical stress for seven days and aggregates were measured by size exclusion chromatography (SE-HPLC). Consequently, the surface hydrophobicity did not impact nor influence the aggregation propensity of these antibodies. Measuring unfolding and aggregation as a function of temperature was monitored by fluorescence spectroscopy with an extrinsic dye, ANS. These results indicate that small structural changes may be present in the antibody solutions; however, large unfolding events must occur to promote aggregation. Further aggregation studies of mAb Y suggest that a combined thermal and shaking stress, impacts the conformational stability and causes aggregation to a greater degree. The influence of aromatic excipients, tryptophan, phenylalanine, and phenol, on the attractive protein-protein interactions of mAb X was monitored by DLS, however this study showed no significant decrease in the protein-protein interactions.

**Keywords:** Hydrophobicity; Protein Aggregation; Protein Unfolding; Fluorescence Spectroscopy; Monoclonal Antibodies

## 2. Introduction

Aggregation is a major physical stability issue amongst monoclonal antibody therapeutics and is a critical concern in developing safe and stable protein liquid formulations.<sup>1-4</sup> Developing methods to predict aggregation in the initial screenings of the formulation process would be beneficial to detect problematic antibodies in the early stages of product development.<sup>5</sup> One type of interaction that is identified as being a major contributor to aggregation is hydrophobicity.<sup>6,7</sup> However, recent advances in experimentally relating hydrophobicity of protein molecules to aggregation prove to be unsuccessful.

The hydrophobicity of a protein affects stability in two ways. Initially, when a protein folds into its native state, the driving force is the hydrophobic effect. This effect is due to the unfavorable change in free energy resulting from the decrease in entropy due to lack of interaction between nonpolar amino acids and water. Therefore, most nonpolar amino acids will bury themselves within the core of the protein, increasing entropy of water and decreasing free energy, which results in the native, folded structure of the protein.<sup>8</sup> However, once the protein is folded into its native structure, a portion of the nonpolar amino acids are not buried within the core, but are exposed on the protein surface.<sup>9,10</sup> It has been suggested that these solvent accessible nonpolar amino acids contribute to hydrophobic protein-protein interactions leading to stability issues of the protein formulation such as aggregation and self-association.<sup>11,12</sup>

Although it has been hypothesized that hydrophobic interactions are one of the major causes in protein aggregation, obtaining a hydrophobic measurement for a protein can be done a multitude of ways. Measuring hydrophobicity, either theoretically by the primary amino acid sequence or by experimental methods to determine the surface hydrophobicity can give a vast difference in the hydrophobicity value obtained and therefore relating to stability issues like

aggregation can be difficult.<sup>13-15</sup> In a publication by Shieh et al, the authors try to correlate aggregation induced by the air/water interface to properties including surface pressure, surface excess and hydrophobicity.<sup>16</sup> Hydrophobicity was measured by two ways; hydrophobic interaction chromatography (HIC) and theoretical calculation of the amino acid sequence. It was concluded that there was no correlation between aggregation-prone antibodies and theoretical hydrophobicity but some correlation could be drawn from the experiments measured by HIC. However, HIC falsely predicted the stability for three of the antibodies. Accordingly, predicting aggregation by this hydrophobicity method proved to be unsuccessful.

Another literature report used computer modeling, Spatial Aggregation propensity (SAP) to predict hydrophobic-prone areas of monoclonal antibodies that could promote aggregation.<sup>17-20</sup> These studies suggest that the aggregation-prone areas are on the protein surface, however aggregation is induced and stability is measured at high temperatures. High temperatures unfold the protein, exposing hydrophobic amino acids that were previously buried. Thus the “hot spots” that were predicted by the model and contribute to the measured hydrophobicity do not fully contribute to aggregation by partial or full denaturation of the protein. Determining if surface hydrophobicity of a protein can be related to the stability and aggregation of a protein in solution continues to be an issue.

In this study, three monoclonal antibodies (mAb X, mAb Y, and mAb Z) were characterized by multiple methods to measure and compare their surface hydrophobicity. Aggregation was measured at several time points immediately following a stress induced by shaking, heating or both to monitor the physical stability of each antibody. Protein-protein interactions were also measured to elucidate the type of amino acids contributing to attractions in solution by the addition of aromatic excipients.



### 3. Materials and Methods

#### 3.1. Materials

Proteins X, Y and Z are all monoclonal antibodies with a molecular weight of 150 kD and with absorptivities ( $\text{mg} \cdot \text{mL} \cdot \text{cm}^{-1}$ ) of 1.4, 1.73 and 1.45, respectively. To achieve the desired pH for each antibody, the stock solutions were buffer exchanged using Amicon Centrifuge units (10 kD cutoff). Each protein solution was filtered using a 0.22  $\mu\text{M}$  syringe filter. All studies were performed with a sample size of three ( $n = 3$ ) or greater unless stated otherwise.

#### 3.2. Methods

##### 3.2.1. Fluorescence Spectroscopy

Fluorescence measurements were performed using Photon Technology International (PTI) TimeMaster TM TM-200 LED lifetime strobe spectrofluorometer (Birmingham NJ). Heating studies were conducted using a temperature control device from Quantum Northwest, Model TC-125, (Spokane WA). Temperatures were chosen based on the unfolding and melting temperatures seen by differential scanning calorimetry measurements (DSC). Concentrations of antibody and ANS were constant at 0.5 mg/mL and 50  $\mu\text{M}$ , respectively. The excitation wavelength was chosen based on the excitation of the extrinsic dye, ANS, to be 375 nm with an emission scanning from 350 nm to 650 nm at a speed of 2 nm/sec. A total of 4 scans were taken for each temperature, with a temperature ramp of 1  $^{\circ}\text{C}/\text{min}$  with a 120 s equilibration at the temperature chosen. 150  $\mu\text{L}$  of each protein was placed in sample cuvette. The excitation and emission slit width was set to 0.5 mm.

For additional heating studies with mAb Y, 250  $\mu\text{L}$  of 0.5 mg/mL protein were filled in 1.8 mL glass vials. Samples were heated to 65  $^{\circ}\text{C}$  in an oven for one hour. Stressed vials were placed on a Vortex (Fisher Vortex Genie 2) at a dial speed of 5 (out of 8) for five continuous minutes.

Samples were held for 15 minutes to allow bubbles to settle and a 70  $\mu$ L aliquot from the vial was taken for scattering measurement. 9  $\mu$ L of a 1 mM ANS stock solution was added to the vial (final ANS concentration of 48  $\mu$ M), stored in a dark place until measurement. The settings on the fluorescence spectrofluorometer were identical to above measurements.

For initial slope measurements, experiments were conducted similarly to previous methods (Ch. 3). 1 mg/ml stock solutions of each antibody were diluted prior to experiments and concentration was checked using SoloVPE. Subsequent concentrations were diluted from 1.0 mg/ml stock.

### 3.2.2. Hydrophobic Interaction Chromatography

HIC experiments were conducted similarly to previous methods (Ch. 3). A butyl HP and phenyl HP column was used. Buffer conditions were maintained at pH 7.0. Stock solutions of proteins were buffer exchanged in pH 7.0, 15 mM ionic strength phosphate buffer. Samples were then diluted to 1.0 mg/ml with pH 7.0 20 mM ionic strength phosphate buffer and filtered before placed in a HPLC vial to be injected in to the HIC columns. The column was equilibrated prior to injection with a 1.0 M ammonium sulfate pH 7.0 sodium phosphate buffer until a stable baseline was reached. 100  $\mu$ L of each protein was injected into the column at 100% 1.0 M ammonium sulfate. A 30-minute linear gradient was used to elute the protein off the column from 100% to 0% ammonium sulfate. At the end of the 30 minutes, the column continued to run in 20 mM sodium phosphate buffer until the protein eluted off the column entirely and the signal returned to baseline.

### 3.2.3. Nuclear Magnetic Resonance: Transverse Relaxation Time Measurements

All proteins were buffer-exchanged in a pH 7.0, 15 mM ionic strength (8.5mM buffer strength) sodium phosphate buffer to maintain a pH  $7.0 \pm 0.5$ . At the pH desired, proteins were

again buffer exchanged in a pH 7.0 D<sub>2</sub>O buffer until about 90-95% D<sub>2</sub>O was achieved.

Concentration of each protein was measured using SoloVPE, and filtered. Solutions were flushed with nitrogen gas prior to filling the NMR tube. Protein-to-Probe ratio was set at 1:100 and all samples were made 24 hours prior to experiment. Samples were placed in a WGS5BL NMR tube (Wilmad-Lab glass) and DSS was used as the reference peak. All experimental setup was similar to the previous method except for the Big Tau set. For these experiments the Big Tau values were set to 0.05, 0.1, 0.2, 0.3, 0.4, 0.5, 0.6, 0.8, 1.2, 2.0, 3.0, 4.0, 8.0, 12.0 and 20.0.

#### 3.2.4. Dynamic Light Scattering

12 mg/ml stock solutions of each protein were prepared, and filtered. Concentrations were diluted to 10 mg/ml – 2 mg/ml and were performed in triplicates. Accurate concentrations were checked after light scattering experiments using SoloVPE. Diffusion coefficients were plotted versus protein concentration and the  $k_D$  was calculated for each condition as explained previously in Chapter 4.

#### 3.2.5. Mechanical Stress (Shaking) of Antibodies at 25 °C ± 2.0°C

All 5 mg/ml antibody solutions (pH 7.0 and ionic strength 15 mM) were shaken using an 11 x 13 inch Excella E2 platform shaker (New Brunswick Scientific). 10 mL of each protein solution was filtered and checked for concentration prior to the start of each experiment. 1.0 mL of the filtered protein solutions from the 10 mL stock was filled into 1.8 mL glass vials with 9 mm screw thread caps (Fisherbrand) to ensure identical concentration for stressed and unstressed vials. The solutions were shaken at 200 rpm for a period of 5 and 8 days. Three vials for each time point were placed on the shaker, including an additional three vials left at the same temperature but not stressed to act as a control. After the shaking period, the solutions were placed into a 2 mL Eppendorf tube.

Three separate aliquots were taken from the 2 mL Eppendorf tube and checked for insoluble aggregates using the Malvern Zetasizer. The rest of the sample was diluted 1:5 times with the appropriate buffer (pH 7.0, 15 mM ionic strength) into a 1.5 mL Eppendorf tube and spun at 10,000 rpm for 15 minutes using the Eppendorf minispin to be analyzed for SE-HPLC for soluble aggregates.

### 3.2.6. Size Exclusion High-Performance Liquid Chromatography

Before stressing the samples, the protein solution was tested for insoluble and soluble aggregates. DLS was used to assess insoluble aggregates. For the purpose of soluble aggregates, SE-HPLC with an inline UV detector set to 280 nm was used. A sodium phosphate buffer (pH 7.0, 20 mM and ionic strength adjusted with sodium sulfate to 200 mM) was used as the mobile phase. A 7.8 mm inner diameter by 30 cm, TSKgel G3000SW XL, Column # Y02981-08S (TOSOH Bioscience, LCC, Japan) was used with an isocratic flow rate of 1.0 mL/min with a 30  $\mu$ L volume injection. Each vial was injected twice and each time point had three vials.

After dilution and centrifugation of the stressed vials, each sample was injected into the column and analyzed using Peak Simple software 3.88 (SRI Instruments, Torrance, CA).

### 3.2.7. Differential Scanning Calorimetry

DSC experiments were performed on a nano-DSC (TA instruments) to determine  $T_m$  and onset of unfolding for each antibody in pH 7.0 sodium phosphate buffer at 15 mM ionic strength. 1.0 mg/ml of each protein sample was filtered and checked for correct concentration prior to experiment. Each sample was run at a scan rate of 1°C/min from 45 °C to 115 °C with a pre-scan equilibration time of 600 seconds. The corresponding buffer was also run at the same conditions for baseline subtraction. The thermal scans were analyzed and baseline subtracted using the Nano Analyze software.

## 4. Results and Discussion

### 4.1. *Hydrophobicity Characterization*

To investigate the impact of surface hydrophobicity on stability, the surface hydrophobicity of three monoclonal antibodies was determined using fluorescence spectroscopy, HIC and NMR. These methods were established in Chapter 2.

Fluorescence spectroscopy using ANS as an extrinsic dye was performed and the initial slopes measured are shown in table 1. MAb Z has the lowest slope of the three antibodies meaning the fluorescence intensity does not overwhelmingly increase or shift in wavelength different than from ANS in water. MAb X has the largest slope of the three proteins. However the values for the three proteins are relatively low, meaning there is not a significant interaction between ANS and these antibodies.<sup>21</sup>

HIC data is shown in Figure 1(a) and 1(b), representing a phenyl column in the former and a butyl column in the latter. The protein that exhibits the least hydrophobicity will elute off the column at an earlier retention time.<sup>22</sup> In both columns it can be seen that mAb Z elutes off the column first, making it the least hydrophobic independent of the type of column used. The order of elution for the three antibodies does not change by the change in column, however the sharper peaks on the phenyl column for all the mAbs are indicative of the phenyl column holding stronger interactions of the two. MAb Y has a very subtle and hardly noticeable peak on the butyl column, however has a small yet distinguishable peak on the phenyl column showing that the phenyl column compared to the butyl column has a stronger interaction between proteins. From the results above, it is difficult to assess which of the two proteins, mAb X and Y, is more hydrophobic because there isn't a clear difference in retention times.

The NMR results, using *tert*-butyl alcohol, as the small molecule probe is shown in figure 2. A decrease in the  $T_2$  relaxation time of the (protein + probe) compared to the  $T_2$  of the probe alone indicates an interaction between the probe and protein.<sup>23,24</sup> It can be seen that there is no decrease in the  $T_2$  relaxation time for *tert*-butyl alcohol when combined with any of the three proteins. Figure 3 shows the percent change for each antibody with the corresponding phenol relaxation time measured the same day to account for day-to-day variations in the relaxation time of phenol (no variations seen with *tert*-butyl alcohol). The raw data for each  $T_2$  relaxation experiments are reported in Table 2. The phenol data shows that there is a less percent change for mAb Z than for both mAb Y and mAb X, consistent with previous results found from HIC and fluorescence spectroscopy. Mab Z, which shows the lowest  $S_0$  value, elutes off both columns first in HIC, also illustrates the least amount of change/interaction in the phenol relaxation data. Therefore mAb Z is the least hydrophobic antibody. However, it is still unclear to distinguish the hydrophobicity difference between the two most hydrophobic antibodies, mAb X and Y.

#### 4.2. Physical Stability of MAb X, Y and Z

##### 4.2.1. Effect of Ionic Strength on the Interaction Parameter ( $k_D$ )

Understanding the extent to which surface hydrophobicity affects stability is explored further by mechanical stress (shaking) at low and high ionic strength conditions. However, first using Dynamic Light Scattering (DLS) to measure protein-protein interactions in dilute solutions at these same conditions can provide insight into the type of solute-solute interactions that are significant at these solution conditions. A negative  $k_D$  value indicates attractive interactions, which become significant at short distances and may be a result of hydrophobic, specific charge or Van der Waals (dipole) interactions. Whereas a positive  $k_D$  results from repulsive interactions

and are dominant at long distances between solute molecules. These are a result of electrostatic, charge-charge and steric interactions.<sup>25</sup>

Figure 4 shows  $k_D$  values as a function of ionic strength for all antibodies at pH 7.0. These results illustrate that mAb Y may have significant hydrophobic interactions at high ionic strength conditions. This is observed by the  $k_D$  values for mAb Y becoming more negative, increasing from -21.8 mL/g (15 mM) to -25.45 mL/g (300 mM), indicating an increase in attractive interactions. When attractions become more dominant as charges on the protein are screened, it can suggest that hydrophobic interactions may be governing the protein-protein attractive interactions in solution. These protein-protein interactions can give additional insight into the behavior of the protein on the HIC column. For mAb Y, the protein-protein interactions are strong attractions throughout the ionic strength range tested; therefore elution of mAb Y off the HIC column, which is performed at high ionic strength (much higher than tested here), is a slow broad peak.

The opposite trend is true for mAb X, where electrostatic interactions govern the attractive protein-protein interactions. At 300 mM, mAb X has slight repulsive interactions, however as the ionic strength is reduced, the attractions are increased significantly. These increased attractions indicate that electrostatic interactions are dominant at low ionic strength and as charges are screened, attractive interactions decrease.<sup>25-28</sup> However the difference between mAb X and mAb Y, is that mAb X's attractions are due to electrostatic interactions, although it elutes last, there is still a sharp protein peak on the chromatogram. This would aid in the protein eluting off the HIC column, although the antibody still has hydrophobic patches on the surface seen by a strong interaction between the HIC column and the protein.

Whereas, mAb Z's  $k_D$  values are only slightly negative (less than  $-5.34 \text{ mL/g}$ )<sup>25</sup> at high ionic strengths indicating slight repulsions and  $k_D$  values are neutral at low ionic strength conditions. Thus, during the removal of salt from the HIC column, the protein is actually slightly repulsive and elutes off the column easily.

#### 4.2.2. Aggregation of MAb X, Y and Z under Mechanical Shaking Stress

The effect of mechanical stress as a function of time is shown in figures 5 and 6. Percent aggregates by Size Exclusion Chromatography (SEC) and DLS were monitored at two separate ionic strength conditions. MAb Y, which exhibits hydrophobic attractions at high ionic strength, does not show any increased aggregation. The hydrophobicity of this antibody does not seem to have a significant impact or influence on the tendency to aggregate through shaking stress. For low and high ionic strength conditions, percent aggregates and DLS scattering intensity (data not shown) showed no change from the initial time point over the course of the shaking stress for any of the three proteins. This indicates that although the nonpolar surfaces of a protein may be more favorable for protein-protein and protein-interface interactions, these studies suggest that the surface hydrophobicity does not influence aggregation to a significant extent.

Shieh et al. studied the ability to predict the agitation-induced aggregation of monoclonal antibodies using surface tensiometry. As mentioned earlier, neither hydrophobicity measured by HIC nor the average hydrophobicity calculated were good predictors of the aggregation induced by mechanical stress for the 16 monoclonal antibodies measured. Although hydrophobicity was not a good predictor of aggregation, out of the 16 antibodies, there were proteins that did show aggregates through turbidity and SEC measurements.<sup>16</sup> Another example shows the effect of varying vial type and size, fill height, and speed for shaking studies performed on three antibody formulations.<sup>29</sup> The results found that the antibodies that were shaken at top speed, 200 rpm, with



a 1.0 mL fill in a 2.0 mL vial aggregated in the least amount of time required. One reason may be that the shaking study methods used in the literature placed the vials horizontally, while the antibodies in this study were shaken vertical to ensure that additional influences did not contribute to aggregation such as the interaction between the vial cap and solution. The vertical shaking may not have as large of an interface compared to the horizontal shaking, however, to differentiate between the different variables that arise due to horizontally placing the vials (vial + cap interaction) may introduce complications in regard to the specific type of interaction causing aggregation. For the antibodies studied here, the surface hydrophobicity did not impact or successfully predict aggregation caused by mechanical stress in solution.

#### 4.2.3. Aggregation of MAb-X, Y and Z under Thermal Stress

Surface hydrophobicity of proteins is the result of the nonpolar amino acids that remain on the protein surface after most of the hydrophobic amino acids are folded within the core. Since the surface hydrophobicity of these antibodies had little effect on their aggregation stability, thermal stress was used to determine if the nonpolar amino acids that are exposed after the protein starts to unfold govern aggregation.

Differential scanning Calorimetry (DSC) scans were performed for each antibody to determine both the onset of unfolding and the melting temperatures ( $T_{m1}$  and  $T_{m2}$ ), which are shown in Figure 7. From the DSC scans, temperatures were chosen to monitor unfolding while observing aggregation by light scattering within the same scan.

Figures 8 (a-c) show the changes in light scattering at the wavelength of excitation 375 nm (primary axis) as well as monitoring the changes in wavelength of maximum fluorescence intensity (secondary axis) for the three antibodies. The full scans can be seen in the appendix (A5), which show that with the shift in maximum fluorescence, there is also an increase in

fluorescence intensity as the temperature is increased. Both mAb X and Z show a change in the fluorescence maximum wavelength around 60 °C for X and 65 °C for Z; close to the unfolding temperature seen by the DSC scans. However at these temperatures, aggregation has not yet begun seen by the consistent intensity in light scattering compared to lower temperatures. Once enough of the protein is unfolded, aggregation can be seen by an increase in the light scattering. However, mAb Y behaves slightly different out of the three proteins. There is a shift towards higher wavelengths (slight decrease in intensity) at 50 °C, significantly before the proteins onset of unfolding and thus indicating ANS is in a more polar environment. However as the temperature continues to increase, the environment of ANS changes to a nonpolar environment again as seen by the shift towards lower wavelengths and an increase in fluorescence intensity.

It can be inferred from the heating studies that unfolding occurs prior to aggregation, and aggregation only begins when a substantial amount of protein has partially unfolded.<sup>6,30</sup> This follows the general mechanism of protein aggregation described by the Lumry-Eyring model in the equation below.<sup>31,32</sup>



Where N is the native state of the protein and is in equilibrium with the unfolded/denatured state, U. These unfolded proteins can form a final state, F and form irreversible aggregates in solution. Therefore the unfolding temperatures, seen by the DSC scans, can predict aggregation at the high temperatures studied. However, to extrapolate these results to lower temperatures will not give reliable information on how the proteins will behave in solution at room temperature.

Further studies were performed with mAb Y to illustrate that at high temperatures the probability of aggregation increases as more energy (mechanical stress) is applied. Figure 9 show that the samples at 25 °C and 65 °C without any applied stress exhibit no aggregation. However,

after applying vortex to the vials at those same conditions, more aggregates were found in the 65°C vials than in the 25 °C. The onset of unfolding for mAb Y is 69 °C illustrated by DSC (figure 7) scans. Therefore, slightly before the onset of unfolding there is a shift in the equilibrium favoring the denatured state, thus once additional stress is supplied in the form of vortex, aggregation increased dramatically. However this does not hold true during all structural events of a protein.

MAb Y also goes through a structural perturbation around 50-55 °C (as mentioned earlier) and similar heating and vortex studies were performed (data not shown) at these conditions, 25°C and 55 °C (unstressed and vortexed). However the protein did not show any aggregation after the stress was applied following heating the protein at 55 °C. Thus, indicating there were not enough proteins with a large enough free energy towards the unfolded/denatured state to generate aggregation.

The shift in wavelength of maximum fluorescence was also observed for the stressed and unstressed vials as a function of temperature. Figure 9 illustrates the total shift in maximum wavelength on the secondary y-axis. ANS fluorescence shifts towards lower wavelengths, which indicates that ANS is in a more nonpolar environment. There is a more pronounced shift for the vials at 65 °C, going from 496 nm (unstressed) to 488 nm (stressed), whereas the vials at 25 °C only shift by 4 nm.

#### 4.3. *Effect of Aromatic Molecules on Protein-Protein Interactions of MAb-X*

##### 4.3.1. Protein-Protein Interactions after the Addition of Aromatic Molecules

To try and illustrate the difference between types of aromatic hydrophobic interactions, several amino acids were studied to determine if there is an effect on the  $K_D$  values of mAb X at chosen pH values and ionic strength conditions. Solutions conditions were explored for mAb X

to determine conditions where hydrophobic interactions may be the significant contributor to attractive interactions. The  $k_D$  studies in figure 10 suggest that at pH 5.0 and 5.5, as ionic strength is increased, attractive interactions decreased indicating electrostatic interactions are dominant. However as the salt concentration is increased at pH 4.5, attractive interactions increased suggesting that hydrophobic interactions may be significant at these conditions.

Once the pH and ionic strength where hydrophobicity may be dominate was seen, amino acids were chosen based on their aromatic structure to determine if these aromatic interactions could decrease attractions in solution. Figure 11 illustrates the  $k_D$  of mAb X alone and with the addition of excipients such as phenylalanine, tryptophan, and phenol. Phenol, analogous to tyrosine, was chosen due to its increased solubility over tyrosine in water. Although  $\pi$ - $\pi$  interactions are much stronger in protein solutions,<sup>33,34</sup> there seemed to be no detectable decrease in attractions as the excipients were added. One reason for the lack of decrease in  $k_D$  values after the addition of amino acids could be explained by the low solubility of these amino acids, especially the capped amino acids. Due to the low solubility, there may have not been enough excipient in solution to interact with protein molecules and cause a decrease in the attractive interactions. The only change came from a high concentration of phenol, where the attractions actually increased rather than decreased. This can be explained by the fact that phenol can denature proteins at high concentrations as it is used for DNA extractions and is used as a preservative in multi-dose protein formulations.<sup>35,36</sup> Therefore this may not be the appropriate measure to determine if specific amino acids, such as tryptophan and phenylalanine are responsible for attractive hydrophobic interactions between proteins in solution. Further studies to identify the difference in aromatic and aliphatic hydrophobic interactions would need to be explored.

## **5. Conclusion**

Three methods to measure surface hydrophobicity were studied: HIC, fluorescence spectroscopy, and NMR. Despite the general consensus, the measured surface hydrophobicity had little effect on protein aggregation. Antibodies X and Y, which were relatively more hydrophobic than mAb Z, showed no difference in protein aggregation. However, as the conformational stability of the protein was compromised, aggregation was observed. Thus, using a proteins surface hydrophobicity value to determine aggregation behavior is not always reliable. Both the surface hydrophobicity and the average hydrophobicity will contribute to aggregation depending on the specific manufacturing and processing parameters used during the drug product cycle.

## 6. References

1. Rosenberg, A. S. Effects of Protein Aggregates: An Immunologic Perspective. *The AAPS Journal* 1–7 (2006).
2. Schellekens, H. Factors influencing the immunogenicity of therapeutic proteins. *Nephrology Dialysis Transplantation* **20**, vi3–vi9 (2005).
3. Roberts, C. J. Therapeutic protein aggregation: mechanisms, design, and control. *Trends in Biotechnology* **32**, 372–380 (2014).
4. Jiskoot, W. *et al.* Protein Instability and Immunogenicity: Roadblocks to Clinical Application of Injectable Protein Delivery Systems for Sustained Release. *Journal of pharmaceutical sciences* **101**, 946–954 (2012).
5. Weiss, W. F., IV, Young, T. M. & Roberts, C. J. Principles, approaches, and challenges for predicting protein aggregation rates and shelf life. *Journal of pharmaceutical sciences* **98**, 1246–1277 (2009).
6. Roberts, C. J., Das, T. K. & Sahin, E. Predicting solution aggregation rates for therapeutic proteins: Approaches and challenges. *International Journal of Pharmaceutics* **418**, 318–333 (2011).
7. DeLano, W. L., Ultsch, M. H., de, A. M., Vos & Wells, J. A. Convergent Solutions to Binding at a Protein-Protein Interface. *Science* **287**, 1279–1283 (2000).
8. Kauzmann, W. Some Factors in the Interpretation of Protein Denaturation. **14**, 1–63 (1979).
9. Klotz, I. M. Comparison of molecular structures of proteins: helix content; distribution of apolar residues. *Archives Of Biochemistry and Biophysics* **138**, 704–706 (1970).
10. Englund, S. & Seifter, S. [22] Precipitation techniques. *Methods in Enzymology* **182**, 285–300 (1990).
11. Jones, S. & Thornton, J. M. Protein-protein interactions: a review of protein dimer structures. *Progress in biophysics and molecular biology* **63**, 31–65 (1995).
12. Chothia, C. & Janin, J. Principles of protein-protein recognition. *Nature* (1975).
13. Biswas, K. M., DeVido, D. R. & Dorsey, J. G. Evaluation of methods for measuring amino acid hydrophobicities and interactions. *Journal of Chromatography A* **1000**, 637–655 (2003).
14. Trinquier, G. & Sanejouand, Y. H. Which effective property of amino acids is best preserved by the genetic code? *Protein engineering* (1998).
15. Asenjo, J. A. & Andrews, B. A. Aqueous two-phase systems for protein separation: A perspective. *Journal of Chromatography A* **1218**, 8826–8835 (2011).
16. Shieh, I. C. & Patel, A. R. Predicting the Agitation-Induced Aggregation of Monoclonal Antibodies Using Surface Tensiometry. *Mol. Pharmaceutics* **12**, 3184–3193 (2015).
17. Chennamsetty, N., Helk, B., Voynov, V., Kayser, V. & Trout, B. L. Aggregation-Prone Motifs in Human Immunoglobulin G. *Journal of Molecular Biology* **391**, 404–413 (2009).
18. Chennamsetty, N., Voynov, V., Kayser, V., Helk, B. & Trout, B. L. Design of therapeutic proteins with enhanced stability. *PNAS* **106**, 11937–11942 (2009).
19. Chennamsetty, N., Voynov, V., Kayser, V., Helk, B. & Trout, B. L. Prediction of Aggregation Prone Regions of Therapeutic Proteins. *J. Phys. Chem. B* **114**, 6614–6624 (2010).
20. Agrawal, N. J. *et al.* Aggregation in Protein-Based Biotherapeutics: Computational

- Studies and Tools to Identify Aggregation-Prone Regions. *Journal of pharmaceutical sciences* **100**, 5081–5095 (2011).
21. Greene, F. C. Interactions of anionic and cationic fluorescent probes with proteins: The effect of charge. *Journal of Protein Chemistry* **3**, 1–14 (1984).
  22. Hofstee, B. H. J. Accessible Hydrophobic Groups of Native Proteins. *Biochemical and Biophysical Research Communications* **63**, 618–624 (1975).
  23. Fielding, L., Rutherford, S. & Fletcher, D. Determination of protein-ligand binding affinity by NMR: observations from serum albumin model systems. *Magn. Reson. Chem.* **43**, 463–470 (2005).
  24. Dubois, B. W. & Evers, A. S. Fluorine-19 NMR spin-spin relaxation (T2) method for characterizing volatile anesthetic binding to proteins. Analysis of isoflurane binding to serum albumin. *Biochemistry* **31**, 7069–7076 (1992).
  25. Yadav, S., Shire, S. J. & Kalonia, D. S. Factors Affecting the Viscosity in High Concentration Solutions of Different Monoclonal Antibodies. *journal of pharmaceutical sciences* **99**, 4812–4829 (2010).
  26. Chari, R., Jerath, K., Badkar, A. V. & Kalonia, D. S. Long- and Short-Range Electrostatic Interactions Affect the Rheology of Highly Concentrated Antibody Solutions. *Pharm Res* **26**, 2607–2618 (2009).
  27. Kumar, V., Dixit, N., Zhou, L. L. & Fraunhofer, W. Impact of short range hydrophobic interactions and long range electrostatic forces on the aggregation kinetics of a monoclonal antibody and a dual-variable domain immunoglobulin at low and high concentrations. *International Journal of Pharmaceutics* **421**, 82–93 (2011).
  28. Lockhart, D. J. & Kim, P. S. Electrostatic screening of charge and dipole interactions with the helix backbone. *SCIENCE-NEW YORK THEN ...* (1993).
  29. Eppler, A., Weigandt, M., Hanefeld, A. & Bunjes, H. Relevant shaking stress conditions for antibody preformulation development. *European Journal of Pharmaceutics and Biopharmaceutics* **74**, 139–147 (2010).
  30. Andrews, J. M. & Roberts, C. J. Non-Native Aggregation of  $\alpha$ -Chymotrypsinogen Occurs through Nucleation and Growth with Competing Nucleus Sizes and Negative Activation Energies †. *Biochemistry* **46**, 7558–7571 (2007).
  31. Sanchez-Ruiz, J. M. Theoretical analysis of Lumry-Eyring models in differential scanning calorimetry. *Biophysical Journal* **61**, 921–935 (1992).
  32. Lumry, R. & Eyring, H. Conformation Changes of Proteins. **58**, 110–120 (1954).
  33. Makhatadze, G. I. & Privalov, P. L. Energetics of interactions of aromatic hydrocarbons with water. *Biophysical Chemistry* **50**, 285–291 (1994).
  34. Burley, S. K. & Petsko, G. A. Amino-aromatic interactions in proteins. *Federation of European Biochemical Sciences* **203**, 139–143 (1986).
  35. Remmele, R. L., Nightlinger, N. S., Srinivasan, S. & Gombotz, W. R. Interleukin-1 Receptor (IL-1R) Liquid Formulation Development Using Differential Scanning Calorimetry. *Pharm Res* **15**, 200–208 (1998).
  36. Hutchings, R. L., Singh, S. M., Cabello-Villegas, J. & Mallela, K. M. G. Effect of Antimicrobial Preservatives on Partial Protein Unfolding and Aggregation. *Journal of pharmaceutical sciences* **102**, 365–376 (2013).

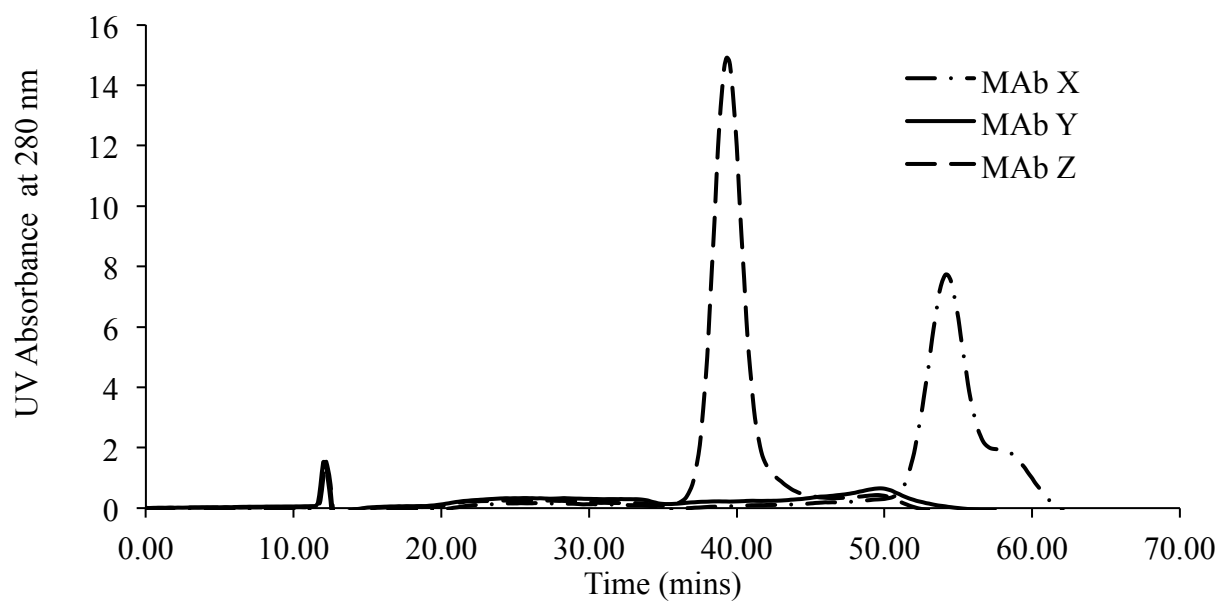
## 7. Figures and Tables

**Table1:** Fluorescence spectroscopy initial slope measurements of three antibodies using ANS as the extrinsic dye

Protein	Slope ( $S_0$ )
MAb X	7.40
MAb Y	5.68
MAb Z	2.53



(A)



(B)

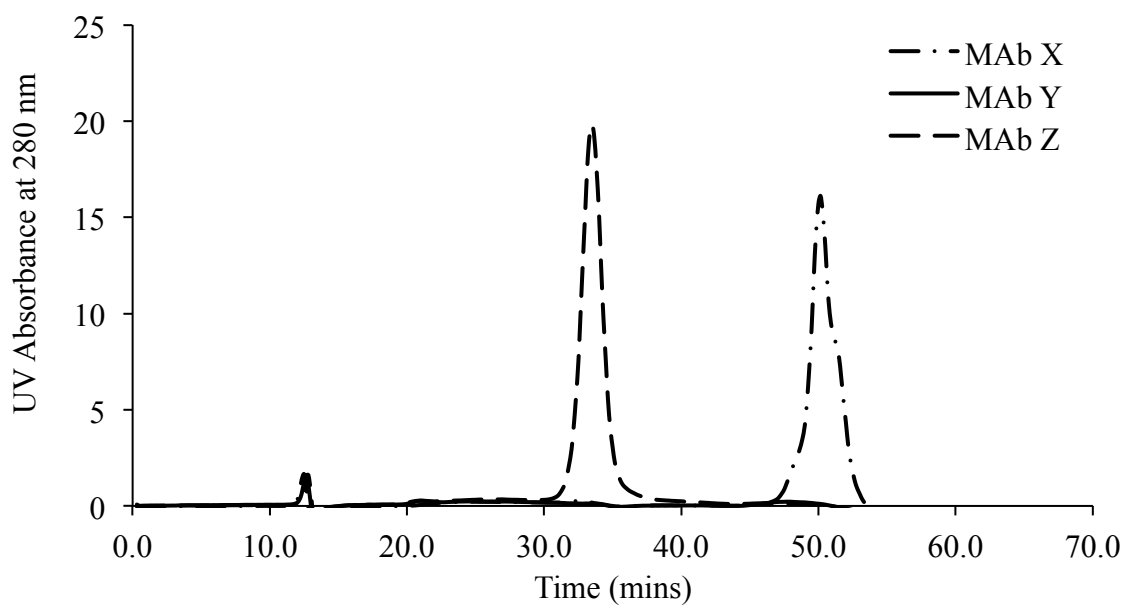


**Figure 1:** Surface hydrophobicity determined by hydrophobic interaction chromatography (HIC) for mAb X, mAb Y and mAb Z at 25 °C on a phenyl column (A) and butyl column (B).

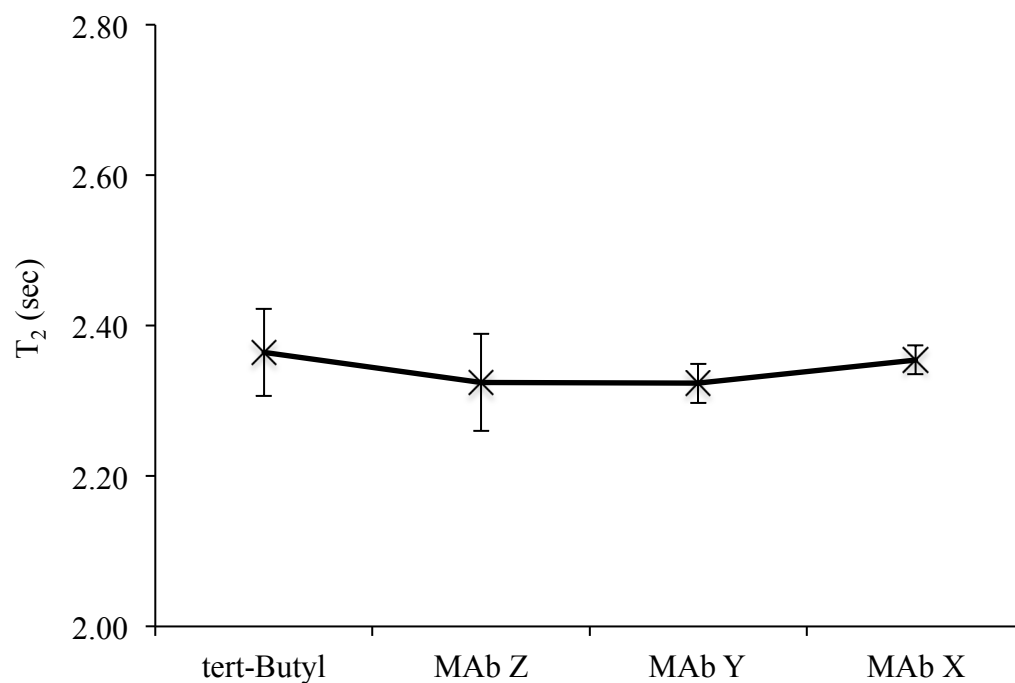


**Figure 2:** T<sub>2</sub> relaxation times for tert-butyl alone and at a 1:100 protein to *tert*-butyl ratio for mAb X, mAb Y and mAb Z. Samples contain about 90% D<sub>2</sub>O pH 7.0 buffer for water suppression. For each sample, the error is standard deviation (n = 3) except for mAb X, which is standard error (n = 2).

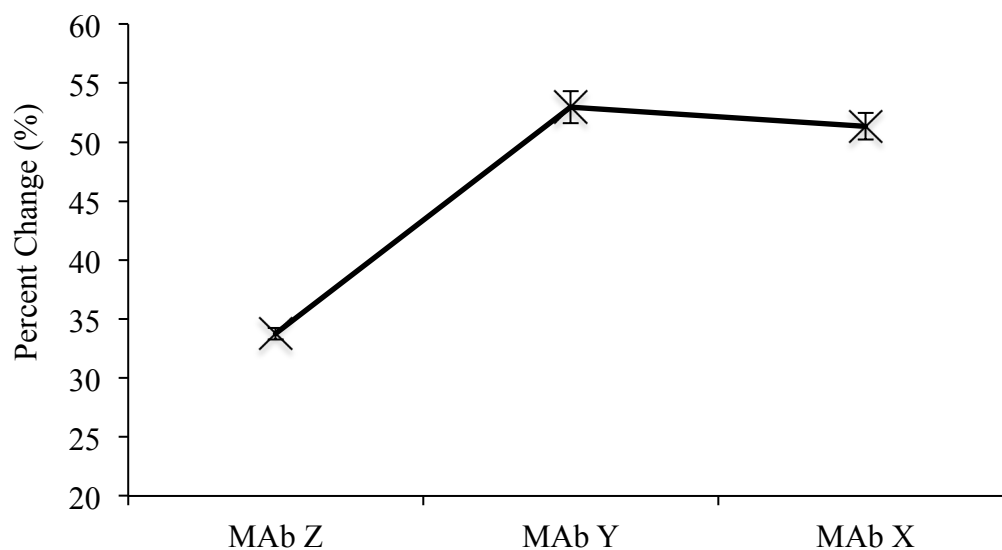


**Figure 3:** Percent change for each antibody with phenol at a ratio of 1:100. The percent change in  $T_2 = 100 \cdot (T_{2f} - T_{2obs}) / T_{2f}$  where  $T_{2f}$  is the relaxation time of the free probe obtained and the  $T_{2observed}$  is the relaxation time of the probe with the antibody. For MAb Z and X the error is standard deviation ( $n = 3$ ) and standard error ( $n = 2$ ) for MAb Y. The buffer conditions were pH 7.0 sodium phosphate buffer (15mM ionic strength) with approximately 90%  $D_2O$ .

**Table 2:** NMR  $T_2$  relaxation times for phenol at a Ratio of 1:100, protein to probe. All  $T_2$  relaxation times are in seconds.

	Phenol	MAb Z	MAb X		Phenol	MAb Y
$T_2$	$5.379 \pm 0.1846$	$3.56 \pm 0.08153$	$2.578 \pm 0.04505$		$5.415 \pm 0.1788$	$2.48 \pm 0.05928$
	$5.431 \pm 0.077$	$3.627 \pm 0.08383$	$2.609 \pm 0.05149$		$5.297 \pm 0.1451$	$2.479 \pm 0.06505$
	$5.415 \pm 0.1788$	$3.561 \pm 0.06785$	$2.705 \pm 0.06593$			
$T_2$ (DSS)	$3.086 \pm 0.0299$	$3.097 \pm 0.02466$	$3.11 \pm 0.02839$		$3.211 \pm 0.02121$	$3.196 \pm 0.01881$
	$3.125 \pm 0.01491$	$3.107 \pm 0.0216$	$3.13 \pm 0.02802$		$3.161 \pm 0.01669$	$3.18 \pm 0.02314$
	$3.211 \pm 0.02121$	$3.16 \pm 0.01943$	$3.201 \pm 0.02205$			

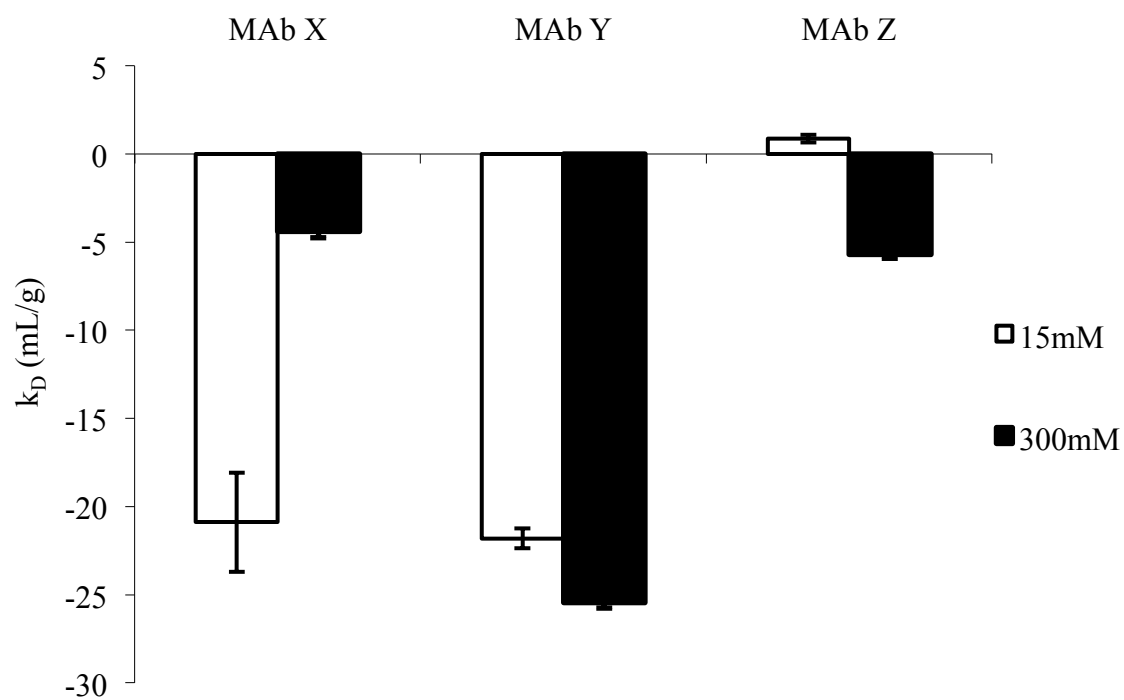


**Figure 4:** Plot of  $k_D$  obtained from Dynamic Light Scattering studies at pH 7.0 at two ionic strengths, 15 mM and 300 mM, adjusted by addition of NaCl. All solutions were analyzed in triplicate.

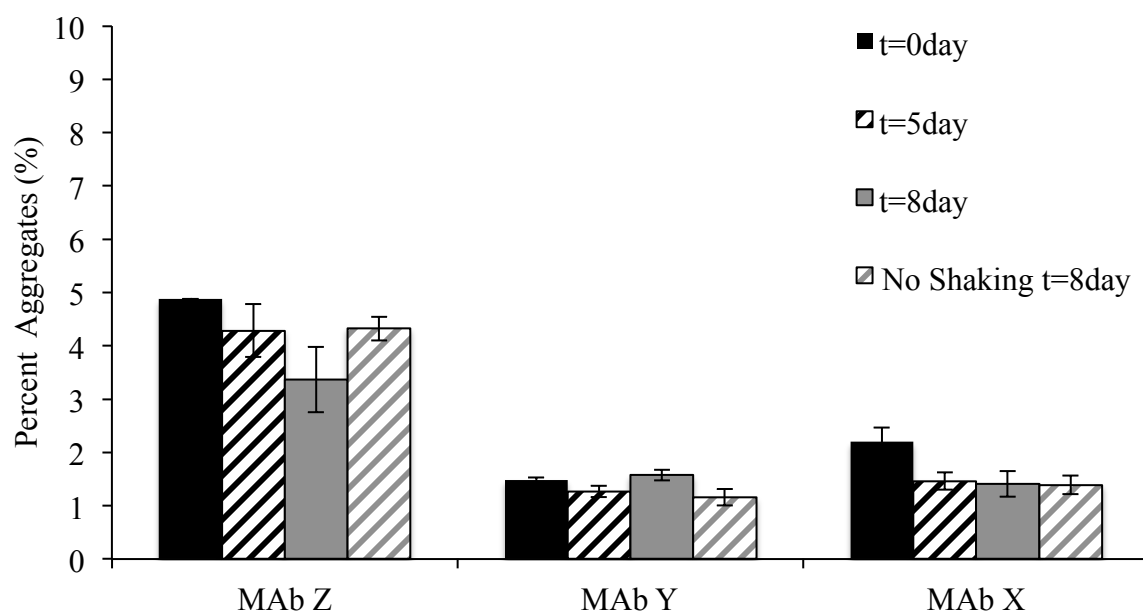


**Figure 5:** Effect of shaking stress was monitored as a function of time at pH 7.0 (15 mM ionic strength due to buffer). 5 mg/ml samples were shaken for a total of 8 days. At each time point, the sample was diluted and analyzed for percent aggregates by SEC at 25 °C. Unstressed samples were analyzed as controls held at the same room temperature. Error bars are standard deviations (n = 3).

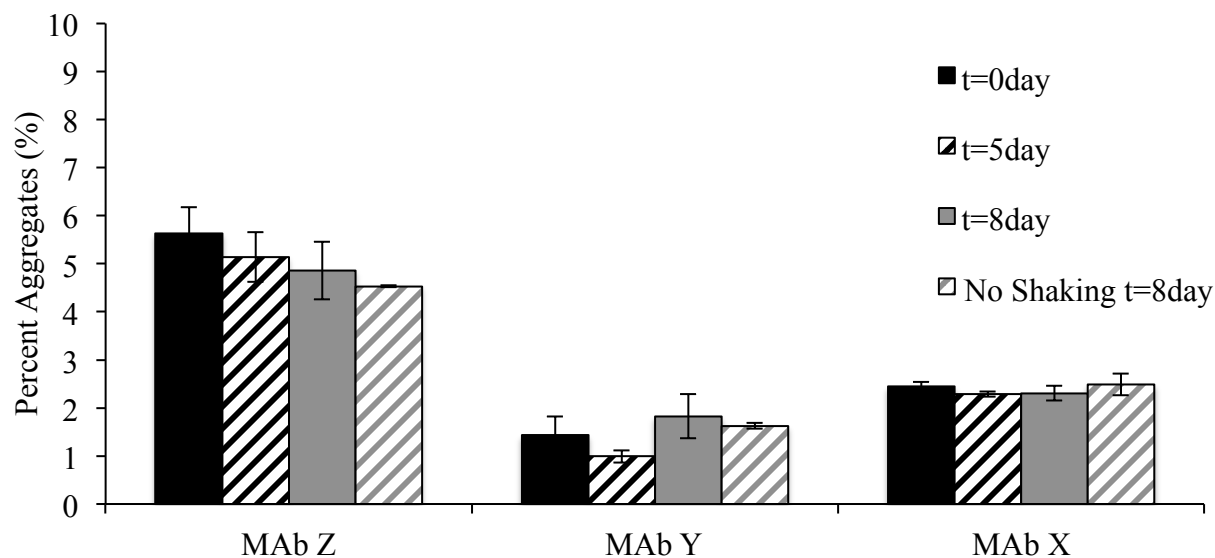
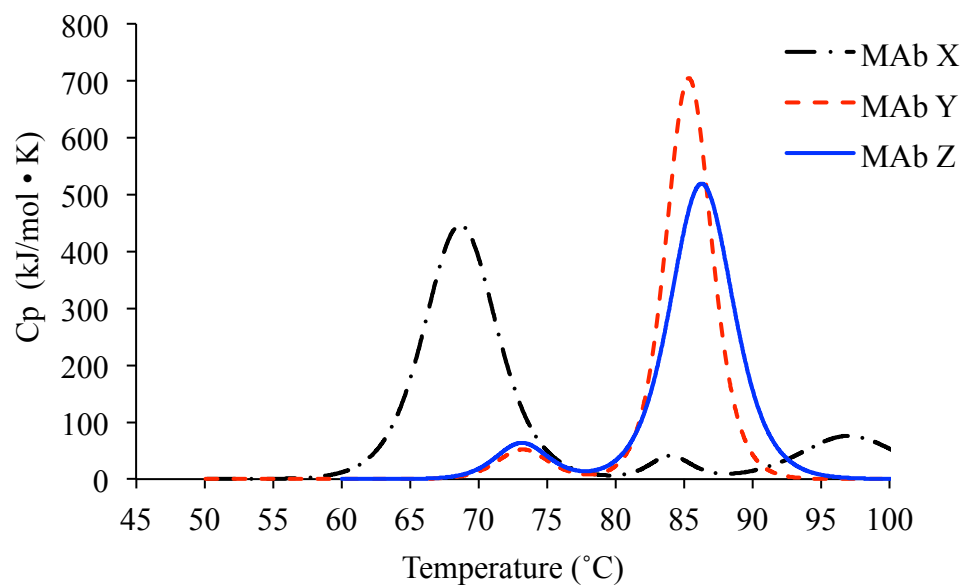


**Figure 6:** Effect of shaking stress was monitored as a function of time at pH 7.0 (300 mM ionic strength added by NaCl). 5 mg/ml samples were shaken for a total of 8 days. At each time point, the sample was diluted and analyzed for percent aggregates by SEC at 25 °C. Unstressed samples were analyzed as controls held at the same room temperature. Error bars are standard deviations (n = 3).

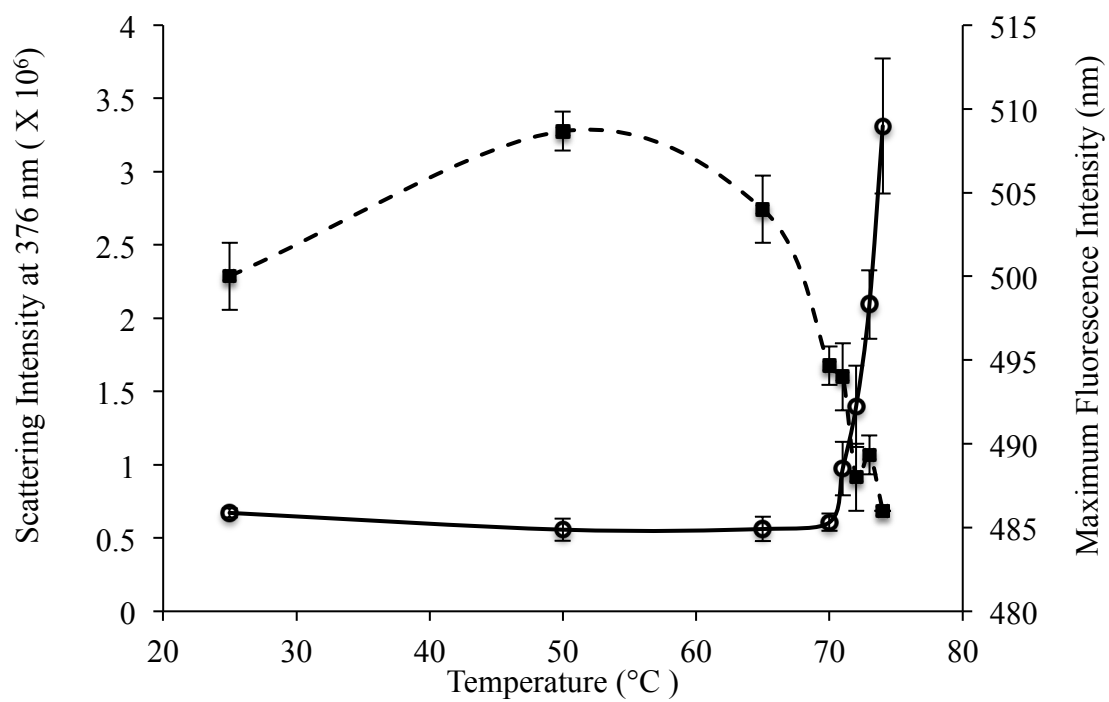


Protein	Onset of unfolding	Tm1	Tm2
MAb X	59.5	68.7	84.01
MAb Y	69.0	73.2	86.3
MAb Z	69.0	73.4	85.4

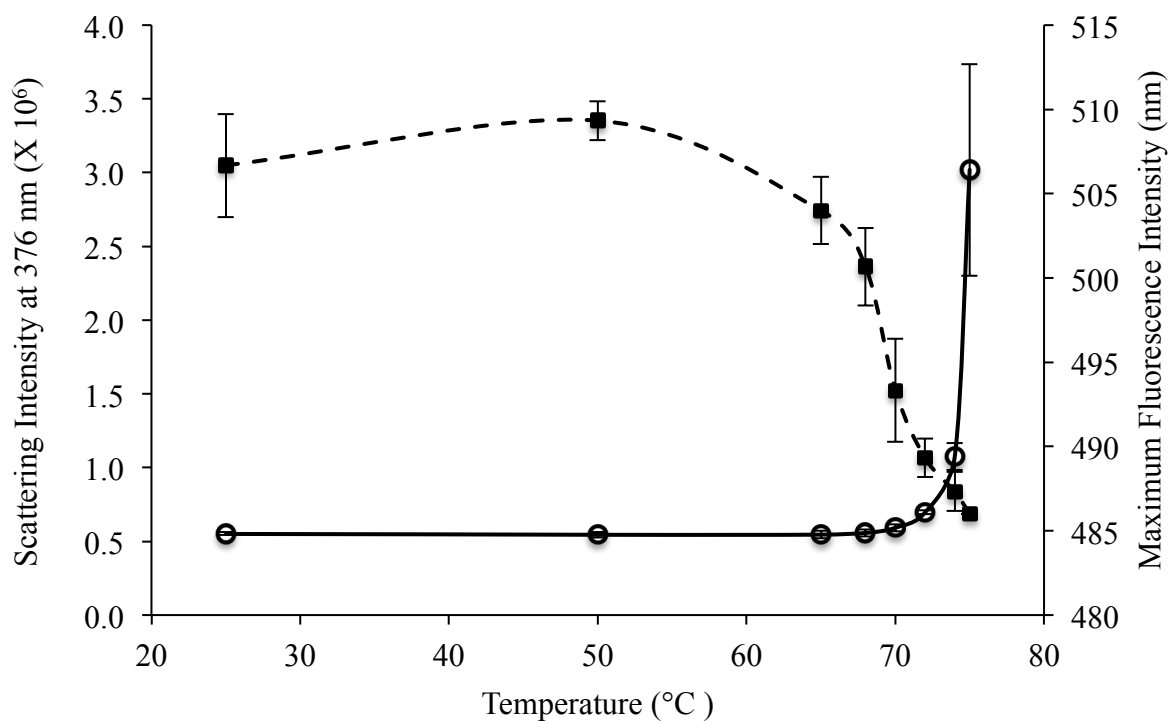
**Figure 7:** Unfolding and melting temperatures of the three antibodies obtained and analyzed by DSC. Scans were performed in duplicate.



(A)



(B)



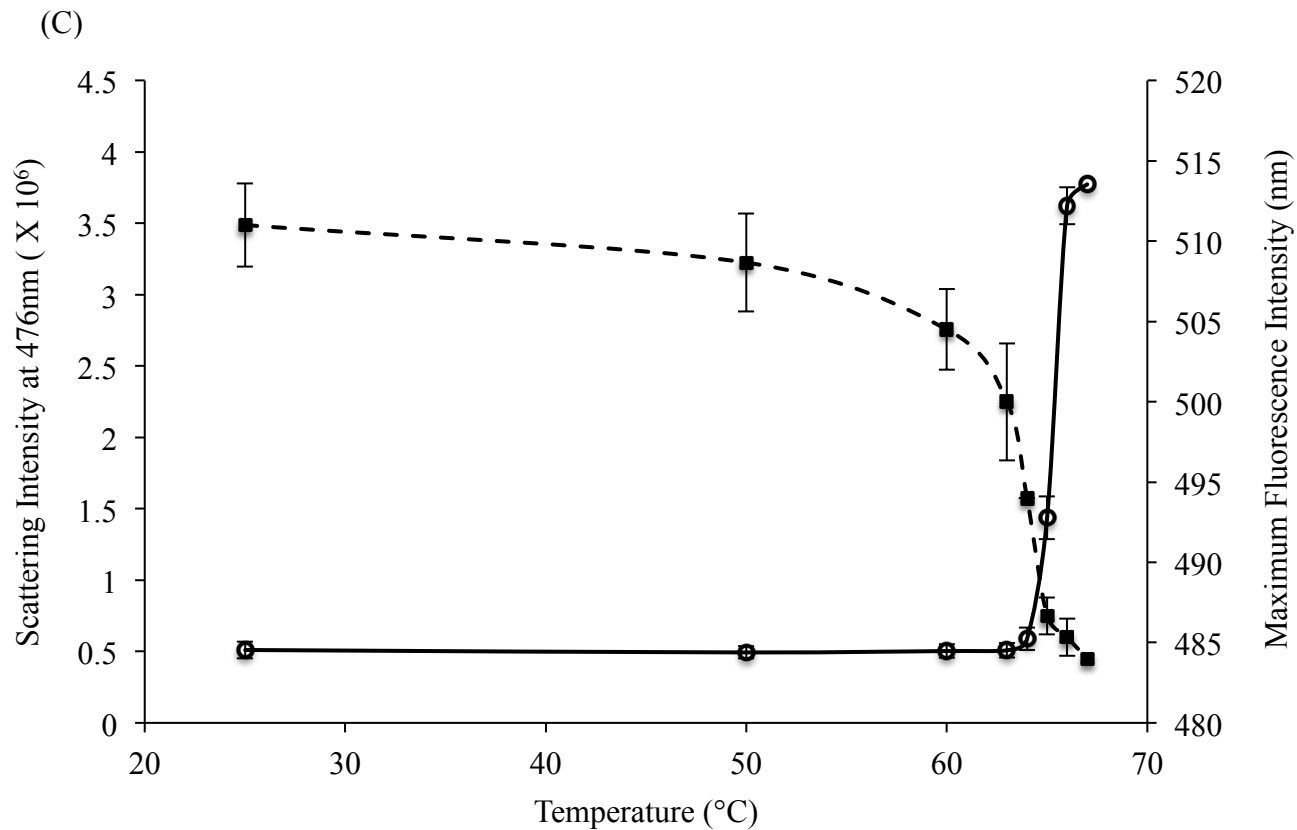


**Figure 8:** Plot of scattering intensity at 376 nm (primary axis – solid line/open circles) and maximum wavelength (secondary axis – dotted line/filled squares) as a function of temperature. All measurements were performed in triplicate. (A) represents MAb Y, (B) MAb Z and (C) MAb X.

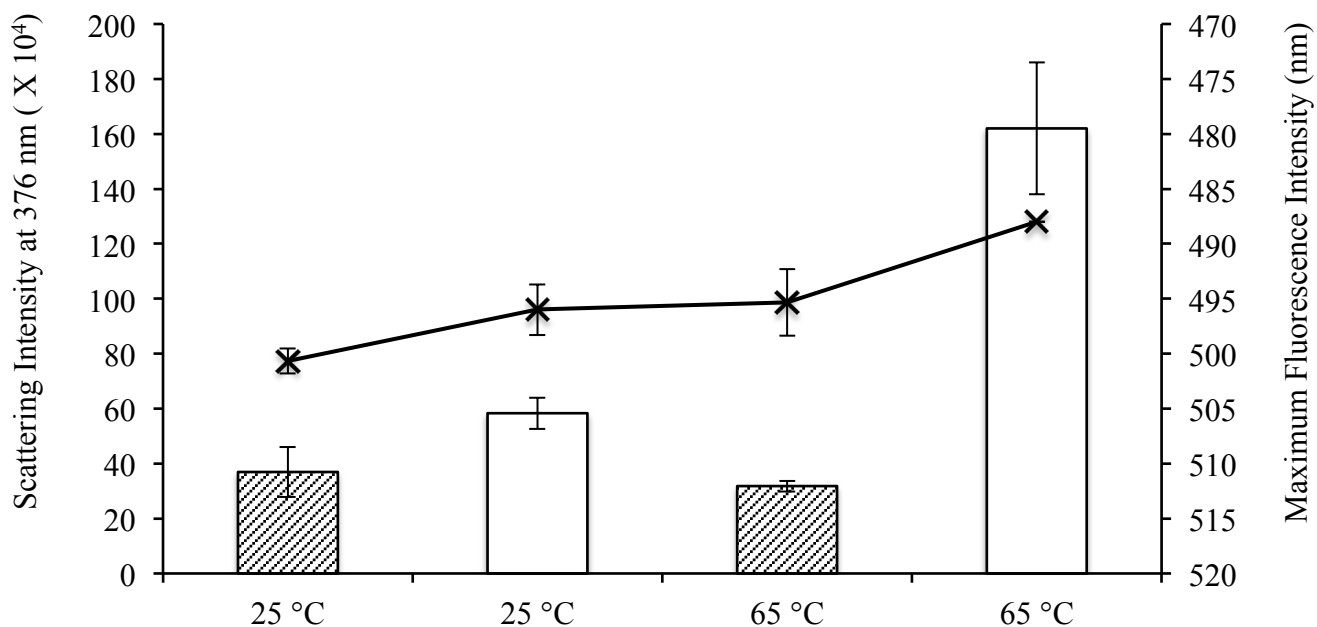


**Figure 9:** The aggregation propensity of MAb Y was monitored at two temperatures and the effect of mechanical stress (vortex) was observed. The scattering intensity (primary y-axis) given by the bar graphs indicates aggregates formed in solution. The shaded and non-shaded bars represent unstressed and stressed samples, respectively. The shift of maximum fluorescence intensity (secondary y-axis, (X) symbols) is the change in the wavelength of maximum fluorescence of ANS. The line is only a guide. Error bars are standard deviation ( $n = 4$ ).

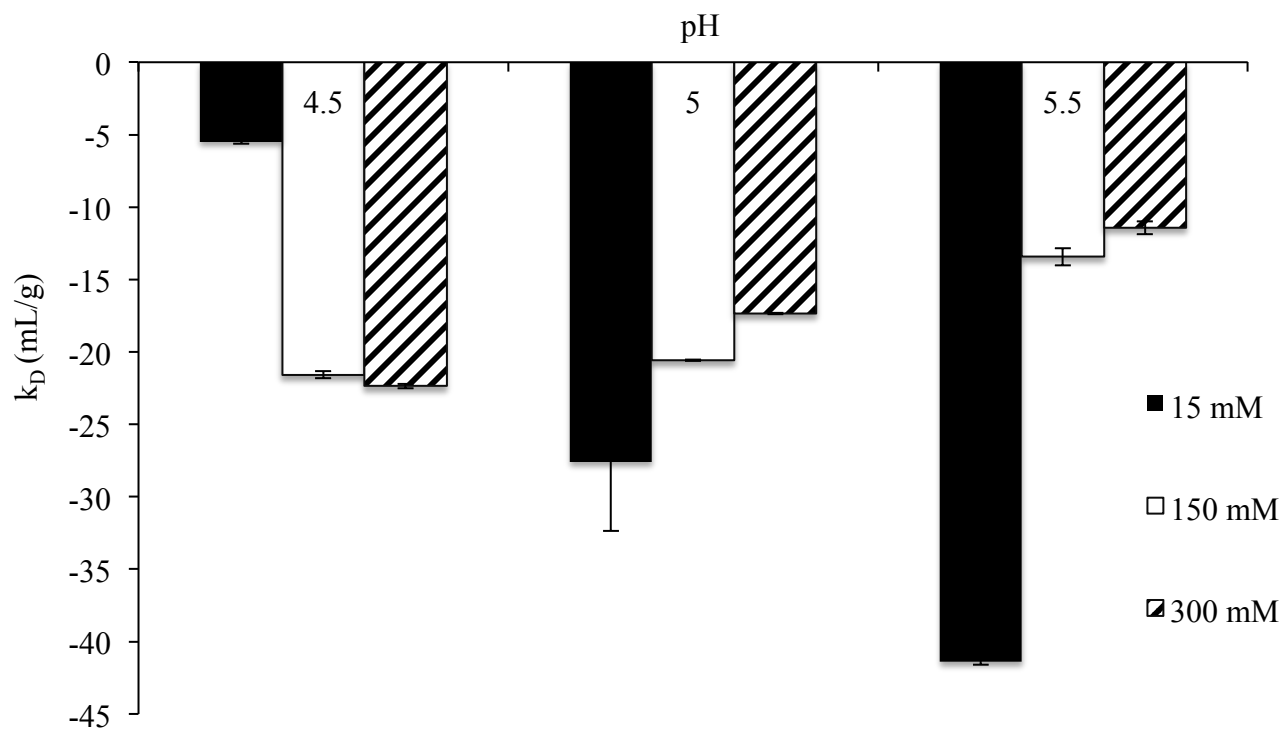


**Figure 10:** Plot of  $k_D$  as a function of pH while varying ionic strength for MAb X. Error bars are standard deviation ( $n = 3$ ).

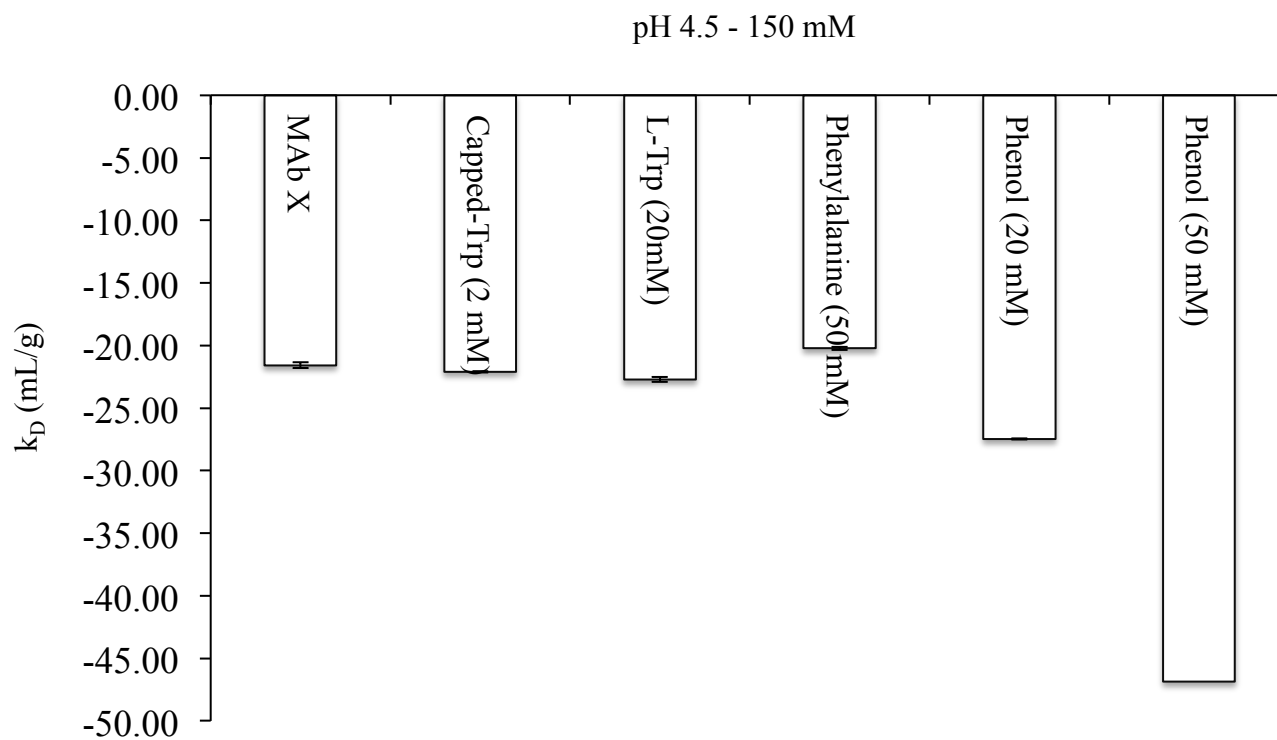


**Figure 11:** Plot of  $k_D$  obtained for mAb X at pH 4.5 and 150mM ionic strength. Each bar represents the  $k_D$  obtained after the addition of excipients with aromatic moieties to the protein solutions. Measurements were performed in duplicate.

## **Chapter 6**

### **Summary**

## 6.1. Summary and Conclusions

Maintaining safe and stable protein therapeutic formulations continues to be a relevant area of research in the pharmaceutical field. A thorough understanding of protein aggregation, specifically predicting proteins that are prone to aggregation has become important in the formulation design. A substantial amount of research regarding certain factors and solution conditions that cause aggregation has led to an understanding of approaches to prevent aggregates or to be cautious of during formulation. Although managing risk is important, understanding the underlying interactions that contribute to aggregation of protein molecules is equally as significant during early stages of formulation and development.

Hydrophobic interactions, whether those that are buried and can be solvent accessible depending on structural changes, or those that remain on the surface after a protein has folded, can both contribute to association and aggregation of protein molecules in solution. Methods measuring hydrophobic interactions lack consistency and are influenced by solutions conditions. Consequently, the main scope of this work was to measure surface hydrophobicity without the influence of solution conditions, and to determine the relationship of hydrophobicity to aggregation promoted either by structural changes or hydrophobic patches on the protein surface of both known model proteins and unknown monoclonal antibodies.

Differences in aromatic and aliphatic hydrophobic interactions were identified using multiple techniques, including a novel method using NMR. Measuring hydrophobicity by HIC using both a butyl and phenyl column showed that there are stronger interactions on the phenyl column, highlighting the significance of  $\pi$  -  $\pi$  interactions. Using NMR, the

transverse relaxation time,  $T_2$  was measured for different small molecules. The degree of decrease in the transverse relaxation time of the probe is due to the interaction with each protein. It was found that phenol showed the most promise as being a successful probe to measure the difference in protein surface hydrophobicity. These studies suggest that using a multi-method approach gave added insight into the type of hydrophobic interaction between two proteins and a well-defined representation of the surface hydrophobicity.

Additionally, it is known that the hydrophobicity of a protein contributes to the adsorption of proteins at the air/water interface. The relationship between the surface hydrophobicity of proteins and how it influenced lateral interactions at the interface was investigated by interfacial rheology studies. It was found from these studies, that the effect of pH influenced elasticity ( $G'$ ) and rigidity at the surface, whereas surface hydrophobicity played a small role. The model proteins were also stressed *via* shaking stress to facilitate aggregation, however surface hydrophobic interactions had no impact on aggregation, whereas, electrostatic interactions contributed to aggregation in both A-ChytA and B-IgA.

Lastly, this work investigated hydrophobicity and aggregation by performing a comprehensive study from characterization of unknown protein molecules to assessing the physical stability of these antibodies in solution. The hydrophobicity of monoclonal antibodies was characterized and the influence of hydrophobicity in protein aggregation was investigated. The antibodies were stressed by both mechanical (shaking) and thermal stresses, and aggregation as well as unfolding was monitored at different solution parameters. The effect of ionic strength or hydrophobicity of the proteins did not



influence aggregation induced by shaking. Consequently, heating the antibodies followed the general aggregation mechanism, where a protein first unfolds and then begins to aggregate in solution. As more energy was applied to the monoclonal antibodies by combining thermal and mechanical stresses, an increased tendency to aggregate was observed. Moreover, the results suggest that the surface hydrophobicity measurements alone cannot be used to predict the degree of aggregation for a protein molecule. It is shown that a combination of both surface and average hydrophobicity influences the physical stability of a protein. These results further imply the significance of understanding the role of surface hydrophobicity measurements in regards to aggregation especially for early protein screening during formulation and development.

## Appendix

**Table A3 - 1: Small Probes**

Protein Probe	Alone	BSA	A-ChytA	B-LgA
<i>Tert</i> -butyl alcohol	2.32±0.01	1.84±0.01 <sup>C</sup>	2.47±0.03 <sup>C</sup>	2.31±0.02 <sup>C</sup>
1-butanol	2.69±0.06	0.71±0.05	2.74±0.01 <sup>A</sup>	2.74±0.10 <sup>A</sup>
1-propanol	3.32±0.04	1.33±0.03	3.41±0.03 <sup>A</sup>	3.25±0.01 <sup>A</sup>
Phenol	5.16±0.03	0.16±0.01	4.60±0.07	4.21±0.04

All  $T_2$  values are presented in seconds. *Tert*-butyl alcohol, 1-butanol and 1-propanol represent aliphatic probes (light grey) and phenol represents the sole aromatic probe (dark grey). The errors for the  $T_2$  values are related to data acquisition and processing (same sample is evaluated multiple times), which shows the accuracy of determining the  $T_2$ . This error does not take into account error associated with sample preparation. All protein:probe samples were prepared at a 1:50 ratio (30  $\mu$ M protein : 1.5 mM probe). 3 mM concentrations for *tert*-butyl alcohol and phenol were used to evaluate  $T_2$  values in the absence of protein, and 6 mM concentrations were used for 1-butanol and 1-propanol. <sup>A</sup> This symbol indicates that protein subtraction was done to limit error due to protein overlap. <sup>B</sup> This symbol indicates that samples were run twice. ND refers to no data. <sup>C</sup> This symbol represents samples that were run once. Deviations shown are based on the deviation of the fit obtained from VnmrJ.

**Table A3-2: Capped Amino Acid Probes**

Protein Probe	Alone	BSA	A-ChytA	B-LgA
Leucine	0.67±0.01	0.28±0.01 <sup>B</sup>	0.61±0.00 <sup>AB</sup>	0.67±0.01 <sup>AB</sup>
Valine	0.83±0.01	0.69±0.01 <sup>B</sup>	0.86±0.00 <sup>AB</sup>	0.86±0.00 <sup>AB</sup>
Phenylalanine	2.04±0.01	0.32±0.00 <sup>B</sup>	2.07±0.01 <sup>B</sup>	1.87±0.01 <sup>B</sup>
Tryptophan	2.20±0.03	0.13±0.01	1.71±0.01	1.79±0.02
Tyrosine	1.46±0.02	0.31±0.02	1.37±0.08	1.51±0.14

All  $T_2$  values are presented in seconds. Leucine and valine represent aliphatic probes (light grey) and phenylalanine, tyrosine and tryptophan represent aromatic probes (dark grey). The errors for the  $T_2$  values are related to data acquisition and processing (same sample is evaluated multiple times), which shows the accuracy of determining the  $T_2$ . This error does not take into account error associated with sample preparation. All protein:probe samples were prepared at a 1:50 ratio (30  $\mu$ M protein : 1.5 mM probe). 3 mM concentrations for all probes were used to evaluate  $T_2$  values in the absence of protein, except for Phe, where 1.5 mM was used. <sup>A</sup> This symbol indicates that protein subtraction was done to limit error due to protein overlap. <sup>B</sup> This symbol indicates that samples were run twice. ND refers to no data.

**Table A3-3: Big Tau Sets**

Probe	Protein	BigTau Set (s)
Tbutyl	None B-LgA A-ChytA	0.1,0.2,0.4,0.6,0.8,1.2,2,3,4,6,8,12,20
Tbutyl	BSA	0.1,0.2,0.4,0.8,1.2,2,3.5,6,8
Butanol	None BSA B-LgA A-ChytA	0.2,0.3,0.5,0.7,1.2,2,3.5,5.5,8,12
butanol	BSA	0.1,0.2,0.3,0.5,0.7,1.2,2,3,4.5,6
propanol	None B-LgA A-ChytA	0.2,0.4,0.6,0.8,1.2,3,6,9,12,20
propanol	BSA	0.1,0.2,0.3,0.5,0.7,1.2,2,3,4.5,6
phenol	None B-LgA A-ChytA	0.2,0.5,0.8,1.2,2,4,6,12,24
phenol	BSA	0.05,0.1,0.2,0.3,0.5,0.7,1.2,2,5
Leu	None B-LgA A-ChytA	0.1,0.2,0.4,0.8,1.2,2,4,8,16
Leu	BSA	0.05,0.1,0.2,0.3,0.5,0.7,1.2,2,5
Val	None BSA B-LgA A-ChytA	0.1,0.2,0.4,0.8,1.2,2,4,8,16
Phe	None B-LgA A-ChytA	0.1,0.2,0.4,0.8,1.2,2,4,8,16
Phe	BSA	0.05,0.1,0.2,0.3,0.5,0.7,1.2,2,5
Trp	None B-LgA A-ChytA	0.1,0.2,0.4,0.8,1.2,2,4,8,16
Trp	BSA	0.05,0.1,0.2,0.3,0.5,0.7,1.2,2,5
Tyr	None B-LgA A-ChytA	0.1,0.2,0.4,0.8,1.2,2,4,8,16
Tyr	BSA	0.05,0.1,0.2,0.3,0.5,0.7,1.2,2,5

Note that the minimum number of points used was nine and that the differing ratios (1:25, 1:50, 1:100) all used the same bigtau set. The above table indicates the combination of protein and probe and their respective bigtau set.

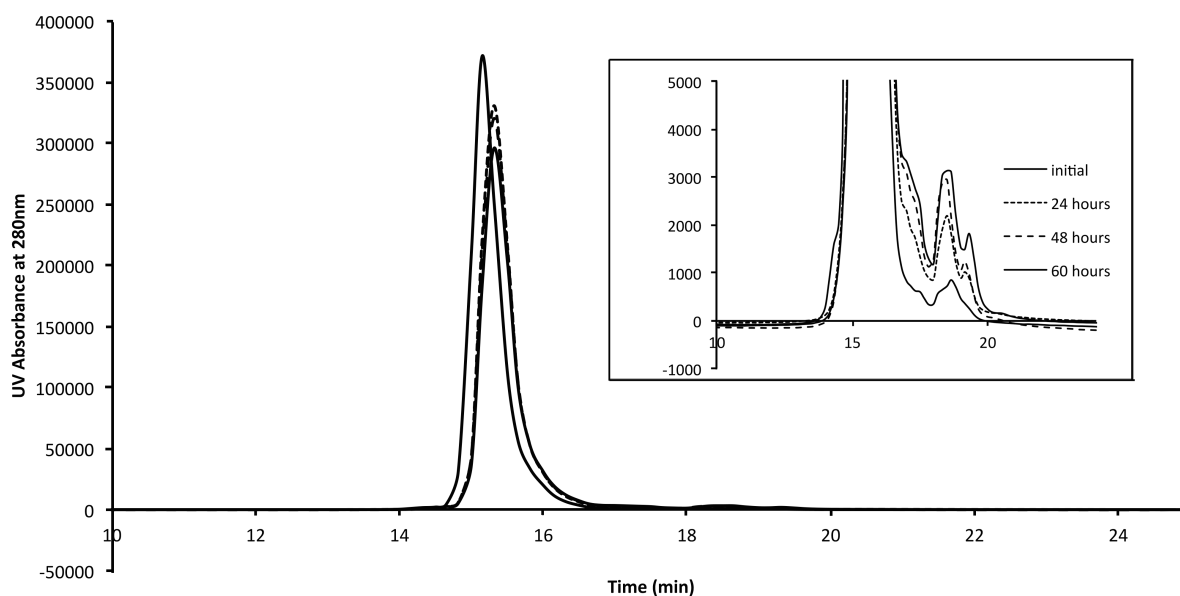


**Figure A3-1:** The physical stability of A-ChytA was monitored as a function of time. UV chromatograms (280nm) of 5 mg/ml A-ChytA at time  $t=0$ , 24, 48 and 60 hours at room temperature. Samples were analyzed at 0.8 mL/min flow rate and with a 100mM pH 7 sodium phosphate buffer with a total ionic strength of 200mM (due to addition of sodium sulfate) used as the mobile phase. The shift in monomer peak is error due to manual injection of the sample.

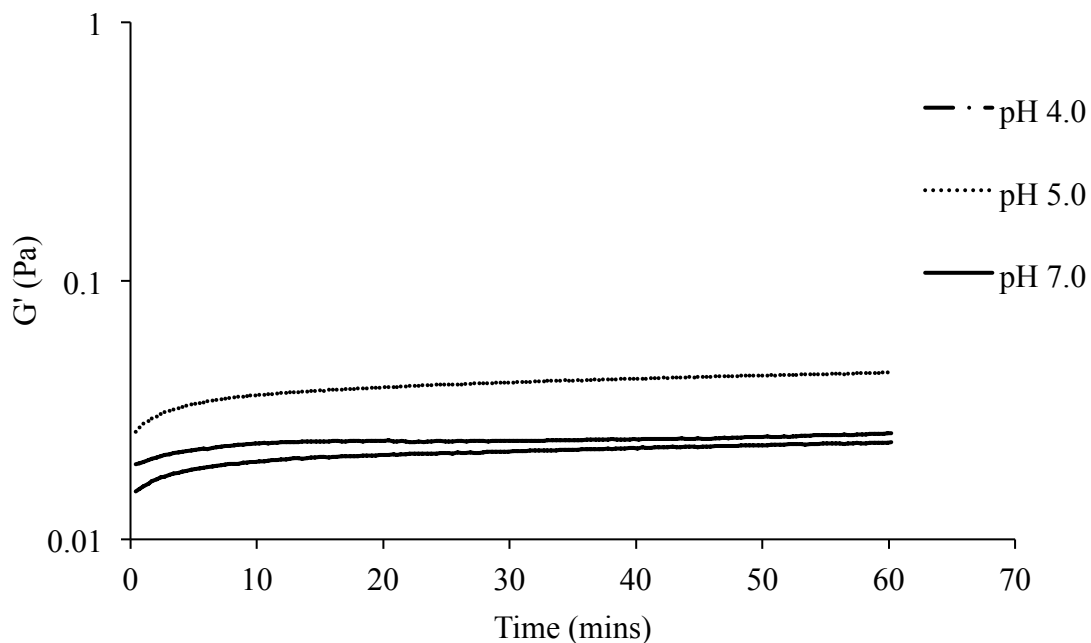


**Figure A4-1:** Elastic Modulus ( $G'$ ) for different pH solutions of BSA measured on an ARG2 Rheometer with a Du Nouy ring attachment. The ionic strength of all solutions was 15 mM. For pH 4.0 and 5.0, measurements were made in duplicates and at pH 7.0 measurements were taken seven times. A time sweep for each pH is one out of the total number of time sweeps for each pH condition.

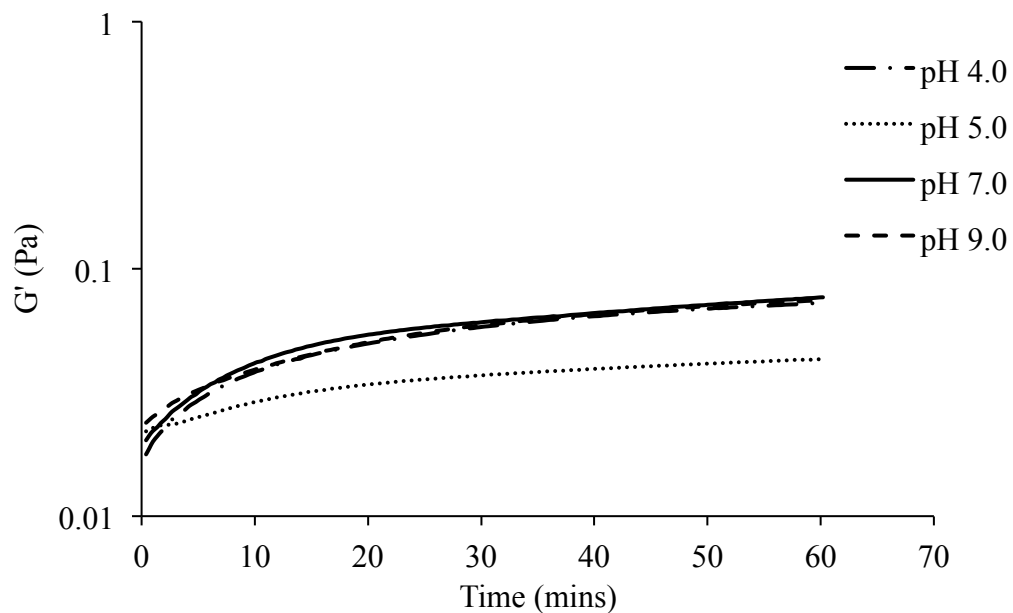


**Figure A4-2:** Elastic Modulus ( $G'$ ) for different pH solutions of A-ChytA measured on an ARG2 Rheometer with a Du Nouy ring attachment. The ionic strength of all solutions was 15 mM. For pH 4.0 and 9.0, measurements were made in duplicates and pH values 5.0 and 7.0 measurements were taken four times. A time sweep for each pH is one out of the total number of time sweeps for each pH condition.



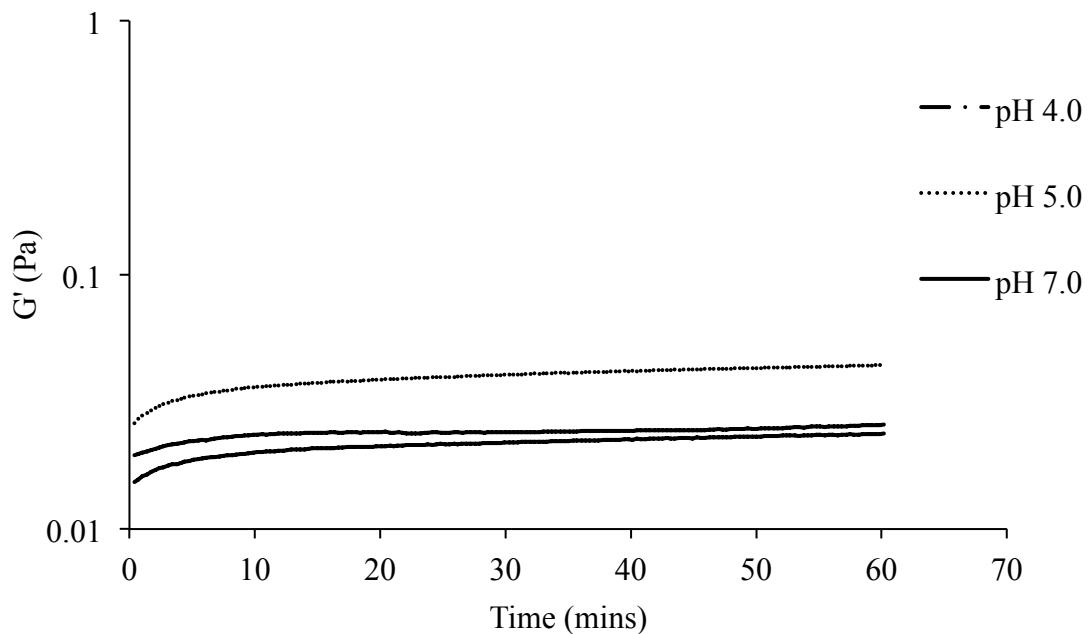


**Figure A4-3:** Elastic Modulus ( $G'$ ) for different pH solutions of B-IgA measured on an ARG2 Rheometer with a Du Nouy ring attachment. The ionic strength of all solutions was 15 mM. For pH 4.0 and 5.0, measurements were made in duplicates and at pH 7.0 measurements were taken four times. A time sweep for each pH is one out of the total number of time sweeps for each pH condition.

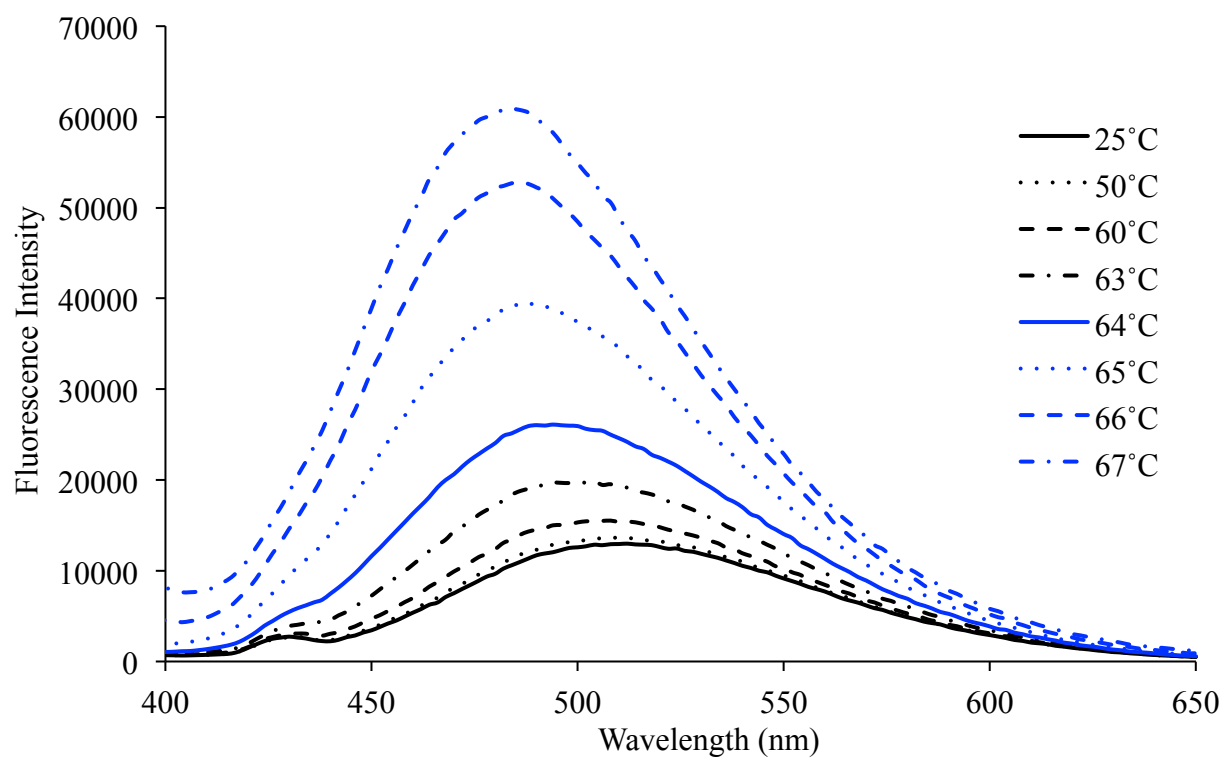


**Figure A5-1:** Fluorescence intensity for MAb X as a function of increasing temperature.

MAb Concentrations were 0.5 mg/ml in a pH 7.0 phosphate buffer (15 mM ionic strength). Temperature ramps were set at 1°C/min

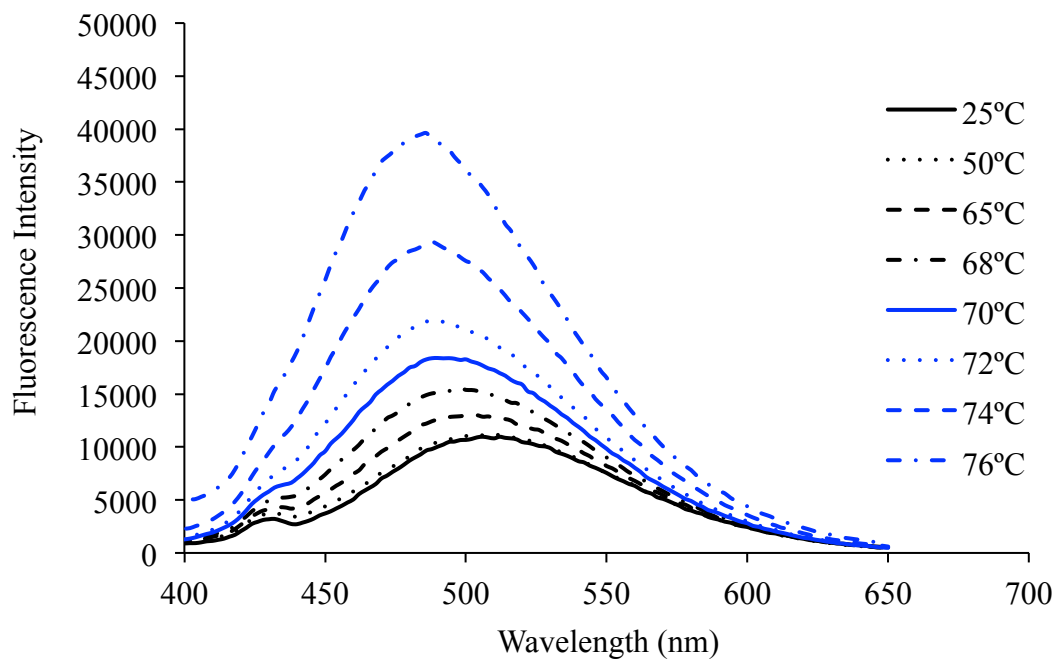


**Figure A5-2:** Fluorescence intensity for MAb Z as a function of increasing temperature.

MAb Concentrations were 0.5 mg/ml in a pH 7.0 phosphate buffer (15 mM ionic strength). Temperature ramps were set at 1°C/min.

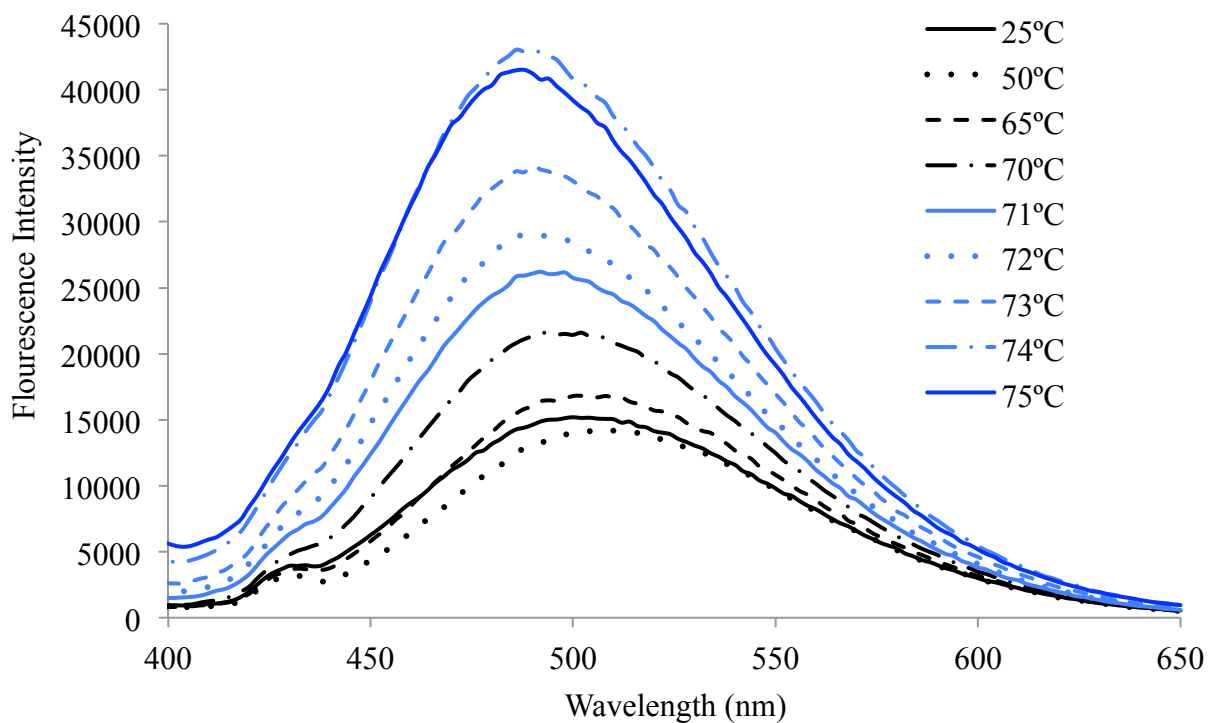


**Figure A5-3:** Fluorescence intensity for MAb Y as a function of increasing temperature.

MAb Concentrations were 0.5 mg/ml in a pH 7.0 phosphate buffer (15 mM ionic strength). Temperature ramps were set at 1°C/min.